



237

Picosecond Lasing Dynamics in Quantum Well Lasers

量子井戸レーザのピコ秒ダイナミックス

A Thesis Presented to
the Graduate School of the University of Tokyo
in Partial Fulfillment of the Requirements for
the Degree of Doctor of Philosophy
in Electronic Engineering

by

Tetsuomi Sogawa

December 21, 1990

To My Parents

Preface

This thesis describes an essential part of the research work carried out at Research Center for Advanced Science and Technology (RCAST), and Institute of Industrial Science (IIS), University of Tokyo, while the author was working as a graduate student of the Department of Electronic Engineering, University of Tokyo, from 1986 to 1991.

For future ultrafast opto-electronics such as ultra high speed optical communication systems and optical information processing systems, development of ultra-short optical pulse generation technology in semiconductor lasers is significantly required. Especially, a gain switching technique is the most important method because of its practical system configurations and possibility of various applications. Up to date, gain switching characteristics and applications to optical communication systems have been investigated with great interest. However, its physical mechanism on the picosecond time scale has not been sufficiently revealed.

In this thesis, picosecond lasing dynamics of gain-switched quantum well lasers are both theoretically and experimentally studied for the purpose of fundamental understandings and future applications to ultrafast optoelectronic systems.

December 1990

Tetsuomi Sogawa

Acknowledgements

I would like to take this opportunity to thank my dissertation supervisor, Professor Yasuhiko Arakawa, Research Center for Advanced Science and Technology, University of Tokyo, for his constant guidance and encouragement throughout my graduate studies at University of Tokyo. His valuable insights proved a great boon to my work, and being a member of his research group expanded my interests to many new areas of quantum electronics.

I am grateful to Professor H. Sakaki, Research Center for Advanced Science and Technology, University of Tokyo, and Professor T. Kamiya, Department of Electronic Engineering, University of Tokyo, for their suggestions and fruitful discussions. I wish to express my special thanks to Professor J. Hamasaki and Professor Y. Fujii, Institute of Industrial Science, University of Tokyo, for their constant guidance and encouragement

I would like to express my gratitude to M. Nishioka, whose technical assistance in the experimental aspects of this thesis was invaluable. I am also indebted to T. Matsusue, who first introduced me to the experimental aspects of picosecond and femtosecond laser technology. A special thanks also goes to Dr. M. Tanaka, who collaborated in much of the work reported here. I am also indebted to T. Takahashi for his help in theoretical analysis. I deeply thank A. Ishikawa for his assistance in the construction of the experimental apparatus used in femtosecond measurements. I am

grateful to many other talented and helpful colleagues, Dr. H. Shoji, Dr. H. Yoshimura, T. Odagiri, N. Hiwasa, S. Tsukamoto, and T. Yamauchi for their guidance, discussions and enjoyable collaborations. I also thank everyone who were working together with me in the Institute of Industrial Science and in the Research Center for Advanced Science and Technology for their kind and valuable cooperations and collaborations.

The fellowship of the Japan Society for the Promotion of science for Japanese Junior Scientists was generously supplied from 1989 April to 1991 March. I also gratefully acknowledge the financial support of the University-Industry Joint Research Program on Mesoscopic Electronics, a Grant-in-Aid from the Ministry of Education, Science, and Culture, the Foundation for Promotion of Material Science and Technology of Japan, the Matsuda Science Foundation, and the Ogasawara Foundation.

Last but not least, I would like to thank my parents for their constant encouragements.

Abstract

The author has established the understanding of the short optical pulse generation and its dynamics in GaAs/AlGaAs quantum well lasers by a gain switching method. The author has addressed following two points as the main purposes.

- 1) Essential improvements in short optical pulse generation by introducing quantum well structures.
- 2) Investigations of the picosecond lasing dynamics of gain-switched quantum well lasers.

With respect to 1), the author has theoretically and experimentally demonstrated the significance of the enhanced differential gain for shorter pulse generation. An extremely short pulse as narrow as 1.3 psec is successfully achieved in a quantum well laser. With respect to 2), the author has clarified the physical process in the picosecond pulse generation by the measurement of time-resolved spectra of gain-switched quantum well lasers as well as the significant dependence of lasing dynamics on quantum well structures. Ultrafast logic gating operations in an optically gain-switched quantum well laser by utilizing novel wavelength switching phenomena are also demonstrated.

Contents

| | |
|---|-----------|
| Preface | iii |
| Acknowledgement | iv |
| Abstract | vi |
| Chapter I Introduction | 1 |
| § 1.1 Background of This Work | 1 |
| § 1.2 Motivations and Objectives of This Study | 6 |
| § 1.3 Synopses of Chapters | 8 |
| Chapter II Picosecond Pulse Generation by a Gain-Switching Method | 10 |
| § 2.1 Introduction | 11 |
| § 2.2 Gain Switching and Rate-Equations | 13 |
| § 2.3 Significance of Enhanced Differential Gain Properties | 15 |
| § 2.4 Picosecond Pulse Generation by an Optical Pumping Method in GaAs/AlGaAs Quantum Well Lasers | 17 |
| 2.4.1 <i>Experimental Procedure</i> | 17 |
| 2.4.2 <i>Measurement of Pulse Durations and Delay Times</i> | 18 |

| | | |
|-------|---|----|
| 2.4.3 | <i>Ultra-Short Pulse (<1.3psec) Generation and Its Stochastic Behaviors</i> | 19 |
| 2.4.4 | <i>Analysis by Travelling Wave Rate-Equations</i> | 21 |
| § 2.5 | Significance of Enhanced Differential Gain Properties for Short Pulse Generation in Detuned Distributed Feedback (DFB) Lasers | 26 |
| 2.5.1 | <i>Introduction</i> | 26 |
| 2.5.2 | <i>Experimental Procedure</i> | 27 |
| 2.5.3 | <i>Measurement of Pulse Durations</i> | 27 |
| 2.5.4 | <i>Discussion</i> | 28 |
| § 2.6 | Concluding Remarks | 30 |
| | Figures | 31 |

Chapter III Spectral Dynamics in Gain-Switching Quantum Well Lasers and Its Dependence on Quantum Well Structures 50

| | | |
|-------|---|----|
| § 3.1 | Introduction | 51 |
| § 3.2 | Dependence of the Number of Quantum Wells | 54 |
| 3.2.1 | <i>The Number of Quantum Wells</i> | 54 |
| 3.2.2 | <i>Experimental Procedure</i> | 55 |
| 3.2.3 | <i>Measurement of Pulse Durations and Time-Resolved Spectra</i> | 57 |
| 3.2.4 | <i>Discussion</i> | 58 |
| § 3.3 | Dependence of the Barrier Thickness | 62 |

| | | |
|--|--|--------|
| 3.3.1 | <i>Coupled QW and Uncoupled QW</i> | 62 |
| 3.3.2 | <i>Experimental Procedure</i> | 63 |
| 3.3.3 | <i>Measurement of Pulse Durations and Time-Resolved Spectra</i> | 63 |
| § 3.4 | Concluding Remarks | 66 |
| | Figures | 67 |
| Chapter IV Repetitive Gain-Switching Characteristics in Quantum Well Lasers | | 78 |
| § 4.1 | Introduction | 79 |
| § 4.2 | Experimental Procedure | 82 |
| § 4.3 | Repetitive Gain-Switching Characteristics | 83 |
| 4.3.1 | <i>Temporal Characteristics</i> | 83 |
| 4.3.2 | <i>Multi-Mode Effects</i> | 84 |
| § 4.4 | Frequency Characteristics of Gain Switching Operation and Small-Signal Modulation | 86 |
| § 4.5 | Concluding Remarks | 89 |
| | Figures | 90 |
| Chapter V Wavelength Switching in Picosecond Pulse Generation and Its Application to All- Optical Logic Gating Operations | | 98 |

| | | |
|-------|--|-----|
| § 5.1 | Introduction | 99 |
| § 5.2 | Lasing Characteristics of Quantum Well Lasers by Localized and Homogeneous Excitation | 100 |
| § 5.3 | Novel Wavelength Switching Phenomena in Picosecond Pulse Generation | 102 |
| § 5.4 | All-Optical Logic Gating Operations | 104 |
| § 5.5 | Concluding Remarks | 105 |
| | Figures | 106 |

| | | |
|-------------------|--|------------|
| Chapter VI | Carrier Capture Process in Quantum Well Structures and Its Effects on Lasing Dynamics | 112 |
| § 6.1 | Introduction | 113 |
| § 6.2 | Carrier Capture Phenomena and Carrier Relaxation Process | 115 |
| 6.2.1 | <i>Experimental Procedure</i> | 115 |
| 6.2.2 | <i>Carrier Capture and Diffusion Process</i> | 116 |
| 6.2.3 | <i>Cooling Process of Hot Carriers</i> | 117 |
| § 6.3 | Effects of Carrier Capture Phenomena and Carrier Heating on Lasing Dynamics of Gain-Switched Quantum Well Lasers | 120 |
| § 6.4 | Concluding Remarks | 123 |
| | Figures | 124 |

| | | |
|-------------------------|--|------------|
| Chapter VII | Conclusions | 133 |
| Appendix | Lasing Dynamics of Quantum-Well Wire Lasers | 136 |
| A.1 | Introduction | 137 |
| A.2 | Gain Properties of Quantum-Well Wire Lasers | 138 |
| A.3 | Theoretical Analysis of Lasing Dynamics of Quantum-Well Wire Lasers | 140 |
| A.4 | Summary | 141 |
| | Figures | 142 |
| References | | 145 |
| Publication List | | 160 |

Chapter I Introduction

§1.1 Back Ground of This Work

High speed semiconductor light sources generating ultrashort pulses with a half-width of a few picoseconds and a peak power equal to or larger than CW power are essential for a broad range of quite different applications. These applications include high bit-rate optical communication, ultrafast optical signal processing, optical sources for optical electronics, picosecond or femtosecond physics spectroscopy, optical disc and so on.

Following the development in other areas of quantum electronics, it has been well established for a number of years that picosecond and sub-picosecond pulses can be obtained in semiconductor laser diodes by active or passive mode-locking, Q-switching, and gain switching. In other laser systems including ion lasers, gas lasers, and dye lasers, the mode-locking techniques such as active mode-locking with acousto-optic (AO) modulators, passive mode-locking with saturable absorbers, and colliding pulse mode-locking (CPM) have remarkably progressed to produce sub-picosecond or femtosecond pulses [1]-[3]. In addition, both a pulse compression technique using optical fibers, pairs of prisms, and pairs of diffraction gratings and a pulse amplification technique

have contributed to shorten the pulse width less than 100 fsec [4]-[8]. As a result, an extremely short pulse as narrow as 6 fsec is successfully achieved [9]. These femtosecond pulses have facilitated investigations in condensed media, carrier dynamics in semiconductors, and chemical reactions [10]-[12].

In semiconductor lasers, in the same way, mode-locking techniques have been investigated using external cavities. Most works on semiconductor laser mode-locking have used active mode-locking [13]-[26], either by modulating the gain of the laser cavity or by modulating the loss of the laser cavity with an external modulator. In this scheme, the external cavity configuration which usually needs an optical etalon to eliminate side modes due to an imperfect anti-reflection coating of facet requires extremely complex optics and careful alignment. In 1988, active mode-locking in a monolithic semiconductor laser was for the first time successfully realized and 4 psec pulse is achieved [21]. In addition, 1.4 psec pulses with a peak power of 10mW at repetition rate of 32.6 GHz is demonstrated in a CPM monolithic semiconductor laser with active modulation [26]. Presently, the shortest pulses (0.56psec) have been obtained with active mode-locking [20]. However, actively mode-locked semiconductor lasers often exhibit instabilities and multiple peaks in their outputs, and the repetition rate should be precisely tuned to that the cavity length determines. On the other hand, in passive mode-locking, microwave oscillators are not required, and the saturable absorber in a passively mode-

locked laser serves to shorten the leading edge of the pulse. Picosecond and sub-picosecond pulses have been obtained by passively mode-locked semiconductor lasers [27]-[30], although the primary problem has been to obtain satisfactory saturable absorbers which have reasonable lifetimes and stability. In both mode-locking techniques, it is inherently possible to produce Fourier transform limit pulses with a pulse width of less than 100 fsec. However, the major draw backs to those methods are the greater cavity complexity due to temperature variations and mechanical vibrations and the limitation to mode-locking at a harmonic of the cavity frequency.

For most important applications such pulses produced by the mode-locking are quite impractical, since they are always emitted in a continuous train without the possibility of a large variation of the repetition frequency and of a ON/OFF signal switching. A gain switching method which is realized by a direct modulation of the injection current is the other basic technique for producing ultrashort optical pulses in semiconductor lasers. No external cavity is needed, and the repetition rate can be varied up to a maximum operation frequency f_{max} which is determined by the relaxation oscillation frequency and electrical parasitic elements present in the semiconductor laser used in the experiment. In GaAs and InGaAsP double-heterostructure lasers, pulse widths of 10 ps~50 ps have been obtained by pre-biasing the laser and superimposing a strong RF modulation current [31]-[36]. For shorter

pulse generation, fast current injection is needed [37], and 4 psec pulse is achieved in AlGaAs V-groove structure laser driven by 100 psec current pulses [38], although the output pulse form includes multiple spike structures with 9 psec interval due to repetitive reflections inside the cavity. For long distance communication systems, short pulses from single-mode semiconductor lasers are required. Picosecond pulses were achieved in distributed feedback (DFB) lasers or distributed Bragg reflector (DBR) lasers [39]-[42]. However, the time-bandwidth product of a gain-switched pulse is typically many times the Fourier transform limit, since the laser chirps during the pulse generation due to the coupling between the gain of the laser and the optical index of the cavity [43]. If a single-mode laser is used, this chirping can be compensated with gratings or optical fibers [44],[45], although the fiber length may be considerable, on the order of 2km. In this way, gain-switched pulses can be compressed from 30 to 5 psec. Another approach to narrower pulse generation is shortening the photon life time in the cavity [46]. In fact, 1.4 psec short pulse is obtained by an ultrashort-cavity semiconductor film laser with cavity length of 1~2 μ m [47], and 4 psec is achieved by a surface emitting GaAs laser [48]. However, the generation of the single short pulse less than a few picosecond in semiconductor lasers with a conventional sample dimension had not been succeeded by the gain switching method. In 1987, significance of high differential gain properties in shorter pulse generation is

proposed by Arakawa [49],[50]. This is not the approach from the design of device structures, but from the modification of material properties by the use of quantum size effects. In fact, an extremely short pulse as narrow as 1.3 psec is achieved in a GaAs/AlGaAs multiquantum well laser [51]. This value is the shortest one so far achieved by the gain switching method.

Q-switching in semiconductor lasers by rapidly switching the intracavity optical loss is also a practical technique for producing picosecond pulses with high peak power and high repetition rate [52]-[57]. Variations in the optical loss can be produced through passive means in which the loss is not directly modulated or active means in which the loss is directly modulated. Passive Q-switching due to saturable absorption was observed in semiconductor lasers with two nonuniformly pumped gain sections [55],[56]. Active Q-switching by direct loss modulation in multi-section semiconductor lasers has an advantage for many applications. 16 psec pulse generation at 4 GHz operation has been achieved in a two section quantum well laser with an intracavity modulator in which quantum confinement stark effect is utilized for efficient loss modulation [58].

The great progress in crystal growth technology such as molecular beam epitaxy (MBE) and metal organic chemical vapor deposition (MOCVD) makes it possible to growth ultra-thin semiconductor heterostructures including superlattice and

quantum well structures [59]. These novel structures have been not only supplying many hot topics in solid state physics, but also providing a variety of new optical and electrical devices such as quantum well (QW) lasers, high electron mobility transistors (HEMT), and resonant tunneling diodes. Since the first investigation of optical properties in quantum wells by Dingle [60] the application of quantum well structures to semiconductor laser diodes [61],[62] has received considerable attention because of physical interest as well as its superior characteristics, such as low threshold current density [63]-[66], low temperature dependence of threshold current [67]-[69], wavelength tunability, and excellent dynamic properties [70]-[72]. Especially, relaxation oscillation frequency is enlarged by a factor of two compared to the conventional double-heterostructure lasers because the differential gain is highly enhanced due to the step like density of states in the two dimensional carrier systems [70]-[74]. Therefore, QW laser becomes a significant candidate which can satisfy the requirements for the applications to ultrafast optoelectronic devices.

§1.2 Motivations and Objectives of This Study

For future ultrafast optoelectronic systems such as high speed optical communication systems and optical information processing systems, improvements of high speed properties in semiconductor

lasers are highly expected. Picosecond pulse generation technology in semiconductor lasers is important for such applications. To this end, many works have been carried out by mode-locking, Q-switching, and gain switching, as described in §1.1. The gain switching method is the most significant candidate owing to its practical scheme for short pulse generation. However, the reported pulse durations by the gain switching method are over 10 ps in single-mode semiconductor lasers and 4 ps in Fabri-Perot type semiconductor lasers, even though theoretical analysis predicts less than a few psec pulse generation which is determined by the photon life time in the laser cavity.

In the gain switching method, short cavity structures have been examined in order to obtain shorter pulses. There is, however, another way to achieve this: that is a modification of material parameters through the use of quantum well structures.

The purpose of this study is to improve the high speed characteristics of gain-switched semiconductor lasers and to understand the ultrafast phenomena in the process of short pulse generation by the gain switching method as well as effects of the QW structures. In this study, picosecond pulse generation in QW lasers and its physical mechanism are systematically investigated. In addition, effects of the QW structures on picosecond dynamics are studied.

§1.3 Synopses of Chapters

In this study, picosecond dynamic properties of QW lasers are investigated in order to comprehensively understand the mechanism of the ultra short pulse generation by the gain switching method and reveal effects of the QW structures. This paper is organized as follows.

Chapter I is the introduction. The background of this study is mentioned.

In Chapter II, the principles of the gain switching method in short pulse generation are described. Theoretical treatment on the basis of conventional rate-equations is provided, demonstrating significance of QW structures for short pulse generation. In order to investigate inherent high-speed characteristics of GaAs/AlGaAs QW lasers, experiments by optically pumped gain switching are carried out. Travelling wave rate equations are analyzed to explain the experimental results. In addition, detuned distributed feedback lasers are also used to obtain the systematic evidence of the effects of the differential gain in short pulse generation.

In Chapter III, spectral dynamics of the gain-switched QW lasers are investigated. Effects of the number of the QWs and the barrier thickness on picosecond dynamics are revealed. Theoretical discussion employing multi-mode rate equations is also provided.

In Chapter IV, repetitive gain switching characteristics are both theoretically and experimentally studied. Frequency response characteristics of the gain switching operation and small signal modulation are investigated in order to discuss the maximum operation frequency in the gain switching.

In Chapter V, novel wavelength switching phenomena in short pulse generation are provided. Applications of the picosecond wavelength switching to all-optical logic gating operations (AND/NOT) are successfully demonstrated.

In Chapter VI, carrier capture phenomena and carrier relaxation process are studied the pump-probe measurements using 100~150 fsec pulses. It is revealed that the relaxation time by the cooling of hot-carriers is 0.3~1 psec and that the capture time is about 20 psec which is due to the carrier diffusion. The effects of carrier capture process and the carrier thermalization on the lasing dynamics of gain-switched QW lasers are also investigated, demonstrating the overflow of carriers significantly influences the lasing dynamics.

Chapter VII is the summary and the conclusions of this work.

Chapter II Picosecond Pulse Generation by a Gain-Switching Method

abstract

The mechanism of short optical pulse generation by the gain switching method is described. The significance of the enhanced differential gain is theoretically discussed on the basis of rate equations. Picosecond light pulses are generated in GaAs/AlGaAs MQW lasers which are gain-switched by optical-pumping pulses from a dye laser. The shortest pulse width achieved in this experiment is 1.3 psec. This is the narrowest pulse width so far achieved in semiconductor lasers without external cavity. We believe that this short pulse generation results from enhanced differential gain due to two-dimensional properties of carriers in the quantum wells. In order to discuss these results theoretically, analyzed are spatial dependent rate equations, in which the stochastic process of the spontaneous emission and the travelling effect of spontaneously generated optical wave packets are included. In addition, detuned distributed feedback lasers are used to obtain the systematic evidence of the effects of the differential gain in short pulse generation.

§ 2.1 Introduction

Picosecond pulse generation technology in semiconductor lasers is important for certain applications such as high speed optical communication systems. For this purpose, mode locking method [13]-[30], gain switching method [31]-[51] and Q-switching method [52]-[58] have been investigated. In contrast to the mode locking method, the gain switching method as well as the Q-switching method has the advantage that no external cavity is required. The narrowest light pulse so far achieved in semiconductor lasers without external cavities is 4 psec by the gain switching method [38].

In the gain switching method, short cavity structures have been examined in order to obtain shorter pulses [46]-[48]. There is, however, another way to achieve this: that is a modification of material parameters through the use of quantum well structures [49],[51],[70]-[72].

In this chapter, firstly the principles of the gain switching method in short pulse generation and theoretical treatment on the basis of conventional rate-equations are provided, demonstrating significance of QW structures for short pulse generation. In order to investigate inherent high-speed characteristics of GaAs/AlGaAs QW lasers, experiments by an optically pumped gain switching using dye laser picosecond pulses excited by mode-locked Nd⁺-YAG laser are carried out. Travelling-wave rate equations are analyzed to explain the experimental results. In addition, detuned distributed

feedback lasers are used to obtain the systematic evidence of the effects of the differential gain in short pulse generation.

§ 2.2 Gain Switching and Rate-Equations

The gain switching is a peculiar method to semiconductor lasers, which is in principle realized by a simple direct current modulation. As illustrated in Fig.2.1, the small-signal direct modulation uses the linear region of the I-L characteristics beyond threshold and light output is sinusoidally modulated. On the other hand, the gain switching method utilizes the nonlinearity of I-L characteristics around the threshold and produces short pulses with high peak power. Figure 2.2 shows the time charts of modulation current, carrier density, and photon density when pulse current is injected into a semiconductor laser. Gain-switching effects are described as follows. Firstly, current pulse injection increases the carrier density. When the carrier density goes over threshold, lasing action starts and the photon density rapidly increases. Strong stimulated emission, on the other hand, decreases the carrier density below threshold and lasing stops. As a result, short optical pulse is generated. This is the principle of the short pulse generation by the gain switching method. Note that a narrower optical pulse is produced compared to the pulse width of the injected current pulse. These dynamic behaviors in the gain switching can be theoretically discussed on the basis of conventional single-mode rate equations [75],[76], which are described as follows.

$$\frac{dP}{dt} = \Gamma c_g g P - \frac{P}{\tau_p} + \beta \frac{n}{\tau_s} \quad (2.1)$$

$$\frac{dn}{dt} = J(t) - c_g g P - \frac{n}{\tau_s} \quad (2.2)$$

, where n is the carrier density, $J(t)$ is the injected carriers, P is the photon density, τ_s is the carrier lifetime, τ_p is the photon lifetime, c_g is the group velocity of light, Γ is the optical confinement factor [72], g is the bulk gain as a function of carrier density n , and β is the spontaneous emission factor [77]-[79]. If the laser is pumped by an highly injected short pulse (i.e. $J(t)$ is nearly equal to $n_0 \delta(t)$: $n_0 \gg 1$), an approximate solution for the pulse width $\Delta\tau$ can be obtained as follows [49].

$$\Delta\tau = \tau_p + \frac{1}{c_g g' n_0} \quad (2.3)$$

, where the gain $g(n)$ is assumed to be a linear function and expressed by $g(n) = g'(n - n_T)$: g' is called the differential gain which is defined as dg/dn and n_{T0} is the carrier concentration at transparent condition. Eq. (2.3) indicates that the pulse width is a sum of the photon lifetime and a term of $1/(c_g g' n_0)$. Therefore, higher differential gain g' as well as higher excited carriers n_0 leads to shorter pulse generation.

§ 2.3 Significance of Enhanced Differential Gain Properties

Figure 2.3 shows the carrier distribution in bulk material and quantum well (QW). In the bulk, the density of states is given by the parabolic function. In the QW, on the other hand, the density of states becomes the step-like function because of the two dimensional properties of carriers. As illustrated in Fig.2.3, the energy broadening of carrier distribution is reduced in the QW compared to the bulk. This narrow carrier distribution influences lasing characteristics, improving threshold current density [63]-[66], temperature dependence of the threshold current [67]-[69], spectral line width [70]-[72], and modulation band width [70]-[74]. Especially, the enhancement of differential gain g' is the most important for lasing dynamics [49],[70].

In QW lasers, the step-like density of states narrows the gain spectrum compared to the bulk material, which leads to an increase of differential gain g' which is defined as the ratio of the derivative of the bulk gain to the derivative of the carrier concentration n (i.e. $g' = \partial g / \partial n$). Figure 2.4 shows a calculated differential gain, plotted as a function of the QW thickness L_z . Note that infinite L_z corresponds to a double heterostructure (DH) laser. This figure indicates that the differential gain of the MQW laser with $L_z = 50 \text{ \AA}$ is enhanced by a factor of four compared to the DH laser. As the higher differential gain leads to shorter pulse generation, we can expect it in a MQW laser.

Figure 2.5 shows a numerically calculated result of pulse width for a MQW laser with $L_z=100 \text{ \AA}$ on the basis of single mode rate equations, plotted as a function of carrier concentration n , where we assume a pumping pulse width of 15 psec. The carrier concentration n is normalized by threshold carrier concentration n_{th} for laser oscillation. For comparison, the pulse width of a DH laser is also plotted. As indicated in this Figure, the pulse width can be reduced by a factor of two compared to that of DH laser under the same excitation level.

§ 2.4 Picosecond Pulse Generation by an Optical Pumping Method in GaAs/AlGaAs Quantum Well Lasers

2.4.1 *Experimental Procedure*

In order to investigate inherent high-speed characteristics of GaAs/AlGaAs QW lasers, experiments by an optically pumped gain switching using dye laser picosecond pulses excited by mode-locked Nd⁺-YAG laser are carried out [49]. The device structure of a GaAs/AlGaAs MQW laser prepared for this experiment was grown by molecular beam epitaxy in a Riber 2300 R&D system. The following layers were subsequently grown on a (100) oriented n⁺-GaAs: a 0.5 μm GaAs buffer layer, a 1.5 μm Al_yGa_{1-y}As cladding layer (y=0.39), a 725 Å Al_xGa_{1-x}As waveguide layer (x=0.19), an active region consisting of four 100 Å GaAs wells separated by 50 Å Al_xGa_{1-x}As barriers, a 725 Å Al_xGa_{1-x}As waveguide layer, 1.5 μm Al_yGa_{1-y}As cladding layer, and 100 Å GaAs cap layer. All layers are nondoped. In Figure 2.6, the associated band diagram is illustrated. After this growth the wafer is cleaved for making a Fabry-Perot resonator with cavity length of 150~300 μm.

In Figure 2.7, the experimental system is illustrated. A dye laser (Pyridin 2) pumped by a mode-locked Nd⁺-YAG laser with a cavity dumper (Spectral Physics) is used for optical pumping of the MQW laser. The repetition rate can be varied in the range between 41 MHz and 400 Hz. The emission power of the dye laser is 60 mW

at 4.1 MHz. To measure the temporal characteristics of the laser emission, a *synchronously scanning* streak camera system (Hamamatsu C1587 + M1955) or a *single-shot* streak camera system (Hamamatsu C1587 + M1952) is used. The camera has an S20 extended red photo-cathode with a radiant sensitivity of 1 mA/W at 8500 Å. The temporal resolution of the streak camera system is larger than 1.5 psec. The laser light from the dye laser is focused through a cylindrical lens on the MQW laser. The stripe width is defined by focusing the pumping laser light with a cylindrical lens, and is less than 20 μm. The wavelength of the dye laser is 7000 Å (1.77 eV) so that only the active region, including the waveguide layers and barrier layers which have a bandgap of 1.64 eV, is excited. The pulse width of the dye laser is estimated to be about 15 psec by the streak camera. All experiments were done at room temperature.

2.4.2 *Measurement of Pulse Durations and Delay Times*

First, we observed output light forms by the streak camera with synchronously scanning mode. In this case, detection sensitivity is very high though timing jitter broaden the measured pulse durations. Figure 2.8 shows the time trace of dye laser and outputs from the QW laser at various excitation power measured by synchronously scanning streak camera. Clear short pulses can be produced when the pumping power is beyond the threshold.

intensity. Figure 2.9 shows the pulse duration as a function of excitation intensity normalized by the threshold intensity. With the increase of excitation intensity, the generated pulse duration becomes shorter. We achieved pulse duration less than 15 psec with high excitation. Under the same condition, the pulse duration of double heterostructure laser was larger compared to this result. In addition, this experimental scheme has the advantage that the delay time from excitation to the pulse generation can be measured. Shorter delay time is required for high bit-rate operation. Figure 2.10 shows the delay time as a function of the normalized excitation intensity. With the increase of excitation intensity, the delay time is reduced. Note that the delay time is shortened so short as 15 psec which corresponds to three times round trip time of light inside the cavity.

2.4.3 *Ultra-Short Pulse (<1.3psec) Generation and Its Stochastic Behaviors*

To measure the temporal characteristics of the lasing emission, a *single-shot* streak camera system (Hamamatsu C1587 + M1952) with a time-resolution of about 1.5 psec is used. By using the single-shot mode each pulse can be measured without averaging.

Figure 2.11 shows a time-trace of a short light pulse generated from the MQW laser measured by the streak camera. The pumping power is two times larger than the threshold power with a

repetition rate of 800 kHz. The average output power and the peak power of the MQW laser are $80 \mu\text{W}$ and several W, respectively. The estimated pulse width obtained in Figure 2.11 is less than 1.3 psec, considering the temporal resolution of the streak camera (>1.5 psec). Note that this value is the smallest one so far obtained in semiconductor lasers by the gain switching method.

In addition, it is found that the pulse form varies randomly even under the same excitation condition. In fact, we sometimes observed pulse trains as shown in Figure 2.12. The interval of these two pulses (3.9 psec) is consistent with the calculated round trip time of a pulse in the cavity, using the refractive index $n_r = 3.7$. The pulse train can be thus ascribed to repetitive internal reflections of a single emission [38]. The envelope of the pulse train is also important for discussing energy dynamics in the laser cavity. The estimated F.W.H.M. of this envelope is 5.5 psec on the basis of the result in Figure 2.12.

The spectrum was also measured by a monochromator. The center wavelength of the spectrum is 8570 \AA with a spectral half width of 40 \AA . In the experiment, longitudinal mode structures were not clearly observed, which is due to the fact that the mode selection capability of the laser cavity is almost lost in this very short time interval.

We believe that physical mechanism responsible for this short pulse generation is the enhanced differential gain due to two-dimensional properties of carriers in the MQW. As shown in

Fig.2.11, a pulse train due to repetitive internal reflections was observed in the experiment. The simple rate equation described in Eqs.(2.1) and (2.2) can not give an exact explanation for the pulse train, because for this purpose we should use a model in which spatial evolution of the pulses in the laser cavity is considered. However, even in this model, the role of the differential gain is proved to be the same as the role discussed above for the short pulse generation. Therefore, we can still declare that use of QW structures as well as short photon lifetime leads to our observation of the short pulse.

Appearance of these pulse trains owing to the repetitive internal reflections of a single light pulse travelling inside the cavity suggests existence of locally generated wavepackets, as discussed in §2.4.4.

2.4.4 *Analysis by Travelling Wave Rate-Equations*

In order to understand our experimental results including these stochastic phenomena of output pulse forms and the initial process of the pulse formation in more detail, we analyze evolution of photons inside the cavity, considering spatial dependence of photon distribution. Following rate equations (2.4), (2.5), and (2.6) are formulated on the basis of the slowly varying approximation [80].

$$\frac{\partial S^+(z,t)}{\partial t} + c_g \frac{\partial S^+(z,t)}{\partial z} = (\Gamma g(z,t) - \alpha_{loss}) S^+(z,t) + \Delta^+(z_i, t_i) \quad (2.4)$$

$$\frac{\partial S^-(z,t)}{\partial t} - c_g \frac{\partial S^-(z,t)}{\partial z} = (\Gamma g(z,t) - \alpha_{loss}) S^-(z,t) + \Delta^-(z_i, t_i) \quad (2.5)$$

$$\frac{\partial n(z,t)}{\partial t} = N_{pump}(z,t) - \frac{n(z,t)}{\tau_s} - g(z,t) (S^+(z,t) + S^-(z,t)) \quad (2.6)$$

, where z -axis is parallel to the cavity direction, $S^+(z,t)$ and $S^-(z,t)$ represent photon density which are traveling $+z$ direction and $-z$ direction, c_g is the group velocity of light in the cavity, Γ is the optical confinement factor, $g(z,t)$ is the bulk gain, α_{loss} is the waveguide loss, $n(z,t)$ is the carrier density, $N_{pump}(z,t)$ is the generation rate of carrier density pumped by the dye laser, and τ_s is the carrier lifetime. The boundary conditions at the facets for $S^+(z,t)$ and $S^-(z,t)$ are given by $S^+(0,t) = R S^-(0,t)$ and $S^-(L_z,t) = R S^+(L_z,t)$, where R is the reflectivity and L_z is the cavity length.

$\Delta^+(z_i, t_i)$ and $\Delta^-(z_i, t_i)$ are random variables which represent a spontaneously generated wave packet coupling to $S^+(z,t)$ and $S^-(z,t)$ at time t_i and at the position z_i . We assume that generation time $\{t_i\}$ of the wave packets is determined by Poisson Process. In this case, the average value of the total number $N_{t,t+\Delta t}$ of the wave packets generated into the lasing mode between t and $t+\Delta t$ in the whole cavity is given by

$$\text{Ave} [N_{t,t+\Delta t}] = \beta S_{xy} \Delta t \int_0^{L_z} \frac{n(z,t)}{\tau_s} dz \quad (2-7)$$

, where S_{xy} is the cross-sectional area of the propagating laser beam inside the cavity, and β is the spontaneous emission coefficient which indicates how often the wavepackets are coupled to the lasing mode. Since the coherent behavior of the dipole moment is kept just for intraband relaxation time τ_{in} (~ 0.2 psec), duration of the optical wave packet $\Delta^\pm(z_i, t_i)$ is the order of τ_{in} . Note that the total energy of one wave packet corresponds to one photon energy. On the other hand, it is reasonable to assume that the generation of the wave packet occurs uniformly inside the cavity. Therefore, the probability function of z_i is given by

$$\begin{aligned} P(z_i) &= 1/L_z && (0 \leq z_i \leq L_z) \\ &= 0 && (z_i < 0, L_z < z_i) \end{aligned} \quad (2-8)$$

A simple calculation using Eq.(2.7) shows that the average number of spontaneously emitted photons which are randomly coupled to the lasing mode is about ten during 1 psec over the cavity, provided that the spontaneous emission coefficient β is 10^{-5} and that other device parameters such as carrier lifetime and optically confined volume are typical. Since $N_{t,t+\Delta t}$ is a random variable, it sometimes occurs that a single wave packet is

spontaneously generated without generation of the succeeding wave packets within several picosecond, which leads to significant evolution of only the first wave packet inside the cavity, as illustrated in Fig.2.13 (a). On the other hand, it also occurs that many wavepackets are generated during 1psec and overlapped, which results in generation of a broad pulse, as illustrated in Fig.2.13 (b). Thus, the model based on these rate equations might explain our experimental results random behavior of output light pulses, although this model is not considering interference between wave packets and definition of the mode of photons is ambiguous.

Figure 2.14 shows a typical calculated result for the time evolution of the light pulse traveling inside the cavity. The amplification of a spontaneously emitted seed inside the cavity is observed. Figures 2.15 (a) and (b) show calculated results of output pulses under the same condition ($\beta = 10^{-5}$) using those rate equations. In this calculation, we assume that spatially uniform excitation is realized by a narrow pumping pulse (i.e., $N_{pump}(z,t) = C \delta(t)$, C is a constant). In addition, it is taken into consideration that coupling of the spontaneous emission to the lasing mode occurs randomly as to both time and space. The result indicates that different pulse configurations are generated even under the same condition. This demonstrates stochastic behavior of the spontaneously emitted wave packets. Note that duration of the output light pulse is not bandwidth limited, since each spontaneously emitted wavepacket, which is amplified by electron-

hole pairs, is broadened due to randomness of time at which the electron-hole pairs begin to oscillate for amplified emission. The envelope of those pulse configurations approximately corresponds to the solution of the simple spatially-averaged rate equations.

Small β is required to achieve strong amplification of the first wave packet, since frequent generation of the spontaneous wave packet leads to overlapping of those pulses, which results in broader light pulse generation, as illustrated in Figures 2.13 (a) and (b). Figure 2.16 shows the calculated pulse configuration when β is 5×10^{-4} . These results confirm importance of the small β to explain the stochastic phenomena observed in the experiment. Note that rapid formation of high carrier density in the active layer is also required to obtain our results: Otherwise, many spontaneous wave packets are generated before the first wave packet is dominantly amplified due to the strong stimulated emission effect.

§ 2.5 Significance of Enhanced Differential Gain Properties for Short Pulse Generation in Detuned Distributed Feedback (DFB) Lasers

2.5.1 Introduction

We have been discussing effect of enhanced differential gain on the short pulse generation by the gain switching method, where the differential gain g' is defined as the ratio of the derivative of the bulk gain to the derivative of the carrier concentration n (i.e. $g' = \partial g / \partial n$). Our theoretical calculation predicted that the pulse duration is reduced with the increase of g' [49]. In fact, the generation of a short pulse as narrow as 2ps was successfully observed in a QW laser in which g' is enhanced compared to double heterostructure lasers due to two-dimensional properties of carriers, as described in §2.4. However, more systematic experiment is required in order to confirm the high g' effect. In this section, we investigate short pulse generation from distributed feedback (DFB) lasers, in which g' can be enhanced by detuning Bragg wavelength from the gain peak to a shorter wavelength [81],[82], demonstrating significance of high g' for the short pulse generation [50].

2.5.2 *Experimental Procedure*

In our experiment we used InGaAsP FBH (flat-surface buried heterostructure) DFB lasers (Fujitsu) [83]. Two samples were prepared to examine the detuning effect in the gain switching method: (i) the Bragg wavelength λ_B is tuned to the gain peak; and (ii) λ_B is detuned to a shorter wavelength by 100 Å. The threshold currents under CW operation at 25°C are 8.5 mA and 11 mA, respectively. The structures of both lasers are the same except for the Bragg wavelength. Gain switching is realized by using current pulse trains (1 GHz, 100 ps F.W.H.M., 100 mA_{p-p},) which are generated by a comb generator (HP33005C) with DC bias. The temporal characteristic of the optical pulses is measured by a synchronously scanning streak camera with a sensitivity at the wavelength of 1.3 μm (Hamamatsu C1587 + M1955).

2.5.3 *Measurement of Pulse Durations*

Figure 2.17 shows the measured pulse duration, plotted against the average input current normalized by each threshold current. In this experiment the modulation amplitude is fixed and the direct current is varied. The circles and triangles represent the experimental data for the detuned and tuned lasers, respectively. In both lasers the pulse duration becomes shorter with increasing input current. The shortest pulse is 25 psec in the detuned laser,

while 33 psec is obtained in the tuned laser. This result demonstrated that enhancement of g' through the detuning leads to reduction of the pulse duration. Note that the increase in the pulse duration at higher injected current level is due to the onset of the second pulse through the relaxation effect.

2.5.4 Discussion

Figure 2.18 shows the calculated bulk gain against carrier concentration in InGaAsP lasers at wavelengths of 1300, 1310, and 1320 nm. When the bulk gain necessary for lasing is supposed to be 250 cm^{-1} , the optimum Bragg wavelength λ_B^{opt} for minimizing the threshold current is about 1320 nm. On the other hand, g' which corresponds to the slope of the bulk gain curve is enhanced by detuning λ_B from λ_B^{opt} to 1310 nm or 1300 nm. This indicates that g' can be controlled in DFB lasers by detuning λ_B .

Figure 2.19 shows the calculated pulse duration of lasers tuned to 1300, 1310, and 1320 nm against the averaged input current normalized by each threshold, using the gain profiles in Fig.2.18. The parameter values used in the calculation were as follows: internal loss $\alpha = 30 \text{ cm}^{-1}$, confinement factor $\Gamma = 0.25$, spontaneous emission factor $\beta = 10^{-4}$, carrier lifetime $\tau_s = 3 \text{ nsec}$, and photon lifetime $\tau_p = 3 \text{ psec}$. The injection current pulse is a raised-cosine pulse (150 psec F.W.H.M., five times as large as the threshold

current) added to the direct current. As shown in Fig.2.19, this calculation explains our experimental result, indicating reduction of the pulse duration due to the detuning effect as well as the increase in the pulse duration in the region of high bias current.

In summary, the effect of detuning the Bragg wavelength in picosecond pulse generation in InGaAsP distributed feedback lasers was investigated using the gain switching method. We observed that the pulse duration is reduced in a detuned DFB laser, in which the differential gain is enhanced through detuning the Bragg wavelength from the gain peak to a shorter wavelength by 100 Å. This result demonstrates the significance of the differential gain for short pulse generation.

§ 2.6 Concluding Remarks

The significance of the enhanced differential gain in picosecond optical pulse generation by the gain switching method is both theoretically and experimentally demonstrated.

An extremely short light pulse less than 1.3 psec is successfully generated by the optically pumped gain switching method in a GaAs/AlGaAs multi-quantum well lasers with a cavity length of 200 μ m. This value is the smallest one so far obtained in semiconductor lasers by the gain switching method. This short pulse generation results from the enhanced differential gain due to two dimensional properties of carriers in the quantum wells. In order to discuss the initial process in short pulse generation, spatial dependent rate equations are analyzed. Stochastic behavior of the spontaneous emission inside the cavity is for the first time pointed out.

The effect of detuning the Bragg wavelength in picosecond pulse generation in InGaAsP distributed feedback lasers is investigated. It is observed that the pulse duration is reduced in a detuned DFB laser, in which the differential gain is enhanced through detuning the Bragg wavelength from the gain peak to a shorter wavelength by 100 Å. This result also demonstrates the significance of the differential gain for short pulse generation.

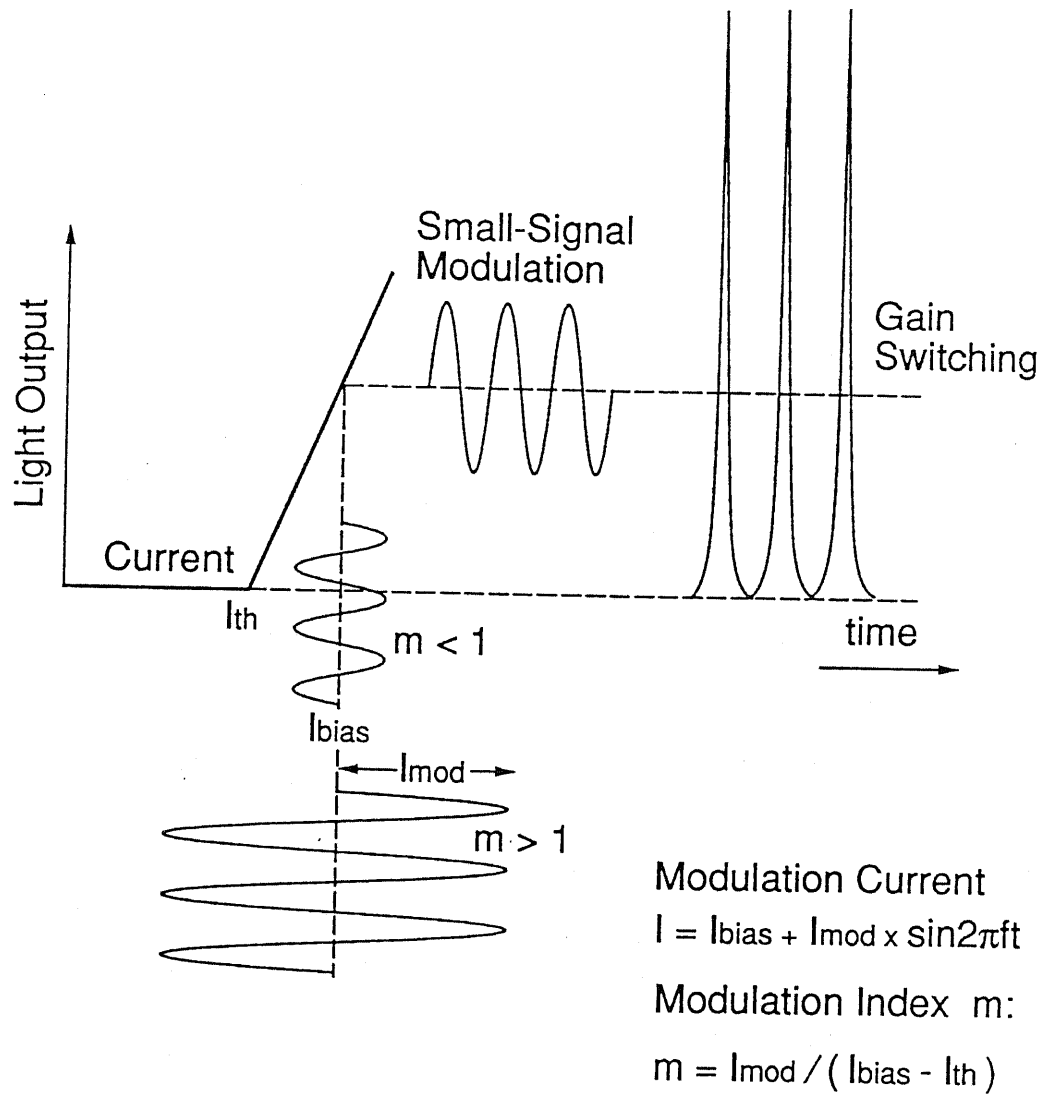


FIG. 2.1 Schematic illustration of operating points and modulation condition of the gain-switching and the small signal modulation in I-L characteristic.

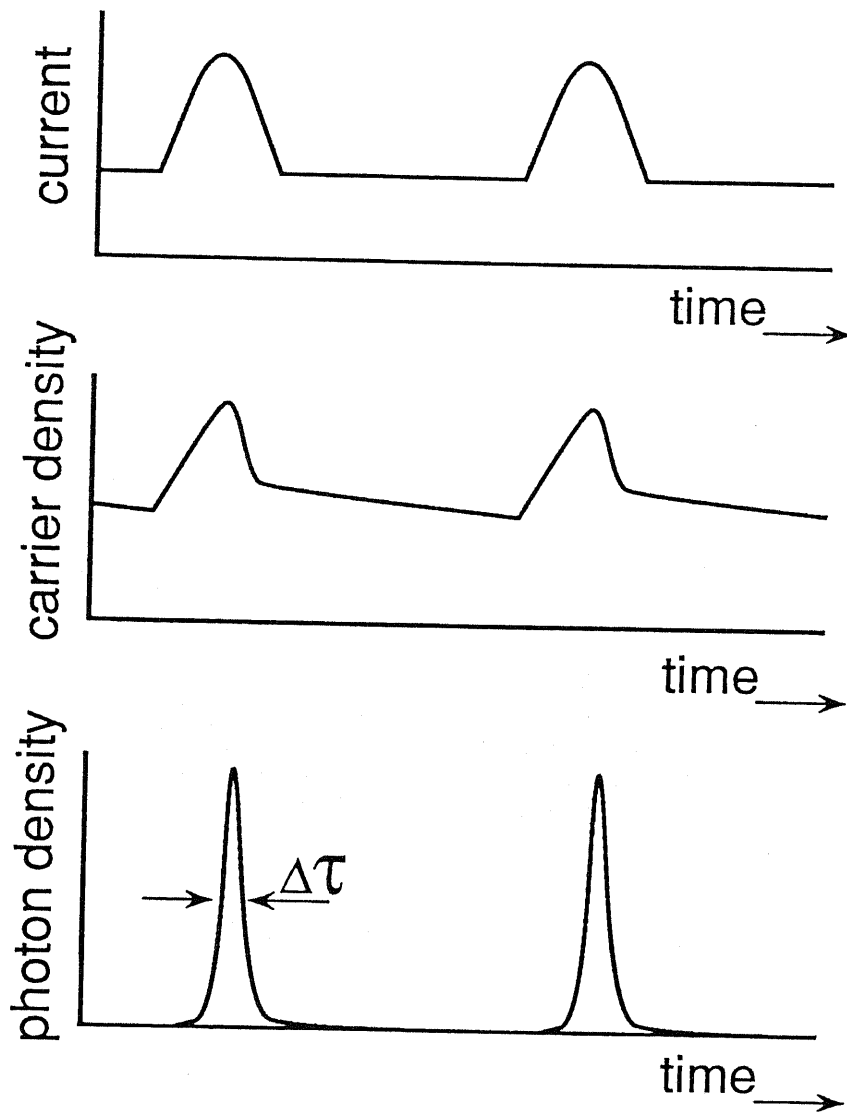


FIG. 2.2 Time charts of modulation current, carrier density, and photon density when the gain switching is realized.

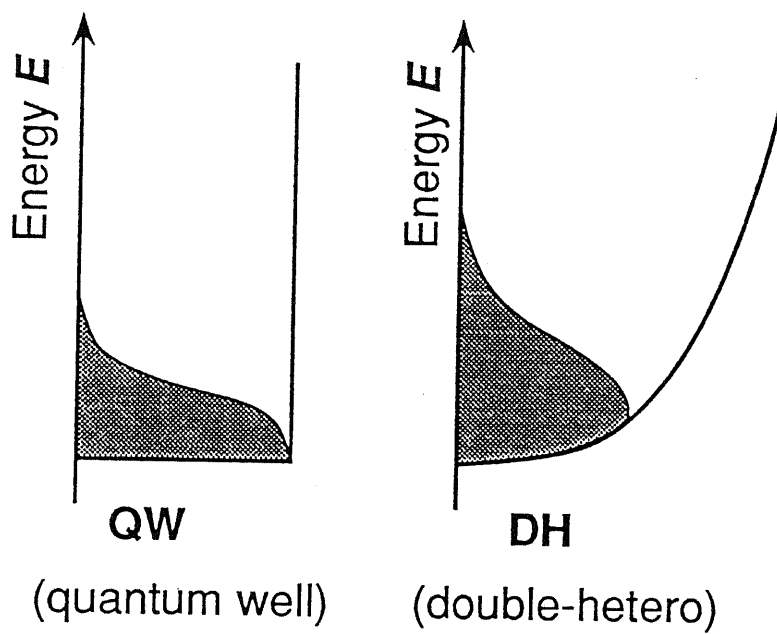


FIG. 2.3 Carrier distribution in bulk material and quantum well (QW). In the bulk, the density of states is given by the parabolic function. In the QW, the density of states becomes the step-like function because of the two dimensional properties of carriers

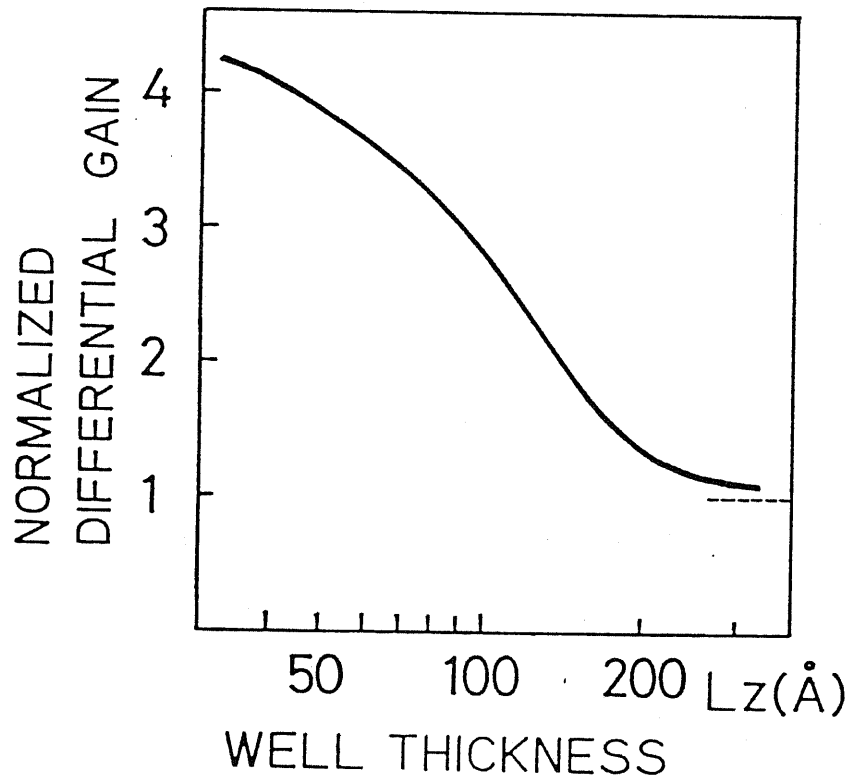


FIG. 2.4 Calculated differential gain properties, plotted as a function of the QW thickness L_z . Note that infinite L_z corresponds to a double heterostructure (DH) laser. The differential gain of the MQW laser with $L_z=50\text{\AA}$ is enhanced by a factor of four compared to the DH laser.

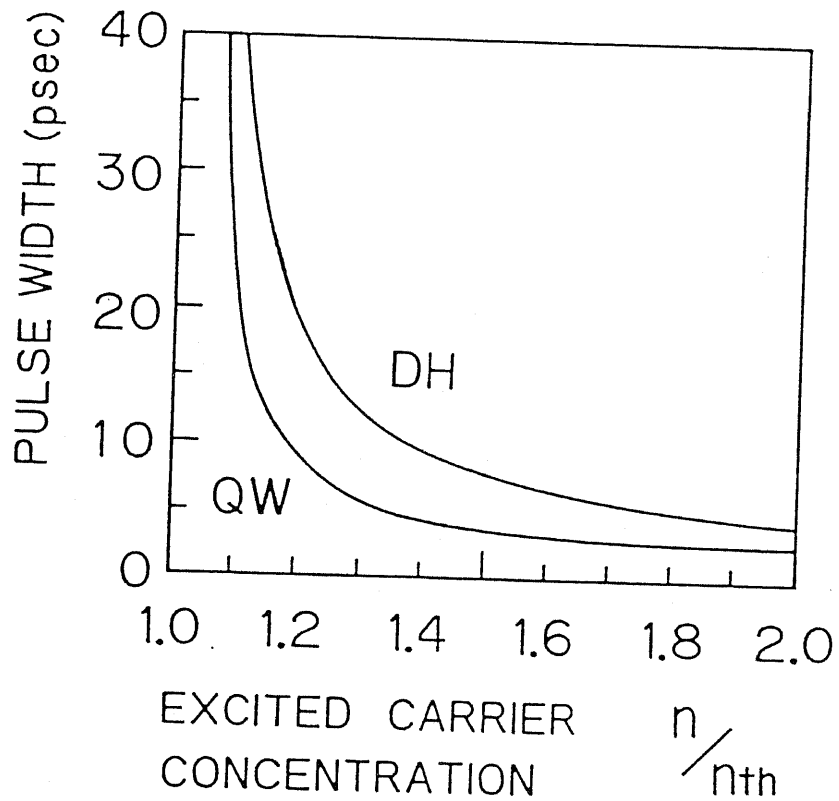


FIG. 2.5 Numerically calculated results of pulse width for a MQW laser with $L_z=100\text{\AA}$ and DH laser on the basis of single mode rate equations, plotted as a function of carrier concentration n , a pumping pulse width is 15psec. The carrier concentration n is normalized by threshold carrier concentration n_{th} for laser oscillation.

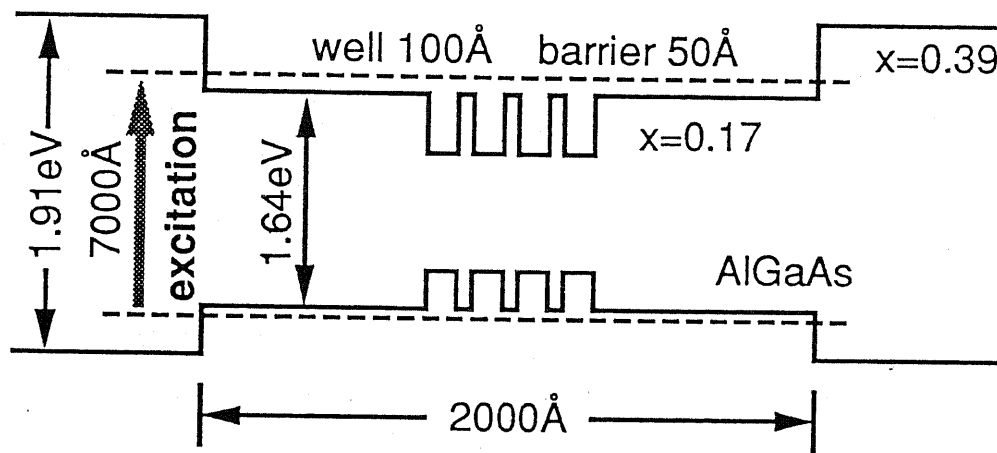


FIG. 2.6 The associated band diagram of QW laser used in the experiments. The following layers were subsequently grown on a (100) oriented n^+ -GaAs: a $0.5\mu\text{m}$ GaAs buffer layer, a $1.5\mu\text{m}$ $\text{Al}_y\text{Ga}_{1-y}\text{As}$ cladding layer ($y=0.39$), a 725\AA $\text{Al}_x\text{Ga}_{1-x}\text{As}$ waveguide layer ($x=0.19$), an active region consisting of four 100\AA GaAs wells separated by 50\AA $\text{Al}_x\text{Ga}_{1-x}\text{As}$ barriers, a 725\AA $\text{Al}_x\text{Ga}_{1-x}\text{As}$ waveguide layer, $1.5\mu\text{m}$ $\text{Al}_y\text{Ga}_{1-y}\text{As}$ cladding layer, and 100\AA GaAs cap layer. All layers are nondoped.

OPTICAL PUMPING

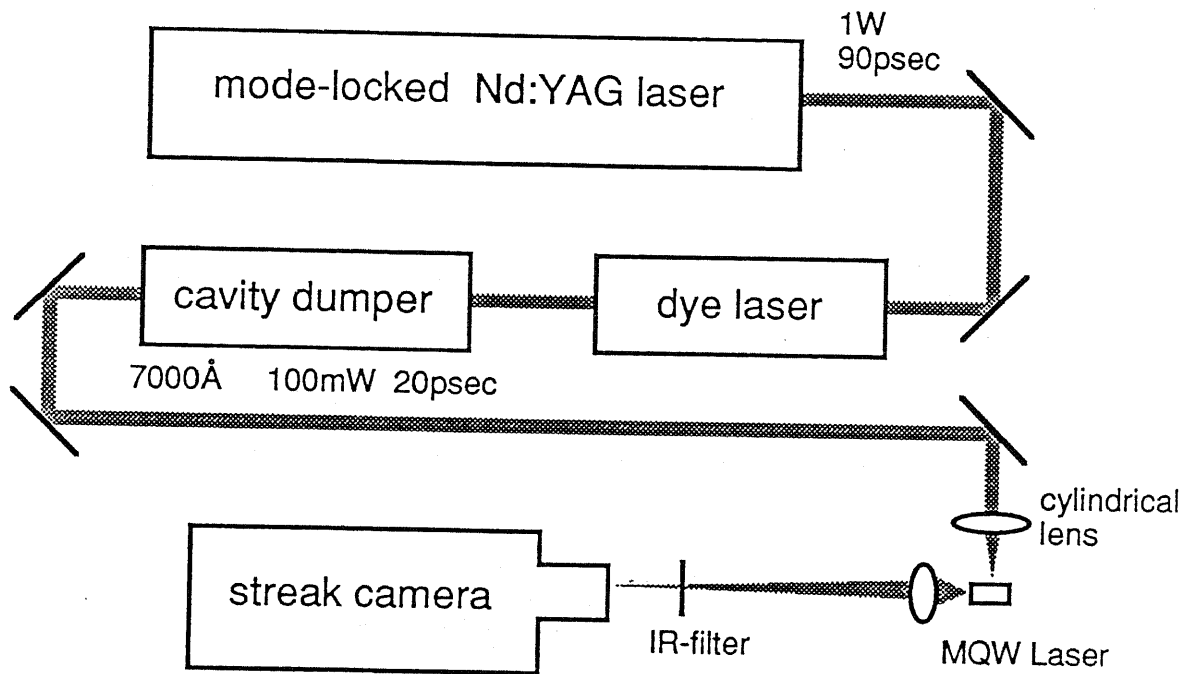


FIG. 2.7 An experimental system is illustrated. A dye laser (Pyridin 2) pumped by a mode-locked Nd^+ -YAG laser with a cavity dumper (Spectral Physics) is used for optical pumping of the MQW laser. To measure the temporal characteristics of the laser emission, a *synchronously scanning* streak camera system (Hamamatsu C1587+M1955) or a *single-shot* streak camera system (Hamamatsu C1587+M1952) is used.

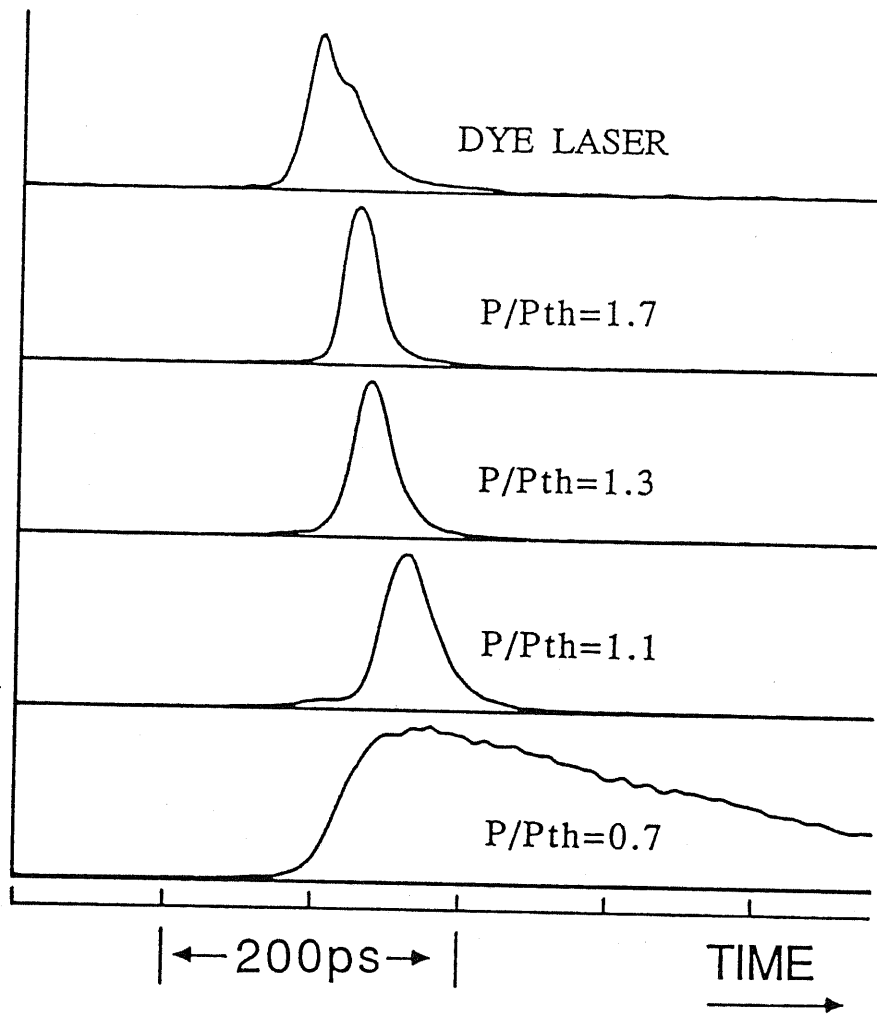


FIG. 2.8 Time traces of dye laser pulse and outputs from the QW laser at various excitation intensities measured by the *synchronously scanning* streak camera.

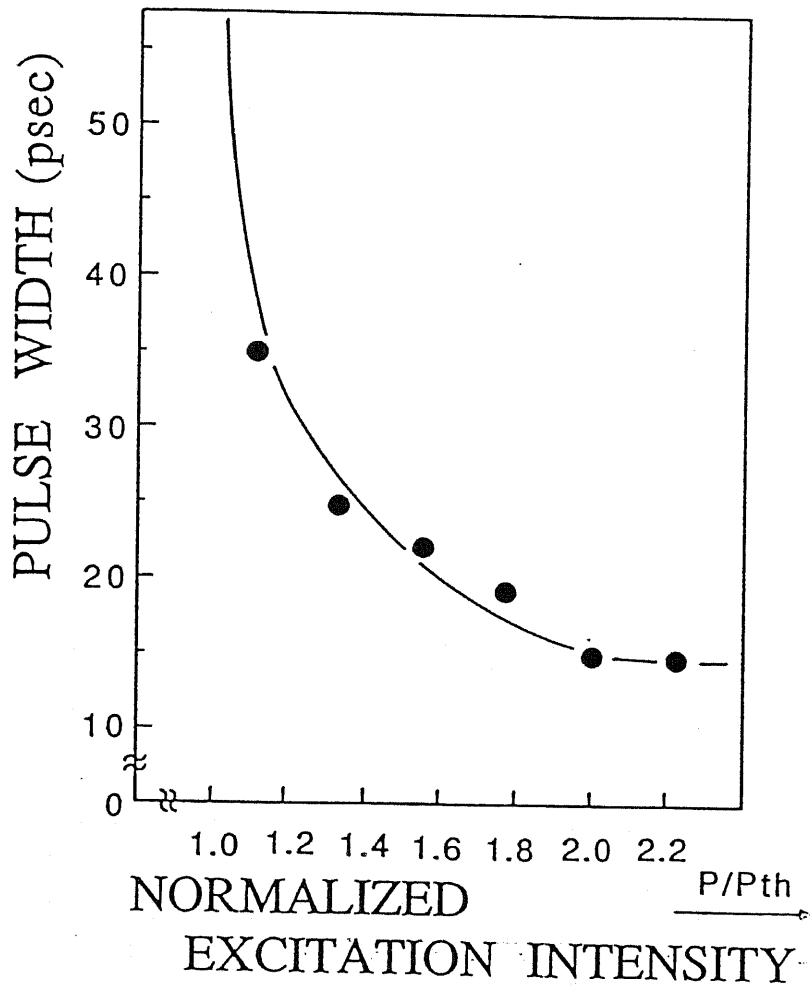


FIG. 2.9 Measured pulse durations as a function of excitation intensity normalized by the threshold intensity.

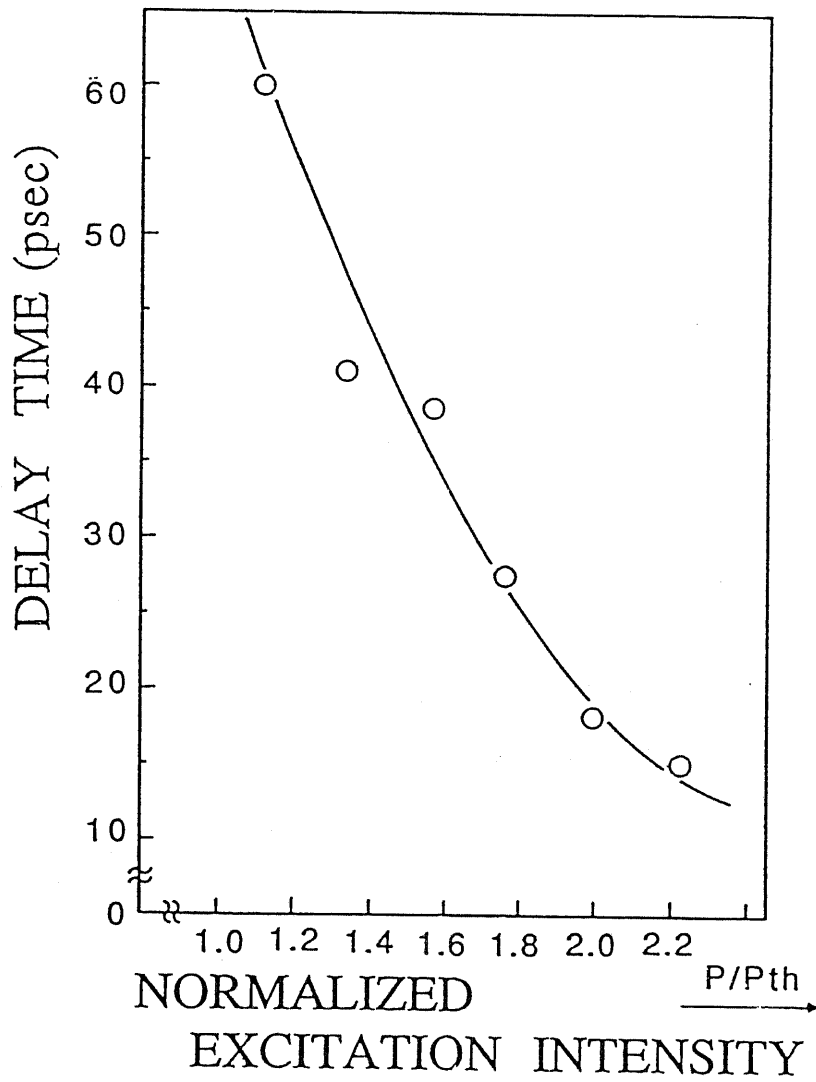


FIG. 2.10 Measured delay time from the excitation peak to the output peak as a function of the normalized excitation intensity.

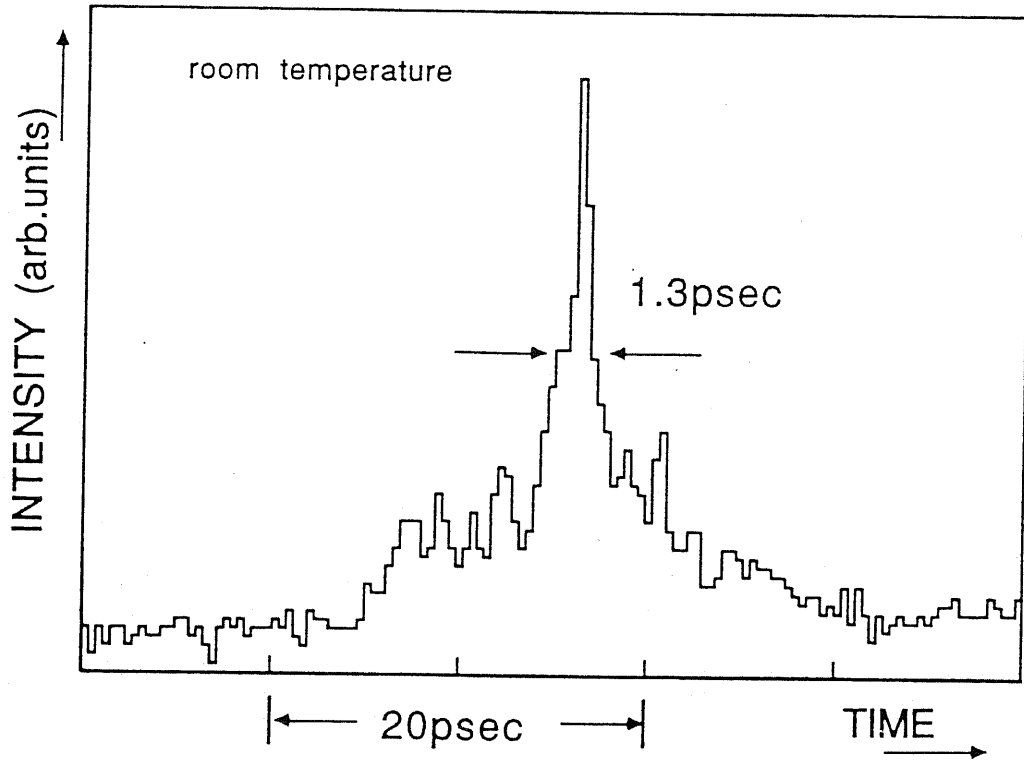


FIG. 2.11 A time-trace of a short light pulse as narrow as 1.3psec from the MQW laser measured by the streak camera. The pumping power is at two times the threshold intensity

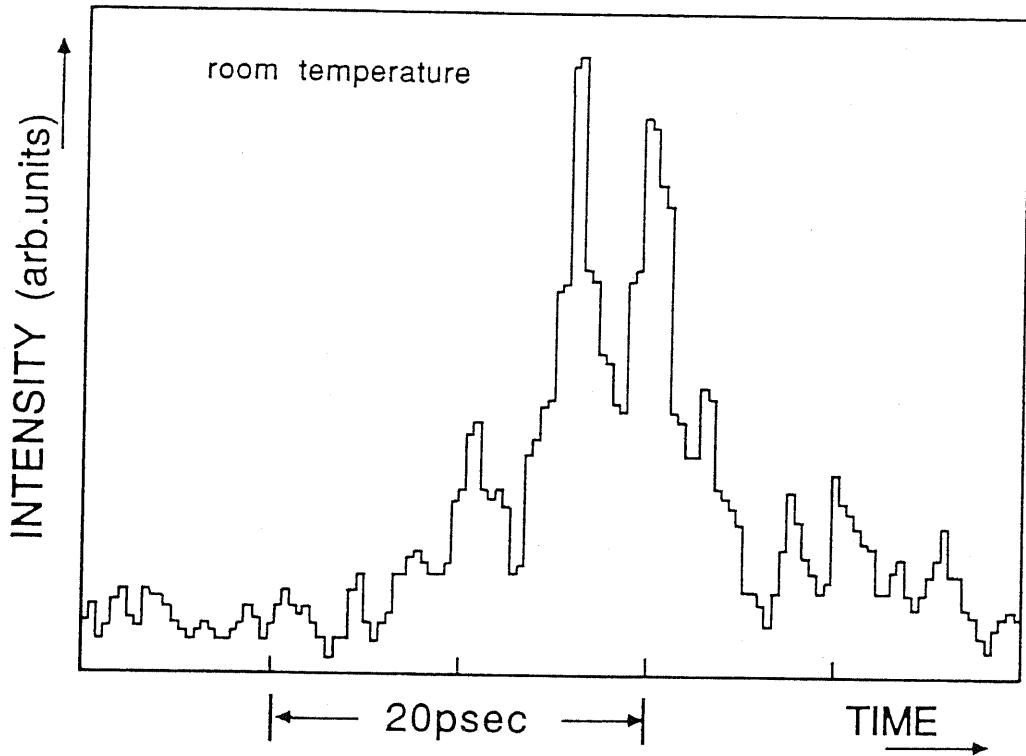


FIG. 2.12 A time-trace of a short light pulse from the MQW laser measured by the streak camera. Repetitive internal reflections of a single emission are observed.

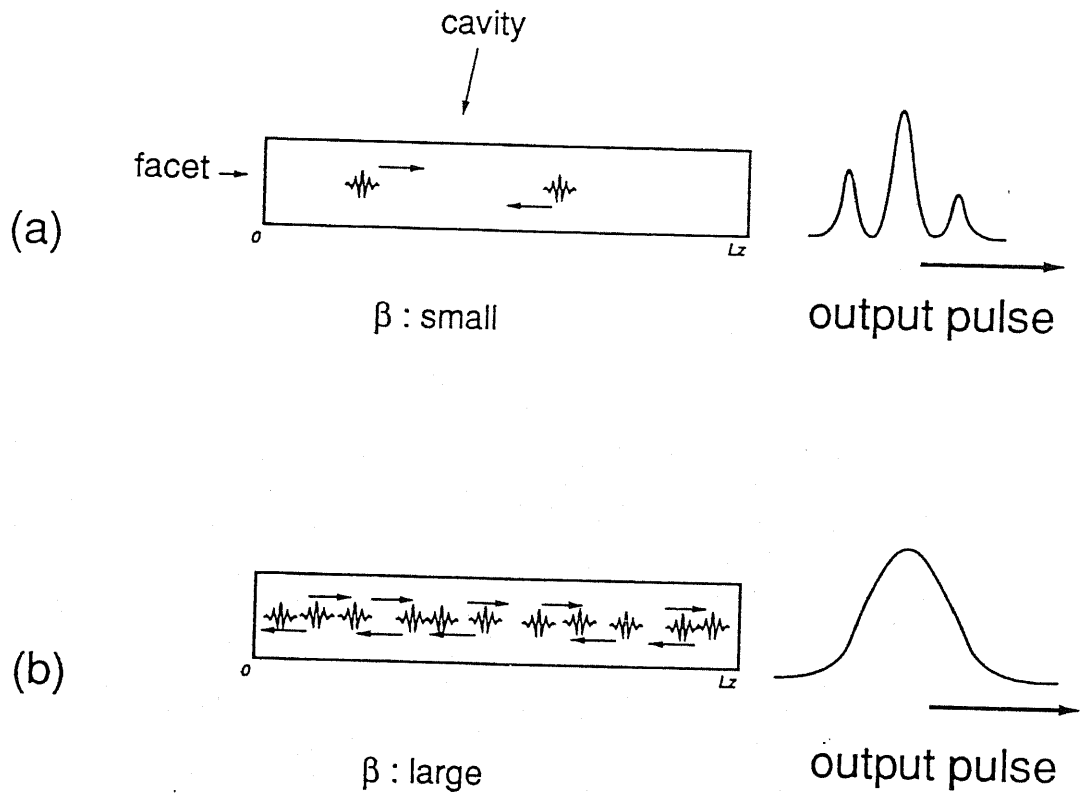


FIG. 2.13 Since $N_{t,t+\Delta t}$ is a random variable, (a) it sometimes occurs that a single wave packet is spontaneously generated without generation of the succeeding wave packets within several picosecond, which leads to significant evolution of only the first wave packet inside the cavity. On the other hand, (b) it also occurs that many wavepackets are generated during 1psec and overlapped, which results in generation of a broad pulse.

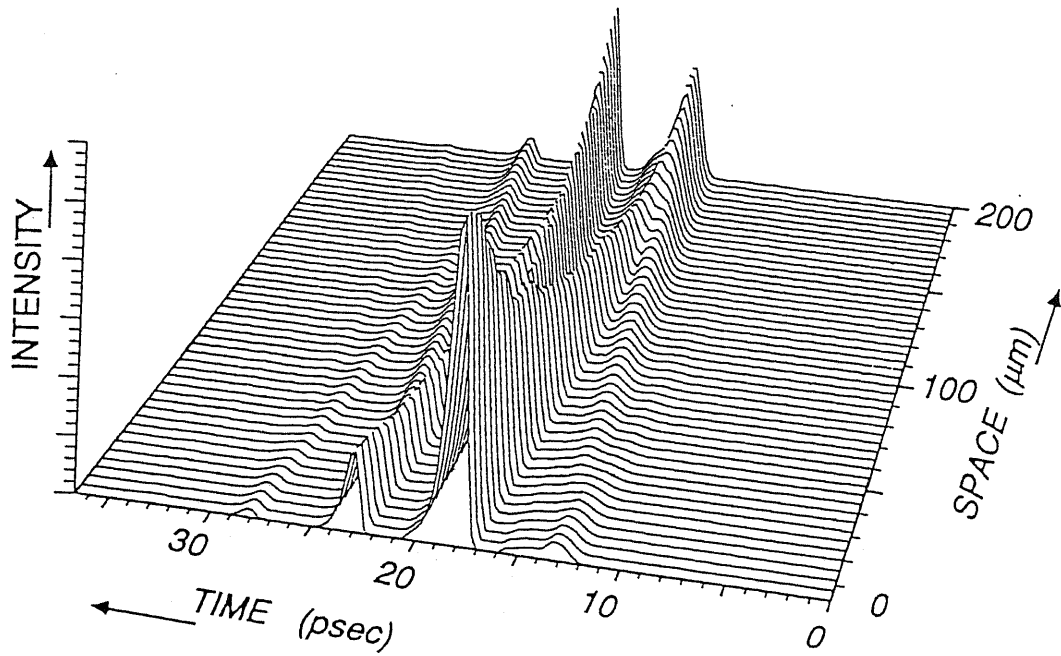
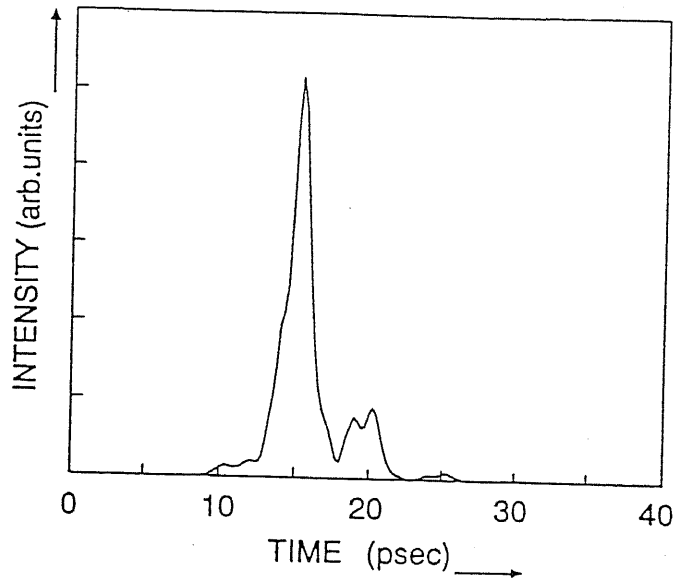
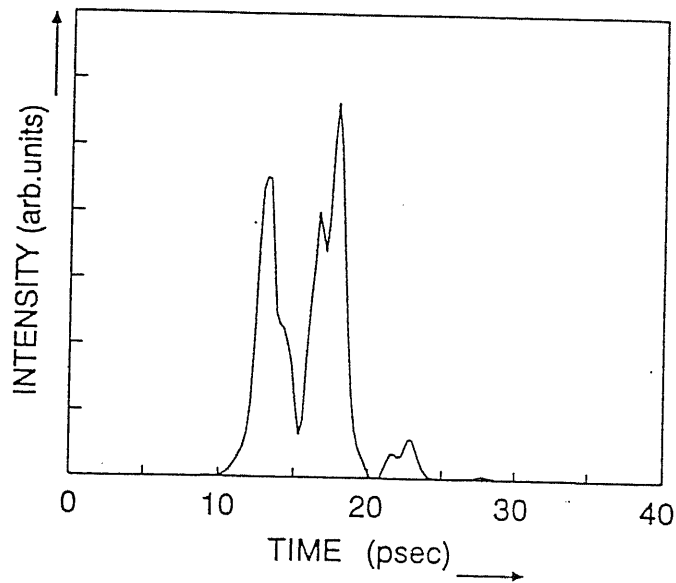


FIG. 2.14 A typical calculated result for the time evolution of the light pulse traveling inside the cavity. The amplification of spontaneously emitted seeds inside the cavity is observed.



(a)



(b)

FIG. 2.15 Two examples of Monte-Carlo simulation result for the output light pulse using spatial-dependent rate equations under the same condition ($\beta = 10^{-5}$). The result indicates stochastic behavior of the output pulse.

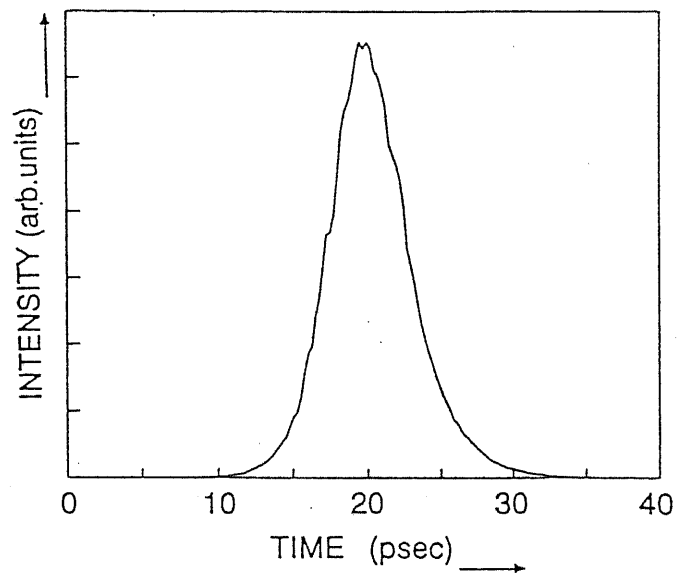


FIG. 2.16 An example of Monte-Carlo simulation result for the output light pulse with $\beta = 5 \times 10^{-4}$.

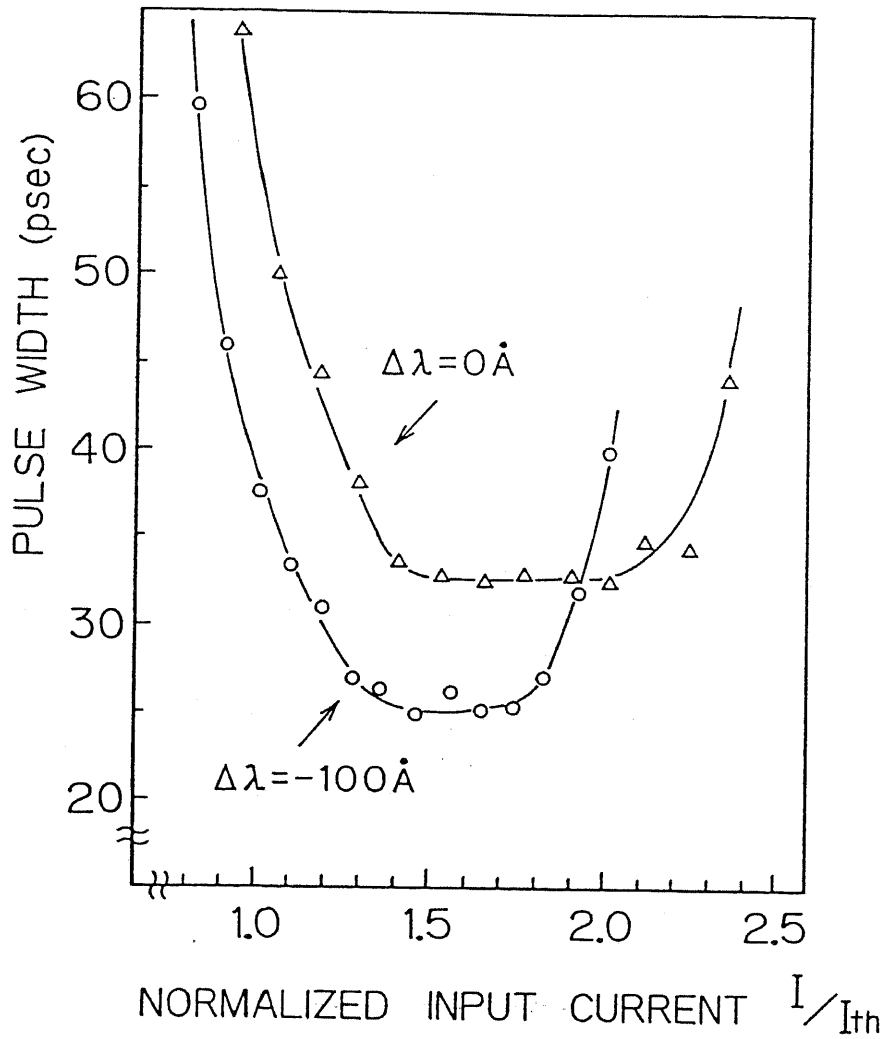


FIG. 2.17 The measured pulse durations of tuned and detuned DFB lasers, plotted against the average input current normalized by each threshold current.

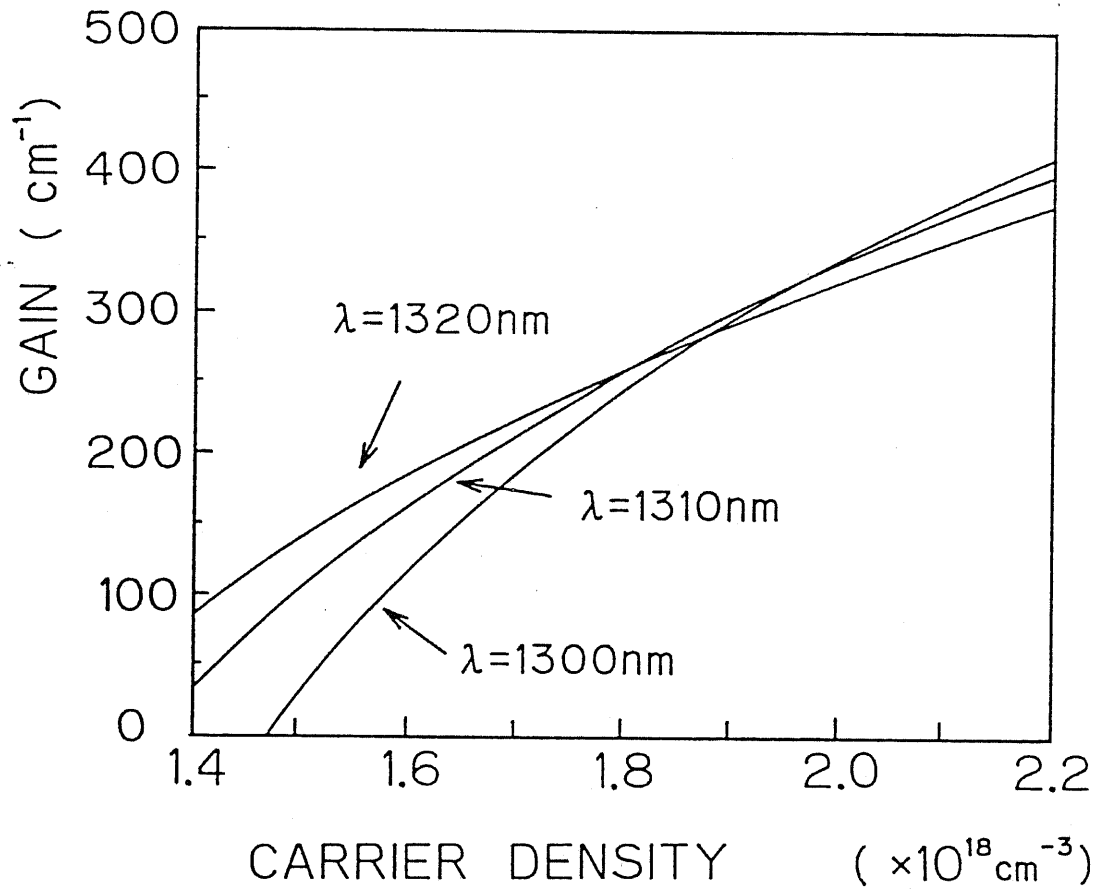


FIG. 2.18 The calculated bulk gain plotted as a function of carrier concentration at various wavelength of 1300, 1310, and 1320nm.

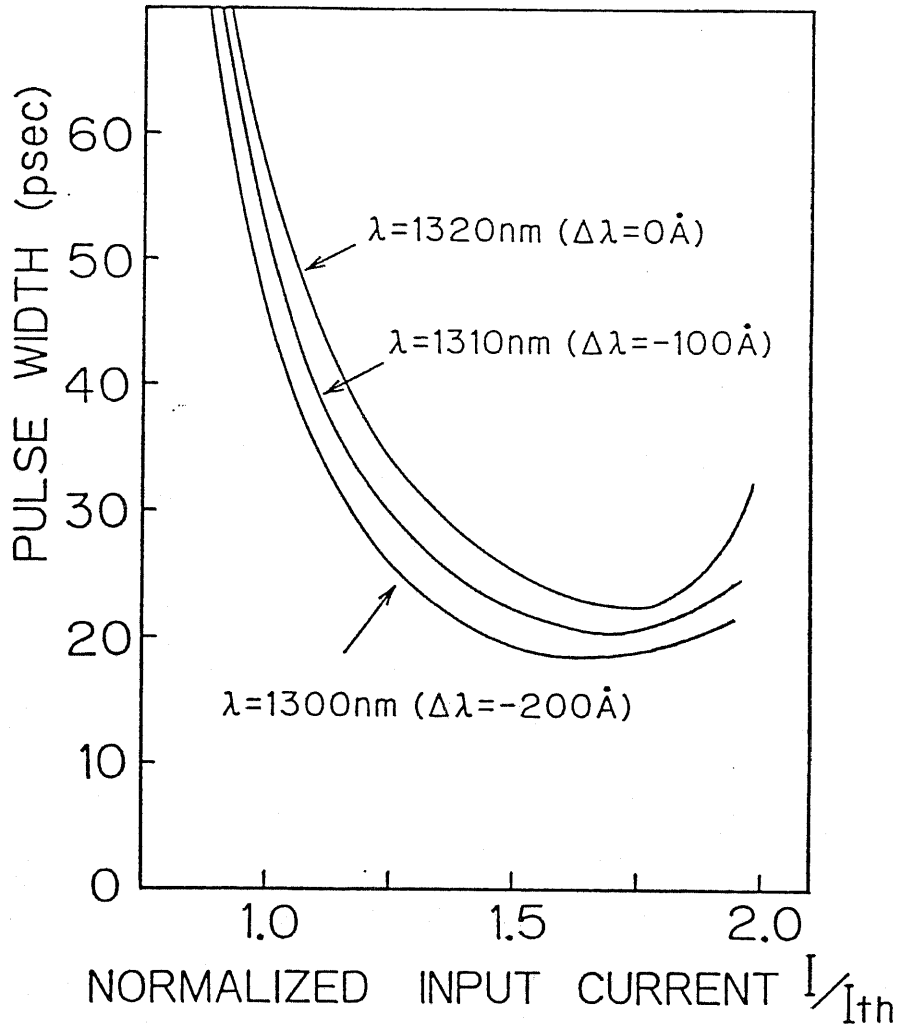


FIG. 2.19 Calculated pulse duration of tuned and detuned (-100Å and -200Å) lasers against average input current normalized by each threshold current.

Chapter III Spectral Dynamics in Gain-Switched Quantum Well Lasers and Its Dependence on Quantum Well Structures

Abstract

Time-resolved spectra of gain-switched GaAs/AlGaAs quantum well (QW) lasers generating picosecond pulses are measured by a streak camera with a monochromator in order to clarify ultrafast lasing dynamics in the wavelength domain. Effects of QW structures such as the number of quantum wells and the barrier thickness on picosecond lasing dynamics are investigated. The results show that both generated pulse forms and dynamic behaviors of lasing spectra strongly depend on the QW structures. In addition, the overflow effect of carriers outside of QWs plays a significant role when the number of QWs is smaller. Theoretical discussions considering dynamic behavior of the gain and the capturing effect of carriers into QWs explain the experimental results well. The significance of two dimensional carrier properties owing to the quantum confinement effects is also demonstrated by comparing the lasing dynamics of an uncoupled QW laser and a coupled QW laser.

§ 3.1 Introduction

For future ultrafast optoelectronic systems such as high speed optical communication systems and optical information processing systems, improvements of high speed properties in semiconductor lasers are highly expected. Picosecond pulse generation technology in semiconductor lasers is important for such applications. To this end, mode locking method [13]-[30], gain switching method [31]-[51] and Q-switching method [52]-[58] have been investigated. In contrast to the mode locking method and the Q-switching method, the gain switching method has the advantage that no external cavity and no sophisticated fabrication technology are required and that the repetition rate can be controlled freely. In §2, it is pointed out that for short pulse generation by the gain switching method the differential gain which is defined by the derivative of gain with respect to carrier concentration plays an significant role [49],[50]. In quantum well (QW) lasers, the differential gain is enhanced by a factor of four compared to conventional double-hetero structure (DH) lasers, leading to improvement of dynamic properties of the semiconductor lasers [70]-[73]. This enhancement is due to the change in the density of states from the parabolic function to the step-like function. In fact, an extremely short pulse as narrow as 1.3 psec is successfully achieved in the QW lasers [51], as described in §2.4.3.

In the gain-switching method, the carrier density at the initial stage of the pulse formation is much higher than the threshold carrier density, which results in multi-mode oscillation in a wide spectral region. In addition, a rapid decrease of carrier density due to the strong stimulated emission causes drastic changes in the spectra. The dynamic behaviors of lasing spectra reveal the transitions of the temporal gain properties in the process of pulse generation. However, the picosecond spectral dynamics of the gain-switched semiconductor lasers have not been sufficiently studied [84].

In this chapter, picosecond lasing dynamics of gain-switched GaAs/AlGaAs QW lasers and its dependence on QW structures are studied by time-resolved spectra measurements.

Firstly, effect of the number of the QWs on the picosecond dynamics is investigated. The results indicate that the pulse duration and spectral width are broadened when the number of QWs is smaller. This mainly results from the differences in the gain profile during the pulse generation due to the difference in the carrier concentration per well (cm^{-2}). Theoretical analysis on the basis of the multi-mode rate equations considering carrier capture process is also carried out, which is consistent with the experimental results.

Secondly, dependence on the barrier thickness is clarified by comparing the lasing dynamics of a coupled QW laser with that of

an uncoupled QW laser. The results indicate that in the uncoupled quantum well lasers, extremely short pulse (<2 psec) is generated, while the pulse duration is about 10 psec in the coupled QW lasers in which the two-dimensional confinement effect is reduced owing to the mini-band formation.

§ 3.2 Dependence of the Number of Quantum Wells

3.2.1 *The Number of Quantum Wells*

Narrow carrier distribution due to the step like density of states in QW improves lasing characteristics such as threshold current density [63]-[66], temperature dependence of threshold current [67]-[69], and dynamic properties [70]-[74], which strongly depend on the designs of QW structure. The number of QWs is important to achieve lower threshold current density [71]. There is an optimum number of QWs which satisfies the given threshold modal gain condition by the lowest current density. In the gain-switching method, the carrier density at the initial stage of the pulse formation is much higher than the threshold condition, resulting in multi-mode oscillation in a wide spectral region. In addition, a rapid decrease of carrier density due to the strong stimulated emission causes drastic changes in the spectra. Therefore, dynamic gain spectra play an important role in the process of pulse generation.

Figure 3.1(a) illustrates a calculated bulk gain of QW lasers with 70 Å wells, plotted as a function of wavelength (or photon energy) for various carrier densities. Double peaks appearing at the first quantum level are due to separation of the light hole energy level and the heavy hole energy level. When we discuss the lasing condition, a modal gain g_{mod} which is given by the bulk gain g_{bulk} multiplied by the optical confinement factor Γ (i.e., g_{mod}

$=\Gamma g_{bulk}$) is important. The modal gain profiles can be modified by varying the number of QWs. Suppose that the total number of carriers excited in the whole active region is the same. The carrier density (cm^{-2}) in each well is smaller in QW lasers with larger N_{QW} , where N_{QW} is the number of the QWs. As a result, the gain profile becomes narrower, as illustrated in Figure 3.1(b). On the other hand, if N_{QW} is small, the gain profile is much broadened. This is due to the fact that the gain flattening effect resulting from the step-like density of states occurs in the QW lasers with extremely high quasi-Fermi energy level, as illustrated in Figure 3.1(c). Moreover, this leads to reduction of the differential gain.

3.2.2 *Experimental Procedure*

In our experiment, we prepared two GaAs/AlGaAs multi quantum-well (MQW) lasers grown by the MOCVD system. Both samples consist of 50 Å GaAs QWs separated by 50 Å AlGaAs barriers; One has 16 QWs (MQW16) and the other has 4 QWs (MQW4). The band-diagrams are illustrated in Figs.3.2 (a) and (b), respectively. The cavity length is about 200 μm for both samples. Short light pulses are generated from the QW lasers which are gain-switched by the optical pumping pulses coming from a dye laser (20 psec, 7000 Å, 1 nJ) excited by a Nd^+ -YAG laser [49]. The optical pumping method makes the excitation of carriers free from

the electrical RC time constant problem. As shown in Fig.3.2, the photon energy of the dye laser pulse (1.77 eV) is a little higher than that of the $\text{Al}_{0.17}\text{Ga}_{0.83}\text{As}$ optical confinement layer (1.64 eV). The total thickness of the optical confinement layer and the QW active layer is the same ($\sim 2000 \text{ \AA}$) for both lasers. The total absorption in the active layer P_{ab} is given as follows:

$$P_{ab} = [1 - \exp\{-\alpha_{QW}L_{QW}N_{QW} - \alpha_{\text{AlGaAs}}(L_{SCH} - L_{QW}N_{QW})\}]P_{input} \quad (3.1)$$

, where α_{QW} and α_{AlGaAs} are the absorption coefficient in the QW and in the AlGaAs ($x=0.2$) barrier and the optical confinement layers, respectively, L_{QW} is the well thickness, N_{QW} is the number of well, and L_{SCH} is the total thickness of the optical confinement layer. Equation (3.1) indicates that the calculated total absorption efficiency in MQW16 and MQW4 at the pumping photon energy of 1.77eV is 34.3% and 28.1%, respectively, that is, the total number of carriers excited in the active region is almost the same for both lasers. As a result, the carrier density per cm^{-2} (or quasi-Fermi-energy level of electrons E_{Fc}) of MQW4 is much higher than that of MQW16.

3.2.3 *Measurement of Pulse Forms and Time-Resolved Spectra*

Figures 3.3 (a) and (b) show typical results of the observed pulse forms of MQW16 and MQW4 under the same excitation condition, respectively, using a streak camera (Hamamatsu C1587 + M1952) without monochromator. To improve time resolution, the single-shot mode was used in the streak camera, resulting in the time resolution of about 1.5 psec. The estimated pulse duration of MQW16 based on the results in Fig.3.2 was less than 2 psec, while that of MQW4 was larger than 10 psec. Threshold excitation intensity is reduced in MQW4 by a factor of 2 compared to MQW16. Therefore, the normalized excitation intensity, which is defined as the excitation intensity divided by the threshold intensity, is much higher in MQW4. However, the pulse duration of MQW4 is much wider compared to MQW16, although it is commonly believed that higher excitation intensity leads to shorter pulse generation [49]. These results suggest that the pulse form should be discussed considering the dynamic behavior of spectra which strongly depend on the number of QWs.

Time-resolved spectra were measured by the streak camera with a monochromator. Figures 3.4 (a) and (b) show measured spectra of MQW16 and MQW4, respectively, indicating multi-mode lasing oscillations as well as a drastic change in picosecond spectra. The lasing oscillation starts in the shorter wavelength

region and the peak of the spectra shifts to longer wavelengths in the process of short pulse formation. In particular, in MQW4, the lasing oscillation occurs with more longitudinal modes and a bigger shift of the peak wavelength compared to MQW16. In addition, as discussed above, pulse duration of MQW4 is much larger than MQW16.

3.2.4 Discussion

The strong dependence of picosecond lasing dynamics on the number of QWs is attributed to the difference in the gain profile of the lasers. In addition, the overflow effect of carriers outside of the QWs is also a significant mechanism. If the number of QWs N_{QW} is large, excited carriers are relaxed immediately into QWs, resulting in the normal carrier distribution. In this case the broadening of the gain profile is suppressed keeping a high modal gain peak, because the density of states is large [as shown in Fig.3.5 (a)]. This leads to a smaller number of longitudinal mode whose gain is bigger than the threshold, resulting in suppressed broadening of the lasing spectra. On the other hand, smaller N_{QW} results in broad gain spectra, as shown in Fig.3.5 (b). In addition, since only the first quantum level exists and the barrier height of the $Al_{0.17}Ga_{0.83}As$ layers is relatively lower in the QW lasers used in our experiment, extremely strong excitation causes the overflow effect of carriers

out of QWs. This overflow effect reduces the maximum gain achieved by the rapid excitation. In addition, the capture process of carriers into QWs from AlGaAs layers also affects the dynamic gain properties of QW lasers.

To discuss our experimental result more quantitatively, lasing characteristics considering the dynamic gain properties are analyzed on the basis of multi mode rate equations which are described by the following equations; Eqs.(3.2) and (3.3) represent dynamics of photon density P_i ($i = 1, 2, \dots$) for each longitudinal mode and the carrier density n , respectively,

$$\frac{dP_i}{dt} = \Gamma c_g g_i P_i - \frac{P_i}{\tau_p} + \beta_i \frac{n}{\tau_s} \quad (3.2)$$

$$\frac{dn}{dt} = N_{pump} - c_g \sum_i g_i P_i - \frac{n}{\tau_s} \quad (3.3)$$

, where τ_s is the carrier lifetime, τ_p is the photon lifetime, c_g is the group velocity of light, Γ is the optical confinement factor, g_i is the bulk gain as a function of wavelength λ_i and carrier density n [i.e., $g_i = g(\lambda_i, n)$], and β_i is the spontaneous emission coefficient. In this calculation, it is assumed that β_i ($=1 \times 10^{-5}$) is the same for all longitudinal modes. N_{pump} is the increasing rate of carrier density

inside the QWs pumped through relaxation of hot carriers generated by the dye laser. To estimate N_{pump} both the carrier overflow effect and capture of carriers into the QWs should be considered.

$$\frac{dn_b}{dt} = -\frac{n_b}{\tau_{cap}} + R_{pump} \quad (3-4)$$

$$N_{pump} = \frac{n_b}{\tau_{cap}} \quad (3-5)$$

, where n_b is the carrier density for the AlGaAs layers, R_{pump} is the pumping rate of carriers by the excitation, and τ_{cap} is the decay time of overflowing carriers due to the capture process including cooling process of carriers. Though the value of τ_{cap} slightly depends on carrier density, excess energy of excited carriers, and QW structures [85]-[88], it is assumed here to be constant for this brief discussion about lasing dynamics.

Figures 3.6 (a) and (b) are calculated results of spectral dynamics of MQW16 and MQW4, respectively when the total carriers excited in the active region is the same. This result clearly indicates that spectral broadening is enhanced with the increase of carrier density and the pulse duration of MQW16 is shorter than MQW4, which is consistent with observed spectral dynamics and

its dependence on the number of QWs in our experiment. The results indicate that the overflow effect is sensitive to the pulse duration as well as the spectral broadening. It is found that τ_{cap} is ~ 3 psec to explain our experimental results. Note that τ_{cap} is usually much longer than the intraband dephasing time [85]-[97]. Details of the capture phenomena will be discussed in § 6.

In summary, we measured dynamic spectra and the pulse form of QW lasers with different number of QWs. The results revealed that the dynamic spectra as well as the pulse form is affected by the number of QWs. These results can be explained by considering the changes in the gain properties due to the band filling and carrier overflow effects.

§ 3.3 Dependence of the Barrier Thickness

3.3.1 *Coupled QW and Uncoupled QW*

Figures 3.7 (a) and (b) are schematic illustrations of the carrier distributions in an uncoupled QW and a coupled QW. In the coupled QW lasers, the formation of the mini-band causes disappearance of the clear step configuration in the density of states near the equivalent band edge. Inset table in Fig.3.7 shows the energy band width of the first mini-band for electron and heavy hole at the room temperature when the GaAs well thickness is 70 Å and Aluminum content of the AlGaAs barrier layers is 0.2. When barrier thickness is 70 Å, mini-band energy width for the electron is 5 meV. If the barrier thickness is thinner than 30 Å, the mini-band energy width becomes broader than 30 meV. On the other hand, if the mini-band energy width is comparable or less than the energy broadening caused by the intraband carrier relaxation (typically several meV), the two dimensional carrier properties are maintained [98],[99]. As indicated in Fig.3.7 (b), the wavelength of the gain peak shifts to shorter wavelengths with the increase of carrier density. This shift results from the bulk like gain properties which have the dependence of gain peak wavelength on the carrier density. Thus, the gain properties of QW lasers can be controlled from a bulk like gain to a complete two dimensional gain by varying the barrier thickness.

3.3.2 *Experimental Procedure*

We prepared two GaAs/AlGaAs QW lasers grown by a metal organic chemical vapor deposition (MOCVD) system; one has ten 70 Å uncoupled QWs (AlGaAs_(x=0.2) barrier thickness is 100 Å), and the other has ten 70 Å coupled QWs (AlGaAs_(x=0.2) barrier thickness is 30 Å), as illustrated in Figs.3.8 (a) and (b). The gain switching is realized by an optically pumping method using dye laser pulses (7000 Å, 15 psec), which enable the excitation of carriers even in the uncoupled QWs. Time-resolved spectra were measured by a streak camera (Hamamatsu C1587 + M1952) in front of which a monochromator is placed. The measurement of dynamic behaviors of lasing spectra reveals the transition of the temporal gain properties in the process of pulse generation which causes drastic reduction of carrier density due to strong stimulated emission.

3.3.3 *Measurement of Pulse Durations and Time-Resolved Spectra*

Figures 3.9 (a) and (b) show the time-resolved spectra of the uncoupled QW laser and the coupled QW laser, respectively, when excitation intensity is as 1.5 times as threshold intensity. In the uncoupled QW laser, the peak wavelength of lasing spectra does not change during the pulse generation, as shown in Fig.3.9 (a). On the other hand, Fig.3.9 (b) shows that dramatic shift of spectra toward

longer wavelengths occurs in the coupled QW laser. This shift is much larger than that caused by the chirping. These differences in the spectral behaviors between the uncoupled QW laser and the coupled QW laser are attributed to the differences in the gain properties near the equivalent band edge, as illustrated in Figs.3.7. These effects clearly appear when the lasing oscillation occurs near the equivalent band edge, which is important for short pulse generation, as discussed in §3.2. In fact, there are no clear difference between the spectral dynamics achieved in an uncoupled QW laser and a coupled QW laser which have four QWs. It is due to the fact that the modification of the density of states near equivalent band edge through the coupling does not have significant influence on the lasing condition which is satisfied by the high quasi-fermi energy level E_{Fc} .

In our experiment, as shown in Fig.3.9, the pulse duration achieved in the coupled QW laser is longer since its pulse shape has a tail structure due to the spectral shift. In this measurement, however, the time-resolution is about 10 psec because of the time broadening caused by the monochromator. The generated pulse forms from the uncoupled QW laser and the coupled QW laser were measured by the streak camera without monochromator, as shown in Figs.3.10 (a) and (b). In the uncoupled QW laser, a short pulse less than 2 psec (F.W.H.M.) is generated. Moreover, this pulse generation is completed within 20 psec and the pulse form has no tail structure. The measured pulse duration is determined by the

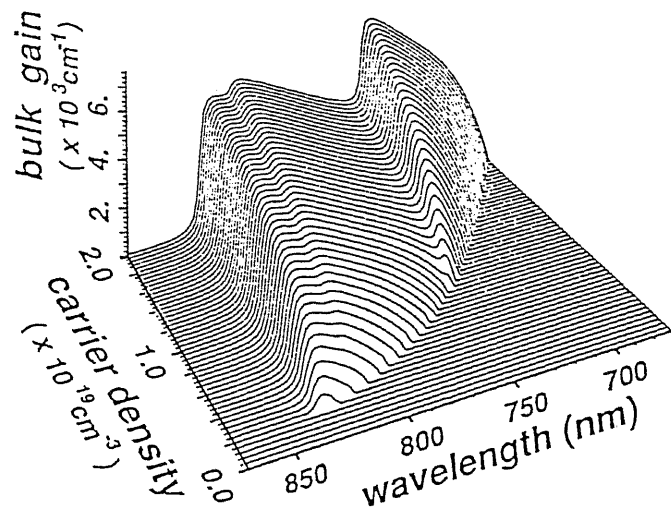
time resolution of our streak camera. On the other hand, in the coupled QW laser, pulse duration becomes much longer. The shift of the lasing wavelength during the pulse generation reduces the efficient stimulated emission, resulting in longer pulse generation.

§ 3.4 Concluding Remarks

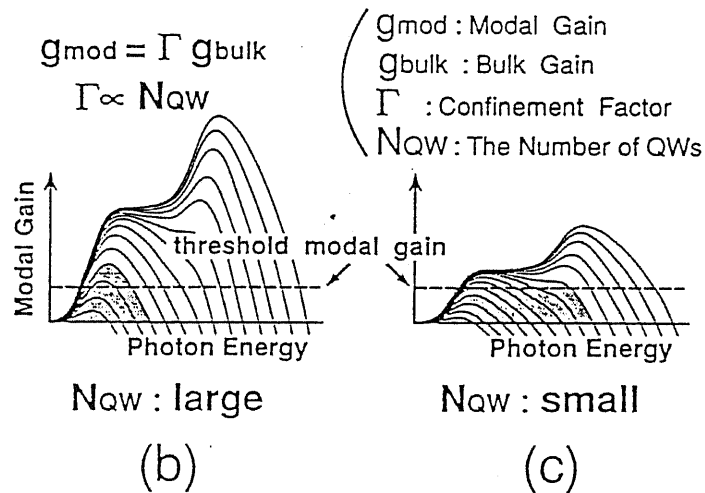
We discussed picosecond lasing dynamic of gain-switched QW lasers and its dependence on the number of QWs and the barrier thickness.

We measured dynamic spectra and the pulse forms of QW lasers with different number of QWs. The spectral dynamics as well as the pulse form is strongly affected by the number of QWs, that is, the pulse duration and spectral width are broadened when the number of QWs is smaller. On the other hand, the larger number of QWs leads to shorter pulse generation with narrower spectra. These mainly result from the differences in the gain spectra during the pulse generation due to the difference in the carrier concentration per well (cm^{-2}). Theoretical analysis on the basis of the multi-mode rate equations which consider the capture process of overflowed carriers explains our results well.

The dependence on the barrier thickness is clarified by comparing the lasing dynamics of a coupled QW laser with that of an uncoupled QW laser. In the uncoupled quantum well lasers, extremely short pulse (<2 psec) is generated, while the pulse duration is about 10 psec in the coupled QW lasers in which the two-dimensional confinement effect is reduced owing to the mini-band formation. These results demonstrate the significance of low dimensional carrier properties in QW structures for short pulse generation.



(a)



(b)

(c)

FIG. 3.1 (a) Calculated bulk gain profiles of QW lasers with 70\AA wells, plotted as a function of wavelength (or photon energy) for various carrier densities. When we discuss the lasing condition, a modal gain g_{mod} which is given by the bulk gain g_{bulk} multiplied by the optical confinement factor Γ (i.e., $g_{mod} = \Gamma g_{bulk}$) is important. (b), (c) If the total number of carriers excited in the active region is the same, the gain profile of the quantum well laser with small number of wells is much broader compared to that of the laser with larger number of wells.

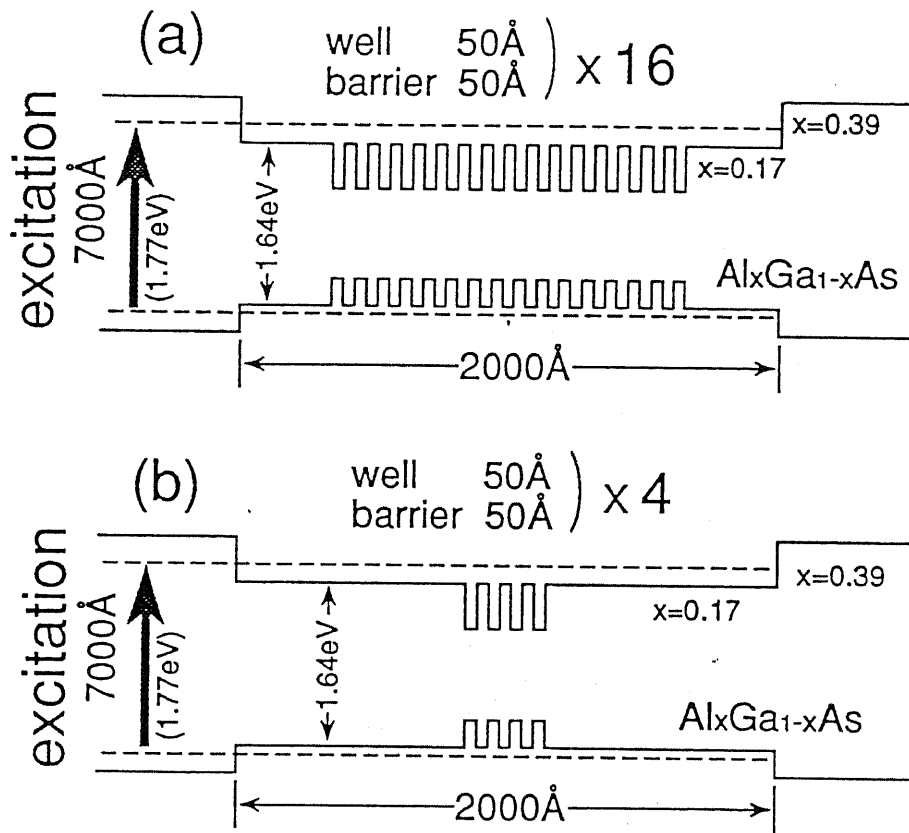


FIG. 3.2 Band diagram for the multi-quantum well (MQW) lasers with (a) 16 QWs (MQW16) and (b) 4 QWs (MQW4).

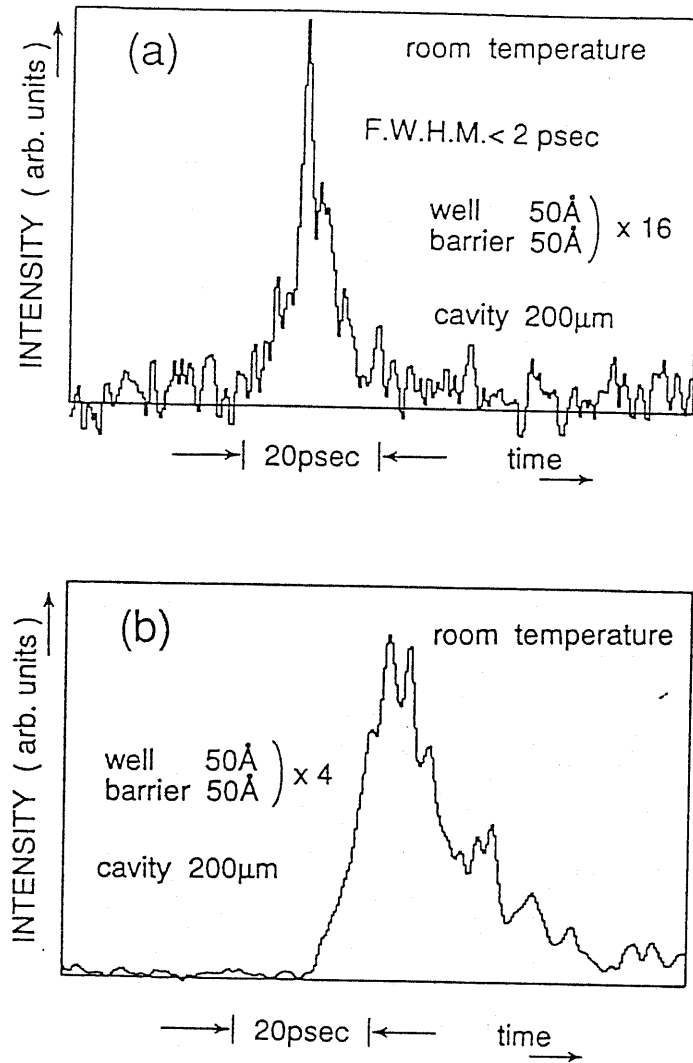


FIG. 3.3 Generated pulse forms measured by a single-shot streak camera; (a) 16 QWs (MQW16) and (b) 4 QWs (MQW4).

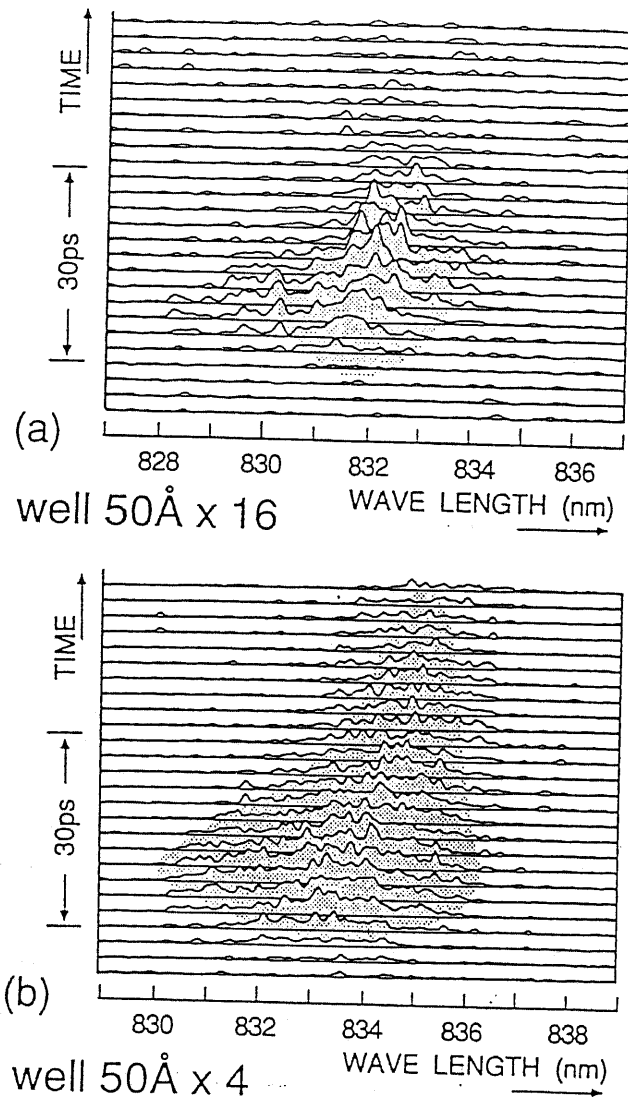


FIG. 3.4 Time-resolved spectra of gain-switched quantum-well lasers with (a) 16 QWs (MQW16) and (b) 4 QWs (MQW4).

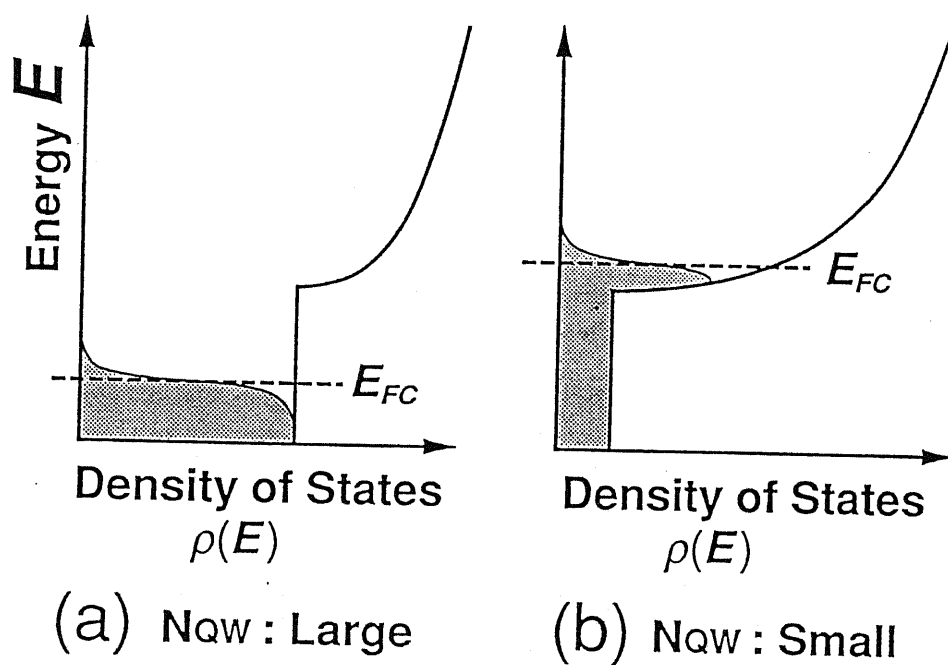


FIG. 3.5 Illustration of carrier distribution in the quantum well laser with (a) a large number of QWs and (b) with a small number of QWs.

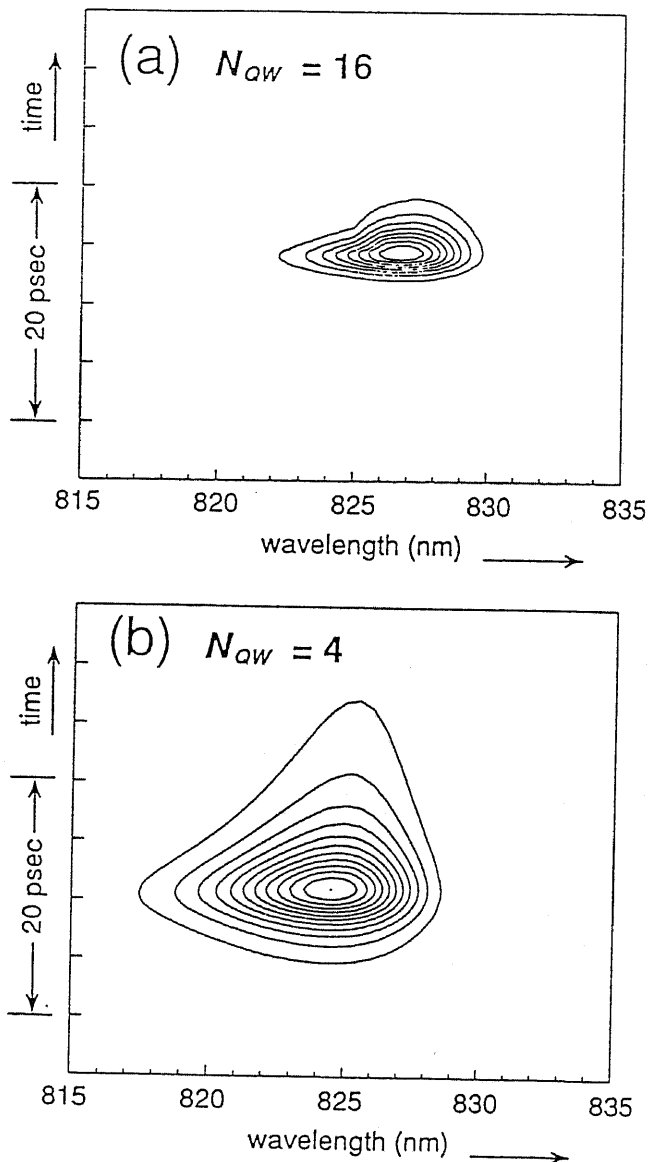
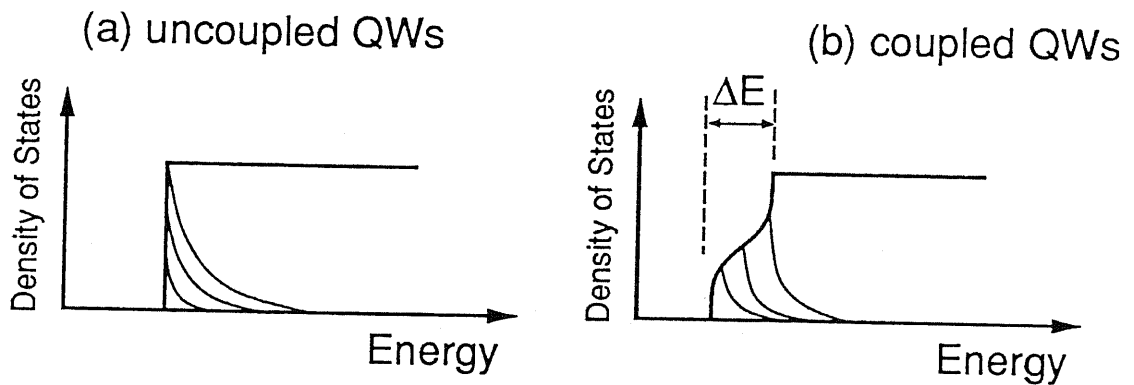


FIG. 3.6 Calculated spectral dynamics of quantum-well lasers with a different number of QWs when the excitation intensity is the same (i.e., carrier density per well n_0 multiplied by the number of QWs N_{QW} is the same); (a) the number of wells N_{QW} is 16 and excited carrier density n_0 is $1.75 \times 10^{12} \text{cm}^{-2}$, and (b) N_{QW} is 4 and n_0 is $7.0 \times 10^{12} \text{cm}^{-2}$.



well 70Å
 barrier
 AlGaAs x=0.2

ΔE : mini-band energy gap

| barrier | ΔE_e | ΔE_{hh} |
|---------|--------------|-----------------|
| 100Å | 1.4meV | ~0meV |
| 70Å | 5.0meV | 0.1meV |
| 30Å | 29meV | 0.5meV |
| 20Å | 45meV | 2.0meV |

FIG. 3.7 Schematic illustrations of carrier distributions in (a) uncoupled QWs and (b) coupled QWs. An inset table shows the energy band width of the first mini-band for electron and heavy hole at the room temperature when the GaAs well thickness is 70Å and Aluminum content of the AlGaAs barrier layers is 0.2.

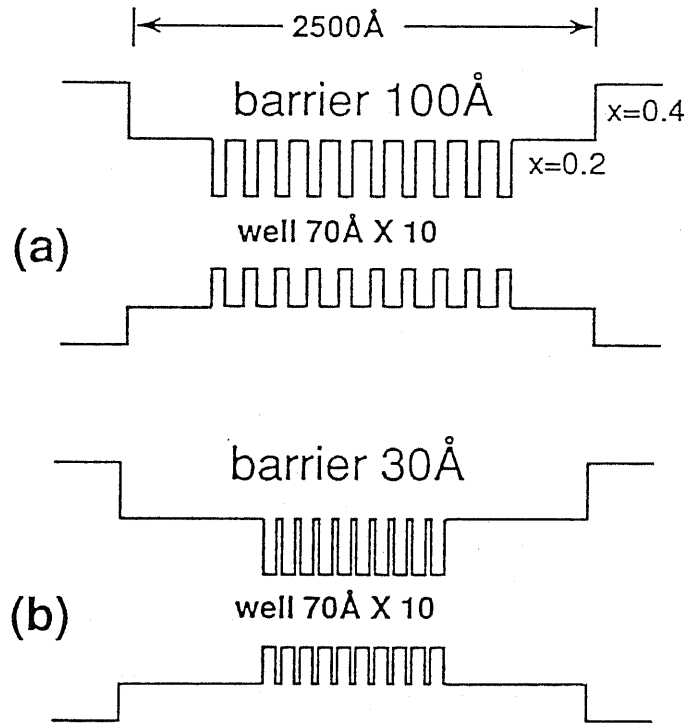


FIG. 3.8 Band diagram for the multi-quantum well (MQW) lasers with (a) uncoupled QWs (barrier thickness is 100 Å), and (b) coupled QWs (barrier thickness is 30 Å).

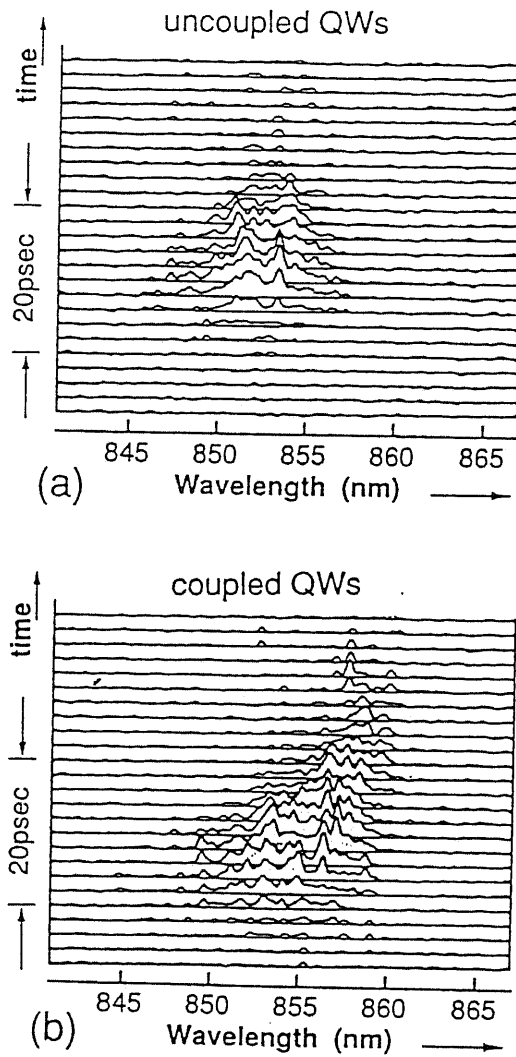


FIG. 3.9 Time-resolved spectra of gain-switched QW lasers (a) with uncoupled QWs and (b) coupled QWs measured by a streak camera together with a monochromator.

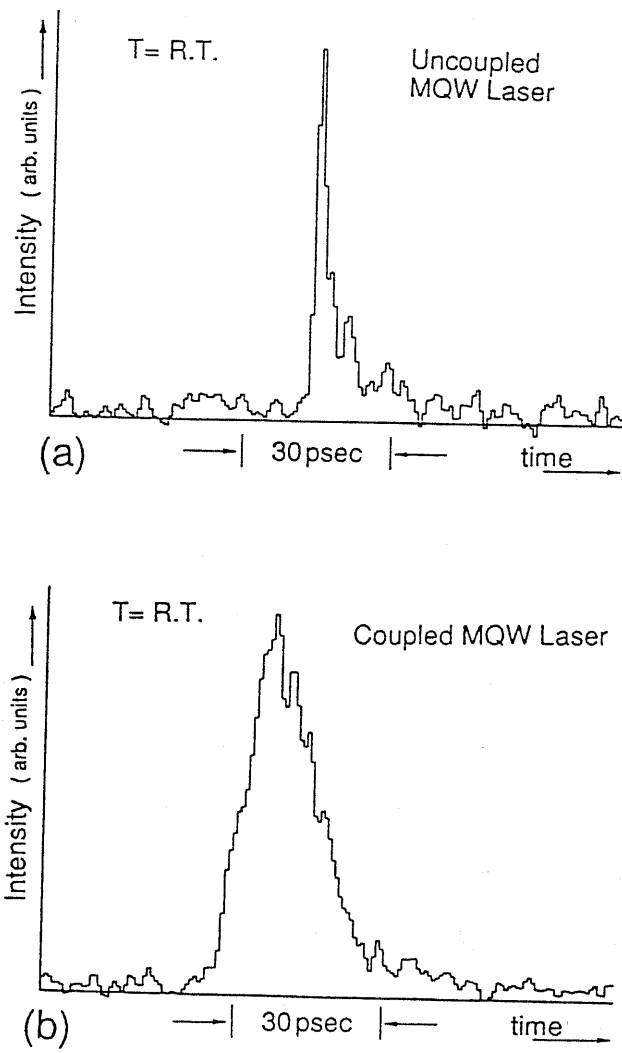


FIG. 3.10 Temporal characteristics of the gain-switched QW lasers (a) with uncoupled QWs and (b) coupled QWs measured by a streak camera.

Chapter IV Repetitive Gain-Switching Characteristics in Quantum Well Lasers

Abstract

Repetitive pulse generation with an extremely short interval of 16 psec is successfully achieved in quantum well lasers through an optically-pumped gain-switching method. This short interval pulse generation is due to the high photon density condition. The significance of two-dimensional quantum confinement for high bit rate short pulse generation is also demonstrated by comparing a coupled and an uncoupled QW lasers. Frequency characteristics of the gain-switching operation is theoretically discussed in comparison with that of the small signal modulation.

§ 4.1 Introduction

For the purpose of ultrafast optical communication systems and optical information processing systems, high-speed performance of semiconductor lasers such as high repetition rate short pulse generation and high frequency modulation is highly expected. It is well known that quantum well (QW) lasers have superior properties as to the high frequency modulation and short pulse generation due to the high differential gain property, which is enhanced by a factor of four compared to conventional double hetero-structure lasers, in two dimensional carrier systems [49],[70].

$$\Delta\tau = \tau_p + \frac{1}{c_g g' n_0} \quad (4.1)$$

$$f_r = \frac{1}{2\pi} \sqrt{\frac{P g'}{\tau_p}} \quad (4.2)$$

As described in Eqs.(4.1) and (4.2), generated pulse duration by the gain switching method $\Delta\tau$ and relaxation oscillation frequency f_r are expressed by these formulas on the basis of conventional rate equations. Eq.(4.2) indicates that f_r is proportional to the square root of the photon density multiplied by the differential gain g' . The most important material parameter for both short pulse generation and high speed modulation is the differential gain. Effects of the

enhanced differential gain on the short pulse generation are demonstrated in §2 and §3. Since high relaxation oscillation characteristic is a required performance for the high bit-rate operation, many works on relaxation oscillation characteristics and modulation band width of semiconductor lasers have been investigated [100]-[108]. The highest relaxation oscillation frequency so far achieved is 30 GHz in a p-type modulation doped QW laser, resulting from the highly enhanced differential gain due to p-type modulation doping in QWs [74].

The gain switching is in principle realized by the simple direct current modulation. As illustrated in Fig.4.1, the small-signal direct modulation uses the linear region of the I-L characteristics and light output is sinusoidally modulated. On the other hand, the gain switching method utilizes the nonlinearity of I-L characteristics around the threshold and produces short pulses with high peak power. In the small signal modulation, the maximum operation frequency is strongly related to the f_r , which depends on operation conditions such as modulation intensity and bias condition as well as device structures. In direct current modulation larger modulation intensity leads to lower f_r . and often causes complicated behaviors in light outputs such as period doubling and multiple spikes [107],[108]. The gain switching is the similar method to the extremely large-signal modulation. Therefore, it is significant to investigate frequency characteristics of the gain switching operation and to clarify the differences from the small-signal modulation.

In this chapter, in order to experimentally investigate the maximum bit rate of the gain-switching operation, optically pumped repetitive gain switching is realized. As a result, repetitive pulse generation with an extremely short interval of 16 psec is successfully achieved in the quantum well lasers. The significance of improved gain properties owing to the two-dimensional quantum confinement for high bit rate short pulse generation is also demonstrated by comparing a coupled QW laser and an uncoupled QW laser. Frequency response of the gain-switching operation is also theoretically discussed in comparison with that of the direct modulation.

§ 4.2 Experimental Procedure

In order to investigate the inherent high-speed characteristics of the MQW laser freely from the RC charging time, we adopted an optical pumping method using picosecond dye laser pulses pumped by a mode-locked Nd⁺-YAG laser. Two pumping pulses are used to excite the QW laser and subsequently modulate the carrier density, as shown in Fig.4.2. One is delayed by an optical delay stage, and the intensity of the second pumping pulse is controlled by a neutral density filter. The excitation wavelength is 7000 Å and the pulse duration is 15 psec. Temporal characteristics of modulated light output were measured by a streak camera together with a monochromator whose time resolution is about 10 psec.

In our experiment, we prepared a GaAs/AlGaAs MQW laser, which has ten 70 Å wells. We adopted 100 Å thick barriers in order to obtain the complete two dimensional carrier properties which is essentially important for shorter pulse generation as discussed in §3.3. And the number of wells is ten because the larger number of wells leads to lower quasi fermi energy level, as discussed in §3.2. In this case, the steep configuration of the density of states near the equivalent band edge is effectively utilized and the enhancement of the differential gain is achieved.

§ 4.3 Repetitive Gain-Switching Characteristics

4.3.1 Temporal Characteristics

Temporal characteristics of modulated light outputs under various pumping conditions are measured. Figure 4.3 shows the time trace of the modulated light output from the QW laser measured by the streak camera. The intensity of the first pumping pulse is twice as large as the threshold intensity. The second pumping pulse is introduced just after the first oscillation. The intensity of the second pumping pulse is controlled by a neutral density filter so as to adequately compensate the decreased carriers. In this case, the time interval from the first oscillation to the second one is 16 psec. Output power is about 30 pJ at 4.1 MHz pumping rate. If continuous operation is assumed, average output power becomes several hundred mW. This high repetition characteristic is attributed to the extremely high photon density condition.

For this high repetition characteristic the improvement of the gain properties due to the quantum confinement effects also plays an important role. In order to investigate the two dimensional effects, we also measure the repetition characteristics of the coupled QW laser which has bulk like gain properties. The barrier thickness is 20 Å, therefore, the steep configuration in the density of states is completely lost because of the formation of the mini-band, as discussed in § 3.3. To find the optimum excitation condition for

the shortest interval time the excitation time interval and the ratio of both excitation intensity are varied. Figure 4.4 shows the time trace of the modulated light output with the shortest interval achieved in the coupled QW laser. In this case, the shortest repetition interval is about 30 psec. These results demonstrate the significance of the two dimensional carrier properties in uncoupled QWs for the high bit rate pulse generation. In this experiment, however, we can not realize the converged condition of repetitive pulse generation by only two excitations even though rough estimation of the upper limit of repetition rate can be achieved. In order to understand our results in more detail we should investigate other factors and mechanism which influence the ON/OFF signal mode (not continuous) pulse generation at a high repetition rate.

4.3.2 Multi-Mode Effects

As discussed in §3.3, there are differences in dynamic behaviors of lasing spectra such as the spectral broadening and spectral shift between the coupled QW laser and the uncoupled QW laser. This spectral shift also influences the high bit-rate pulse generation characteristics. In order to understand the effects of the spectral shift on repetitive pulse generation, the time-resolved spectra were measured. Figures 4.5 (a) and (b) show the spectral dynamics of the uncoupled QW laser and the coupled QW laser when the first excitation is at 2 times the threshold intensity, the second one is at

0.5 times the threshold and the excitation interval time is about 30 psec. In the uncoupled QW laser, there is no clear difference between the lasing wavelength of the first lasing pulse and the second one. On the other hand, in the coupled QW laser, the second lasing occurs in the longer wavelengths compared to the first lasing. It is due to the fact that the residual photons of the first lasing pulse in the longer wavelengths become the seeds of the second lasing pulse. This is a patterning effect in the wavelength domain, which does not appear until repetition rate becomes over 10 Gbit/s. In the longer wavelength side of gain peak, differential gain is small and, in addition, the maximum gain value saturates even if the intensity of the second excitation is enlarged. Therefore, the broad second pulse with a slow rise time is generated in the coupled QW laser. These results demonstrate the shift of lasing spectra during the pulse generation due to bulk like gain properties reduces the maximum bit rate of the ON/OFF signal mode (not continuous) pulse generation. This patterning effect in the wavelength domain is not so significant when the continuous pulse generation is realized, where the differential gain property is dominant for repetition characteristics.

§ 4.4 Frequency Characteristics of Gain-Switching Operation and Small-Signal Modulation

As discussed in §4.2 and §4.3, the short interval pulse generation can be attributed to the high photon density condition and improved gain characteristics in the uncoupled QW laser. Since the roughly estimated repetition rate obtained in §4.2 is beyond 50 GHz which is much higher than the highest relaxation oscillation frequency so far achieved in semiconductor lasers (30 GHz) [74], theoretical analysis of repetition characteristics of the gain switching operation in comparison with the relaxation oscillation characteristic is worth discussing. It is well known that relaxation oscillation frequency is proportional to the square root of the photon density if modulation signal is relatively small compared to the bias current. However, it is reported that the increase of modulation amplitude reduces f_r [103]. Note that the gain switching is realized by the extremely strong current modulation. In this section, we compare the frequency characteristics of the gain-switching operation with that of small signal modulation on the basis of conventional single mode rate equations in order to clarify the relation between the maximum operation frequency of the gain switching and the relaxation oscillation frequency.

Figures 4.6 (a)~(d) show the time traces of the sinusoidal modulation current (dotted line) and the photon density (solid line) when average injection current is kept constant and the

modulation frequency f_{mod} is varied, where the gain switching is realized by extremely strong current modulation: The bias current is 50 times as high as the threshold current and the amplitude of the signal current is the same with the bias current. As the modulation frequencies are extremely high, pulse durations of the injection current are narrow enough to enable the single pulse generation by the gain switching effect, as shown in Fig.4.6 (a)~(c). With the increase of f_{mod} , the peak intensity of generated pulses begins to decrease and finally the gain switching is no longer realized, as shown in Fig.4.6 (d).

Figure 4.7 shows the frequency response of the gain switching operation and the small signal modulation when the average injection current is the same. The horizontal axis is frequency and the vertical axis is the normalized frequency response $\delta(\omega)$ which is defined by the normalized peak to peak output signal intensity by the average output intensity divided by the normalized peak to peak modulation signal current by the average signal current. As to the small signal modulation, $\delta(\omega)$ corresponds to the conventional expression of frequency response and $\delta(\omega) = 1$ means the dc response. In small signal modulation, clear resonant peak owing to the relaxation oscillation appears. In the gain switching mode, on the other hand, the peak is broad and once modulation frequency goes over the resonant frequency of the small signal modulation, the gain switching condition can not be realized, as shown in Figs.4.6 (c) and (d), and the frequency response become the same

curve with the small signal modulation. Figures 4.6 (c) and (d) and Fig.4.7 indicate that the maximum frequency of the gain switching, to which intense pulses can be generated, becomes just below the resonant frequency of the small signal modulation.

Figure 4.8 shows the resonance frequency of the small signal modulation and the maximum frequency of the gain switching operation as a function of the square root of the average photon density, indicating that upper limit of modulation band width of the gain switching operation is slightly lower than that of the small signal modulation under the same photon density condition.

§ 4.5 Concluding Remarks

In summary, repetitive pulse generation with an extremely short interval of 16 psec is successfully achieved in quantum well lasers through an optically-pumped gain-switching method, demonstrating the promising high speed properties of the quantum well lasers as the ultrafast optoelectronic devices. Theoretical analysis indicates that this high repetition frequency results from the extremely high photon density owing to the strong excitation condition. The effects of dynamic spectral shift are also studied by comparing the coupled QW laser and the uncoupled QW laser, demonstrating that the high repetition frequency is due to the complete two dimensional gain properties which have weak dependence of the gain peak wavelength on the carrier density as well as the enhanced differential gain.

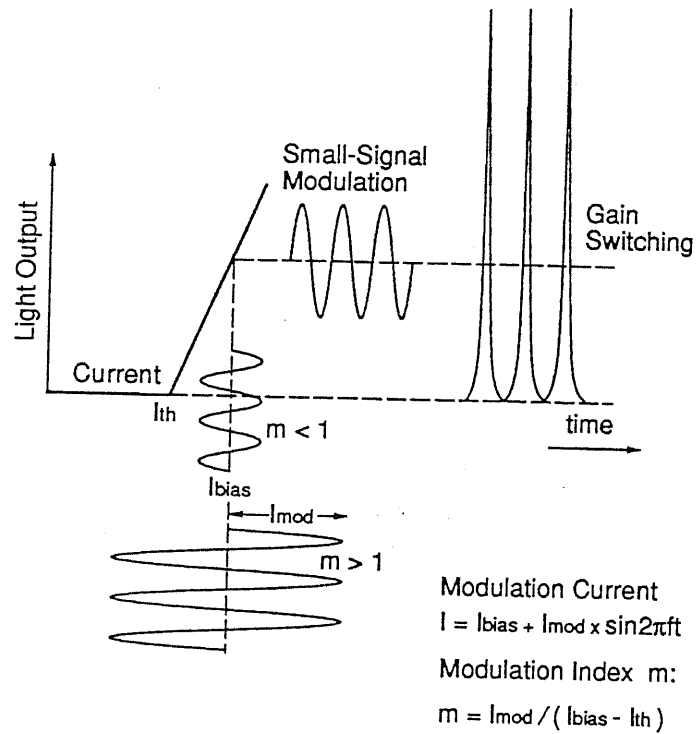


FIG. 4.1 Operating points and modulation condition of the gain-switching and the small signal modulation in I-L characteristic.

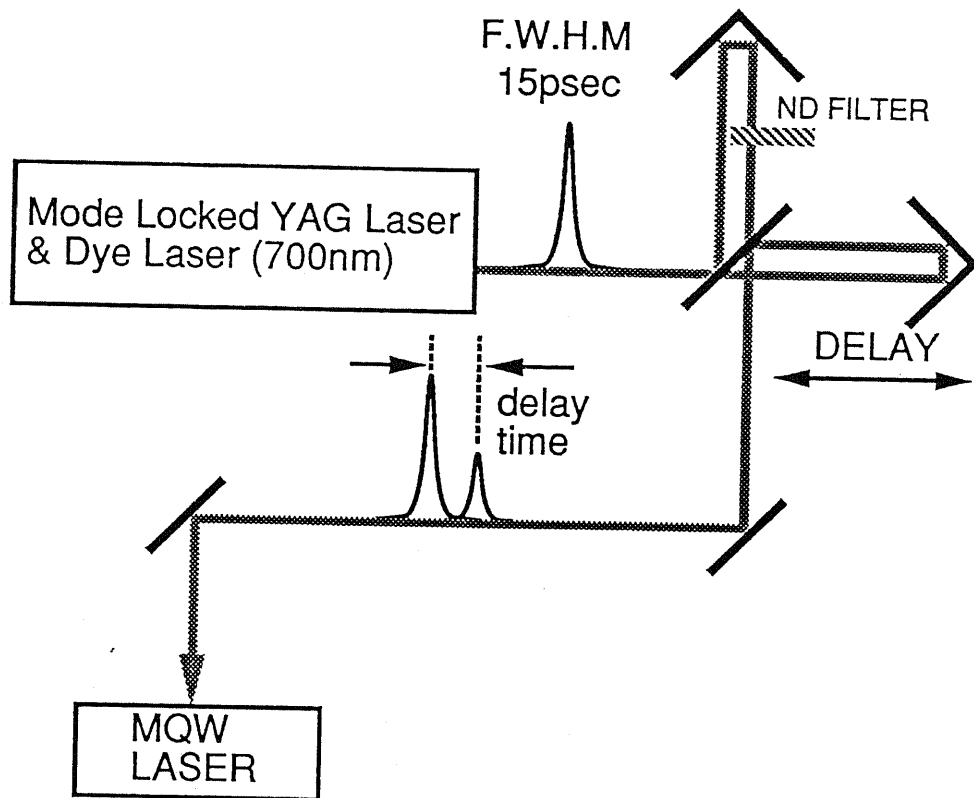


FIG. 4.2 Schematic illustrations of the experimental configuration for an optically pumped repetitive gain switching using picosecond dye laser pulses.

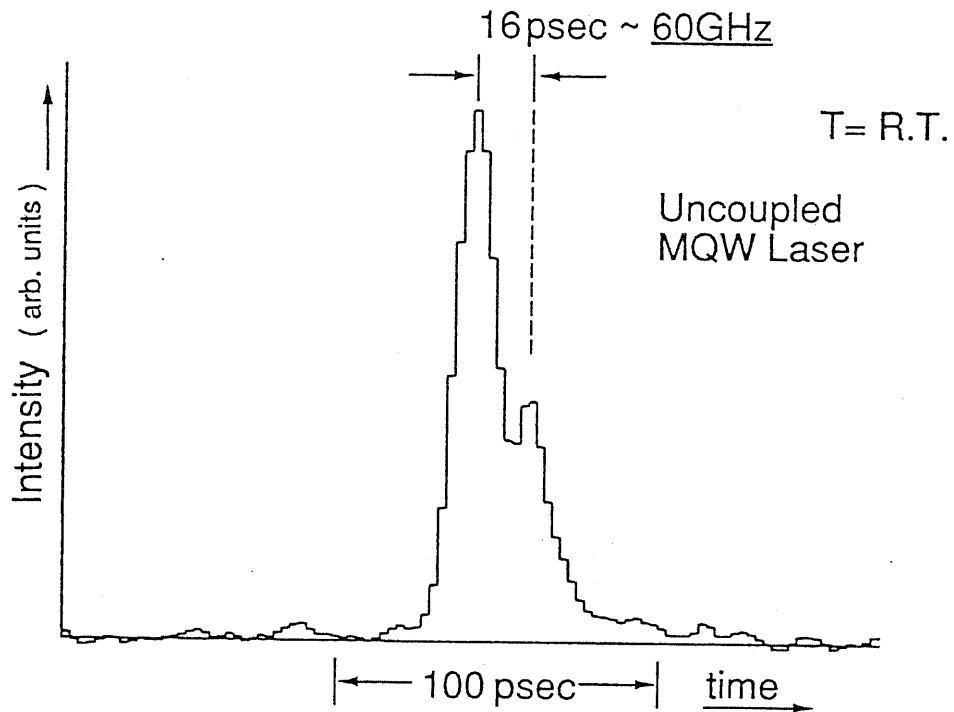


FIG. 4.3 Temporal characteristics of modulated light output from a QW laser (with uncoupled QWs) measured by a streak camera through a monochromator.

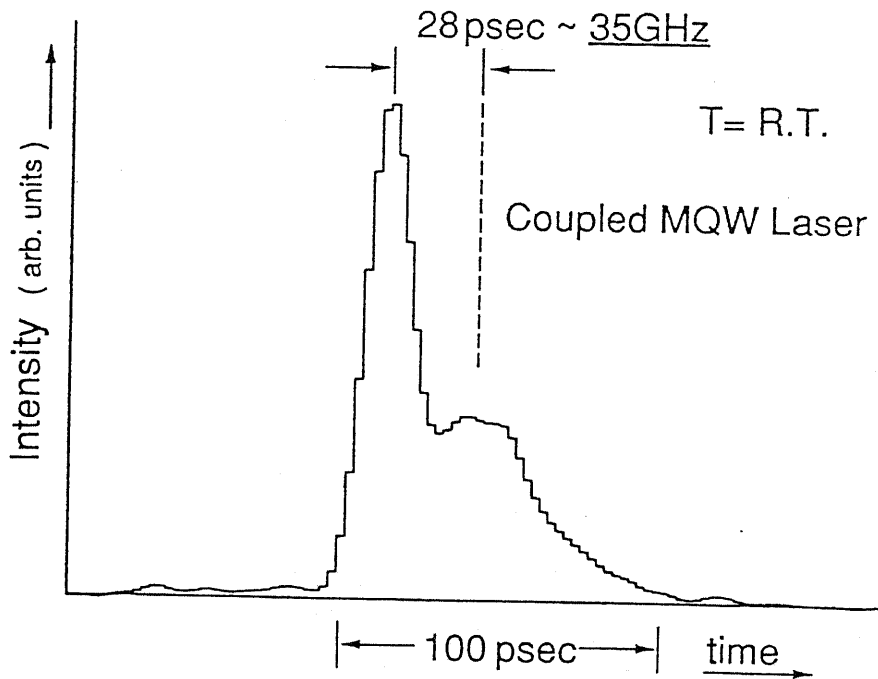


FIG. 4.4 Temporal characteristics of modulated light output from a coupled QW laser which has bulk like gain properties measured by a streak camera through a monochromator.

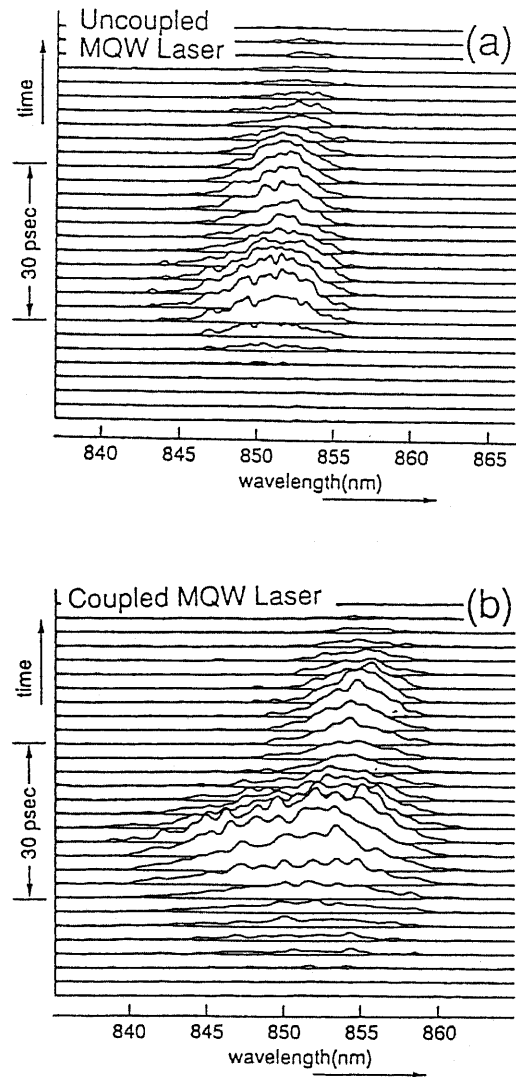


FIG. 4.5 Spectral dynamics of the (a) uncoupled QW laser and the (b) coupled QW laser measured by a streak camera together with a monochromator when the first excitation is at 2 times the threshold intensity, the second one is at 0.5 times the threshold and the excitation interval time is about 30psec.

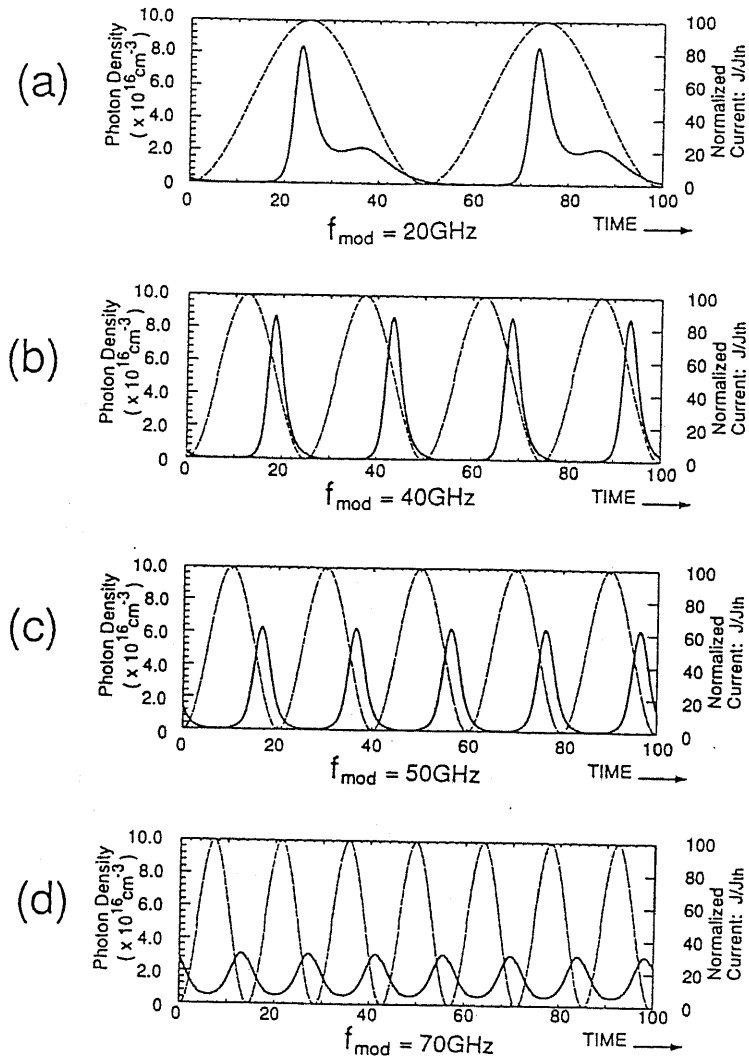


FIG. 4.6 Time charts of modulation current and photon density at various modulation frequencies: (a) $f_{\text{mod}}=20\text{GHz}$, (b) 40GHz , (c) 50GHz , (d) 70GHz .

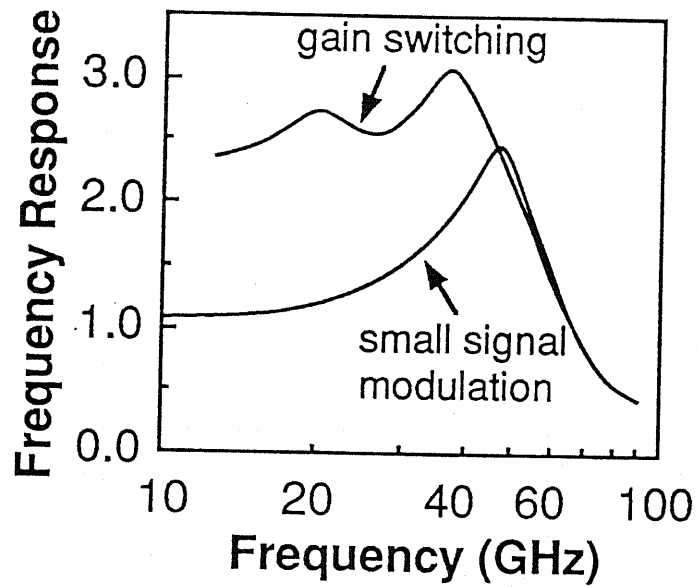


FIG. 4.7 Frequency response of the gain switching operation and the small signal modulation. The bias current is 50 times as high as the threshold current. The amplitude of the sinusoidal modulation current is at 100% the bias current in the gain switching, and at 5% the bias current in the small signal modulation.

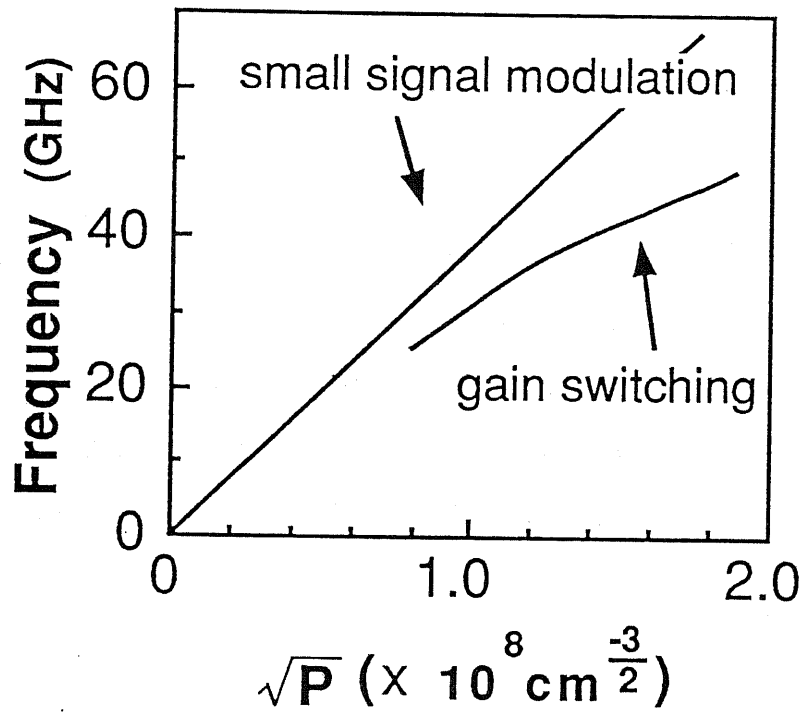


FIG. 4.8 Resonant frequency of the gain switching operation and small signal modulation as a function of the square root of the averaged photon density.

Chapter V Wavelength Switching in Picosecond Pulse Generation and Its Application to All-Optical Logic Gating Operations

Abstract

We developed a novel technique to switch the lasing wavelength of picosecond pulses in an optically pumped quantum well (QW) laser by utilizing spatially localized and homogeneous excitation. The applications of these phenomena to ultrafast logic gating operations are successfully demonstrated.

§ 5.1 Introduction

All optical logic gating operations are important for future ultrafast information processing systems. For this purpose, various ultrafast switching schemes have been investigated. The Optical Stark effect in multi-quantum well (MQW) Fabry-Perot etalons demonstrated high speed logic operations (~ 100 fsec) [109]. In this case, high peak power ($\sim \text{GW}/\text{cm}^2$) is required to achieve the optical stark effect efficiently. Bistable devices such as SEEDs and bistable semiconductor lasers can also achieve the all optical switching operation [110]-[114]. In these devices, however, the logic speed is limited by the carrier lifetime, resulting in switching time of over several hundred psec. To suppress these carrier lifetime, the use of stimulated emission phenomena is promising, which leads to rapid reduction of really-excited carriers in device materials [115].

In this chapter, we demonstrate a novel ultrafast logic operations in quantum well (QW) lasers with gain-switched lasing oscillation as an ultimate case of the stimulated emission. In this operation, picosecond wavelength-switching phenomena which are controlled by the combination of spatially localized and homogeneous optical pulses play a significant role. The gain-switched QW lasers can generate shorter pulses compared to bulk lasers because of the enhanced differential gain properties [49]. In fact, a short pulse as narrow as 1.3psec was achieved in MQW laser [51], in which the short pulse generation was realized by an

optically pumped method in which dye laser pulses with the duration of about 20 psec. Here, such picosecond lasing effects are applied to high speed logic operations.

§ 5.2 Lasing Characteristics of Quantum Well Lasers by Localized and Homogeneous Excitation

Figure 5.1 is a schematic illustration of the experimental configuration for the wavelength switching using spatially localized and homogeneous excitation pulses. Picosecond pulses are generated from a GaAs/AlGaAs multi-quantum well (MQW) laser at room temperature (70 Å ten GaAs wells separated by 100 Å $\text{Al}_{0.2}\text{Ga}_{0.8}\text{As}$ barriers) by the gain-switching method using two pumping pulses whose pulse durations are about 15 psec; one (PULSE1) is focused into a 30 μm circular spot for localized excitation near the edge, and the other (PULSE2) is focused by a cylindrical lens into a 30 μm width stripe for homogeneous excitation along the cavity, as illustrated in Fig. 5.1. The cavity length is 200 μm and the total thickness of the active region is 2500 Å. These pumping pulses are generated from a dye laser (~ 7000 Å) excited by a mode-locked Nd^+ -YAG laser. About 30% of input pulse energy ($\sim 1\text{nJ}$) is absorbed in the active region and gain switching is realized. All experiments were done at room temperature.

Figures 5.2 (a) and (b) show the spectra of the luminescence and the lasing pulses from the MQW laser excited by only PULSE1 and only PULSE2, respectively, at various excitation intensity. Even if the excitation is localized (i.e., only PULSE1 is used), lasing can be realized in the MQW laser because the absorption coefficient in the unexcited region at the lasing wavelength is small due to the band

gap shrinkage effect caused by an extremely high carrier density [116]. As shown in Figs.5.2 (a) and (b), the peak wavelength with the localized excitation are longer compared to the homogeneous excitation by $60 \text{ \AA} \sim 120 \text{ \AA}$, shifting to longer wavelength region with the increase of excitation intensity, demonstrating that this shift is due to the band shrinkage effect in the locally excited MQW laser.

§ 5.3 Novel Wavelength Switching Phenomena in Picosecond Pulse Generation

When both excitation pulses are introduced to the MQW laser, lasing condition is modified by the spatially inhomogeneous gain profile, being significantly affected by the time relation of two excitation pulses. Figures 5.3 (a)~(d) show the picosecond spectral dynamics of generated pulses measured by a streak camera in front of which a monochromator is placed when excitation time interval T_{delay} between the first excitation (PULSE1) and the second excitation (PULSE2) is varied. In this case, the excitation intensity of PULSE1 is about 1.4 times as high as the threshold intensity and that of PULSE2 is about two times as high as the threshold intensity. As shown in Fig.5.3 (a), two gain-switched pulses are generated in the different wavelengths when T_{delay} is longer than 60 psec. When T_{delay} becomes shorter than 30 psec, the peak wavelength of the second lasing pulse becomes close to the wavelengths of the first lasing pulse. This is due to the fact that the residual photons of the first lasing pulse become a seeds of the second pulse, as shown in Fig.5.3 (b). When T_{delay} is less than 15 psec which is comparable with the time-rag of the pulse generation from the excitation, only one pulse is generated in the wavelengths where lasing should occur by the first excitation, as shown in Fig.5.3 (c). In this case, the growing photons by the first excitation becomes the seeds of the lasing. On the other hand, when the both excitation pulses are simultaneously introduced, lasing wavelengths shift to shorter ones,

as shown in Fig.5.3 (d). The mechanism of the wavelength switching is attributed to the dominant amplification of the initially present photons, demonstrating that the wavelength of the generated picosecond pulses can be controlled by the combination of PULSE1 and PULSE2.

Figures 5.4 (a)~(d) shows the averaged spectra of the picosecond pulses under the various excitation conditions when both excitation intensities of PULSE1 and PULSE2 are two times as high as threshold intensity. The measured pulse duration by the streak camera without monochromator is less than 10 psec, which results from the strong excitation condition as well as the enhanced differential gain owing to the two-dimensional properties of carriers in MQW lasers. Fig. 5.4 (b) shows that the peak wavelength of the generated pulse pumped by the only PULSE2 is 848 nm. If PULSE1 excites the laser prior to PULSE2 by about 10 psec, lasing occurs at the wavelength of 858 nm that is the same wavelength of the MQW laser excited by only PULSE1, as shown in Figs.5.4 (a) and (c). On the other hand, Fig.5.4 (d) shows that the lasing occurs at the middle wavelength between the peak wavelengths of Figs.5.4 (a) and (b) if both excitation pulses are introduced to the active layer simultaneously.

§ 5.4 All-Optical Logic Gating Operations

On the basis of these results, this picosecond wavelength switching in short pulse generation can be applied to all-optical logic gating operations. Figures 5.5 (a) and (b) are the experimental results which demonstrate AND gate operation and NOT gate operation, respectively. In Fig.5.5 (a), output pulse forms at the wavelength of 854 nm through the monochromator are shown under the three excitation conditions; i) Only PULSE1 is introduced, ii) only PULSE2 is introduced, and iii) both PULSE1 and PULSE2 are introduced. In this case, both PULSE1 and PULSE2 correspond to input signals which are introduced to the laser simultaneously. Fig.5.5 (a) indicates that the intensity of the output signal pulse at the wavelength of 854 nm becomes stronger only when the two input signals come in, demonstrating the all-optical AND gating operation. In Fig.5.5 (b), output pulse forms at the wavelength of 848 nm are shown when i) only PULSE2 is introduced and ii) PULSE1 is introduced prior to PULSE2 by about 10 psec, where PULSE1 and PULSE2 correspond to the input signal and the clock pulse, respectively. When the input signal does not come in, the output signal pulse appears at the wavelength of 848 nm, demonstrating the NOT gating operation.

§ 5.5 Concluding Remarks

In summary, we demonstrate the wavelength switching phenomena in the picosecond pulse generation by the gain switching method in the MQW lasers using spatially localized and homogeneous pumping pulses. These results are due to the enhanced band gap shrinkage effects and the dominant amplification of the initially present photons. This mechanism can lead to several 10 GHz optical logic operations in the MQW lasers since each physical process is constructed by the gain switching phenomena which achieve a quite high repetition rate up to 60 Gbit/s [117], as described in §4.

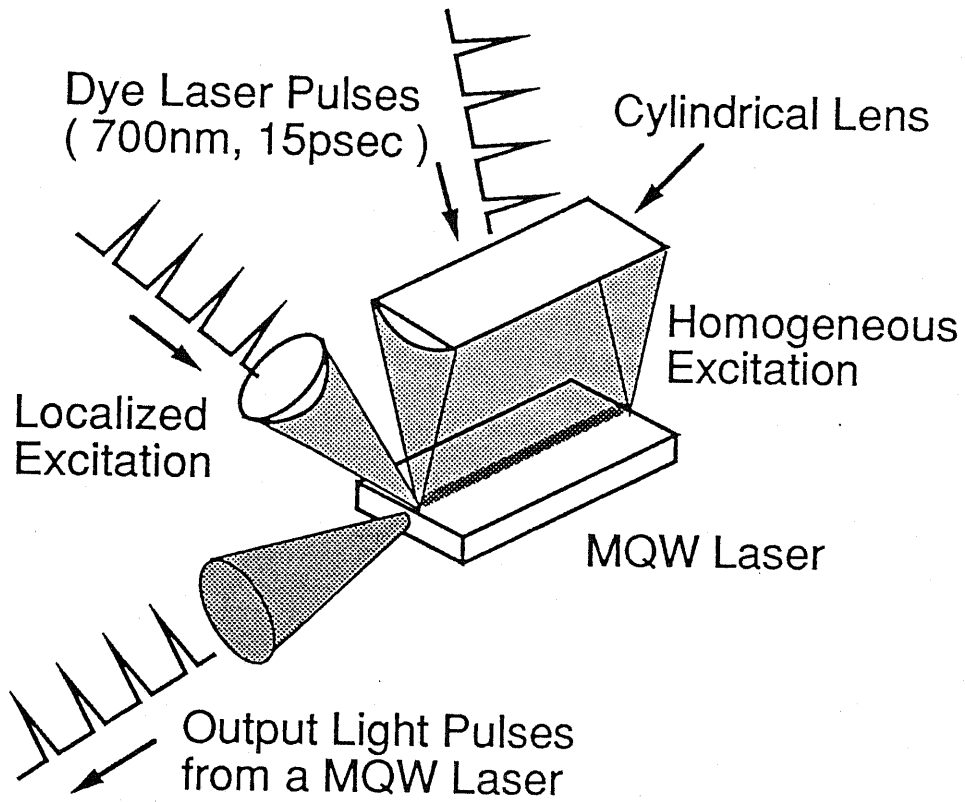


FIG. 5.1 A schematic illustration of the experimental configuration for wavelength switching using spatially localized and homogeneous excitation.

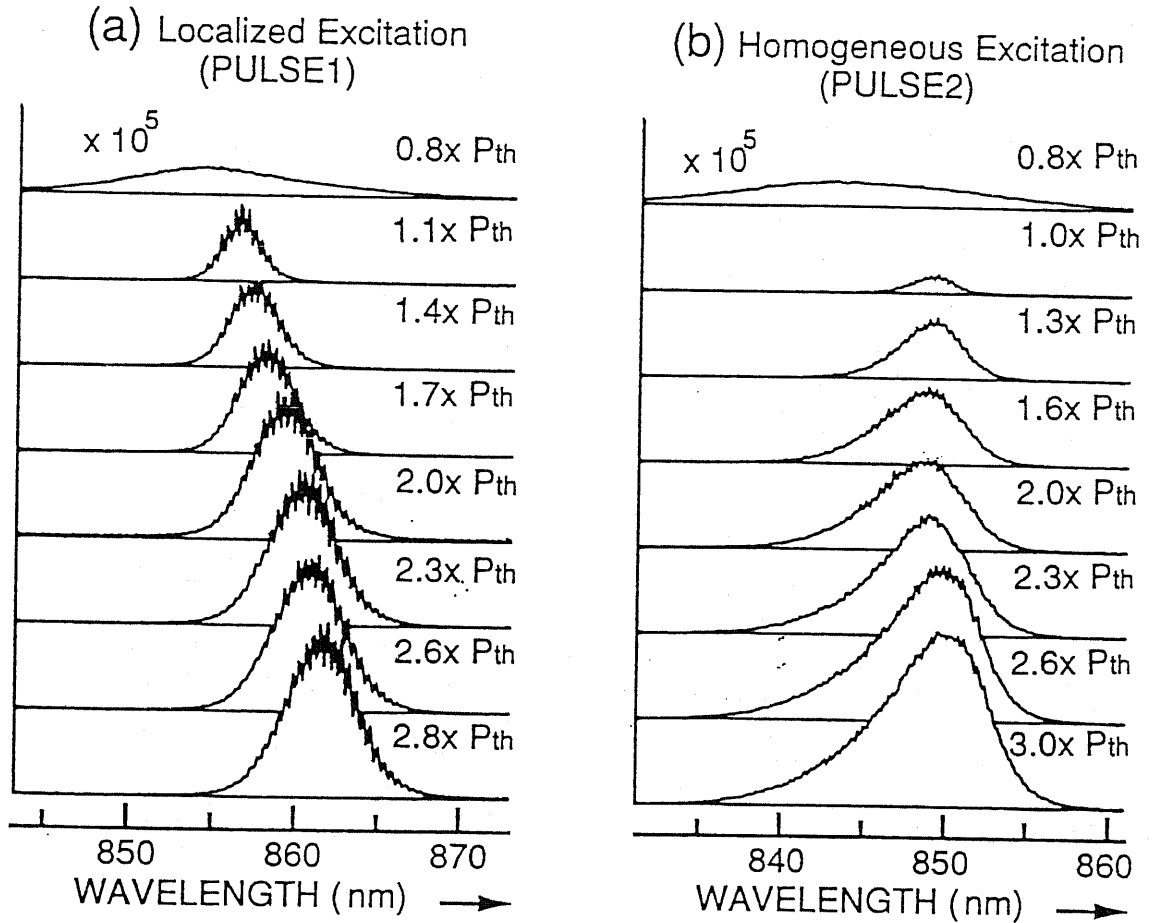


FIG. 5.2 The spectra of the photo-luminescence and the generated pulses from the MQW laser pumped by a) only PULSE1 (localized excitation), b) and only PULSE2 (homogeneous excitation) at various excitation intensity.

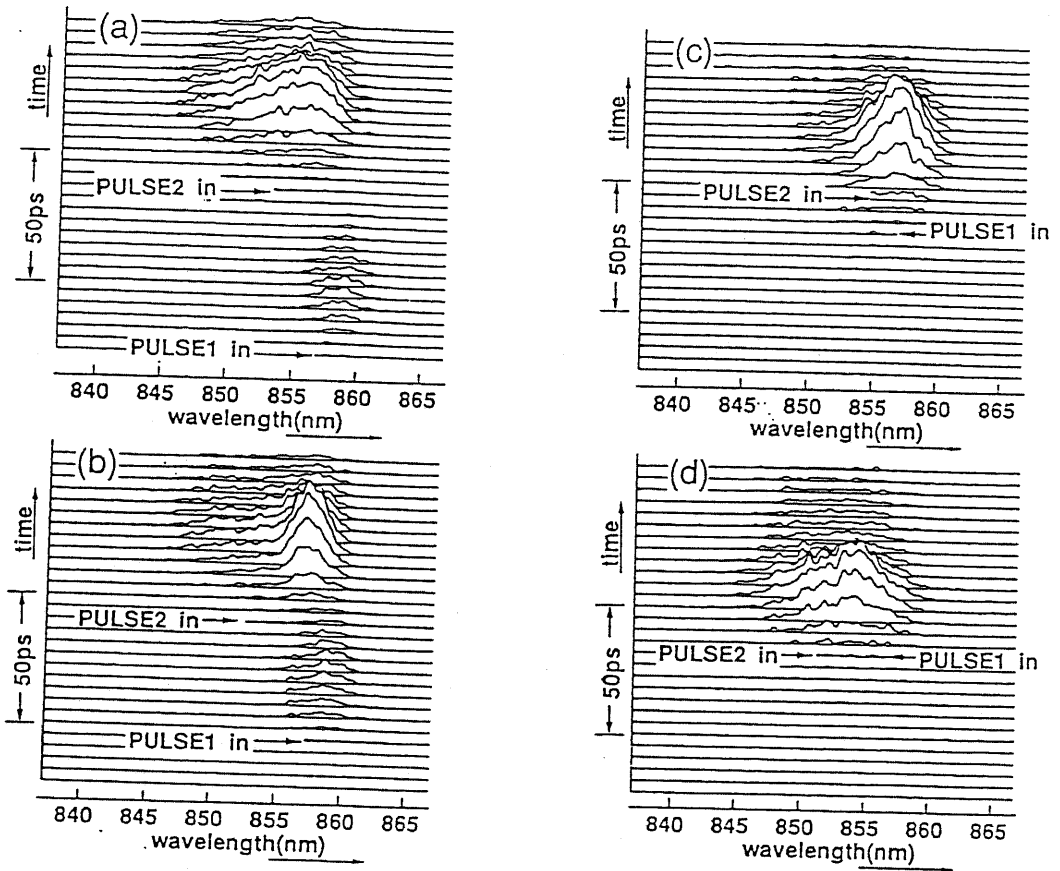


FIG. 5.3 Picosecond spectral dynamics of generated pulses under the various excitation conditions: a) the time delay from the first excitation (PULSE1) to the second excitation (PULSE2) T_{delay} is longer than 60psec, b) T_{delay} is about 30psec, c) T_{delay} is less than 15psec, and d) the both excitation pulses are simultaneously introduced.

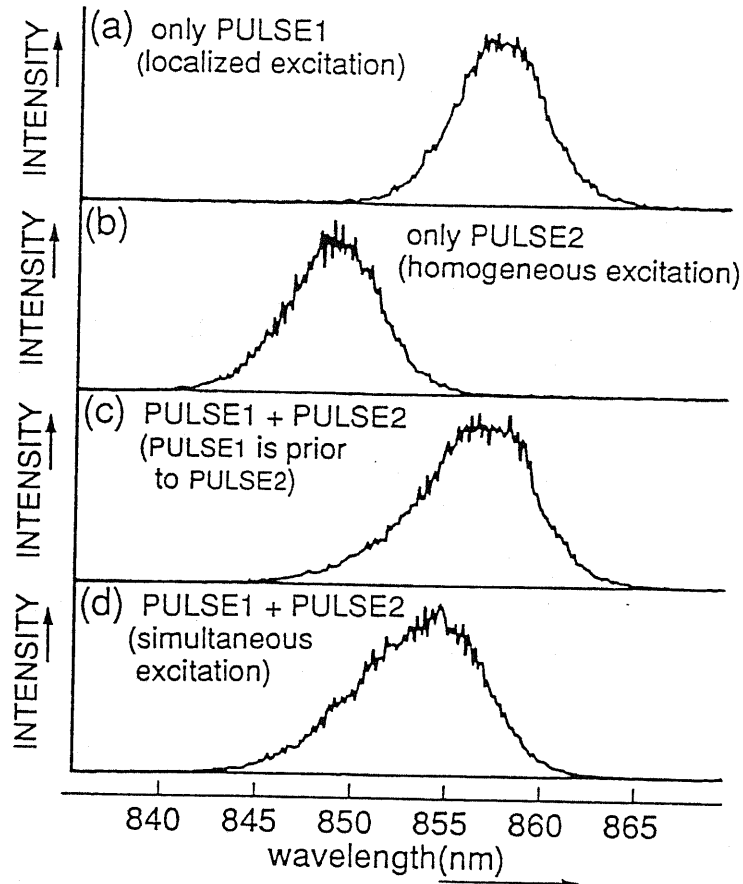


FIG. 5.4 Averaged spectra of picosecond pulses under the various excitation conditions: a) only PULSE1 (localized excitation), b) only PULSE2 (homogeneous excitation), c) PULSE1 is introduced prior to PULSE2 by 10psec, and d) PULSE1 and PULSE2 are simultaneously introduced.

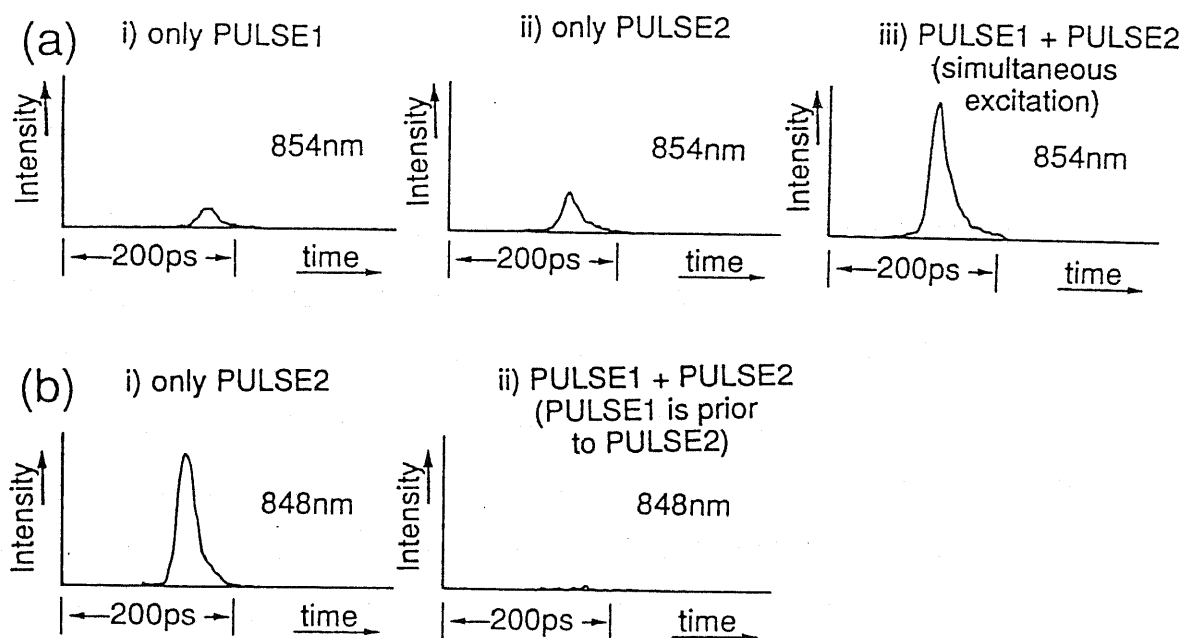


FIG. 5.5 Experimental results of a) the AND gate operation, and b) the NOT gate operation using the combinations of the spatially localized and homogeneous excitation.

Chapter VI Carrier Capture Process in Quantum Well Structures and Its Effects on Lasing Dynamics

Abstract

We observed capture phenomena and cooling process of photo-excited carriers in quantum well (QW) structures by pump-probe measurements using wavelength-tunable 100-150 fsec ultrashort dye laser pulses. It is revealed that hot-carriers thermalize with relaxation times ranging from 0.1 psec to 2 psec, which depends on excess energy of carriers, and that the carrier diffusion speed dominantly determines the capture time of about 20 psec. The effects of carrier capture process and the carrier thermalization on the lasing dynamics of gain-switched QW lasers are also investigated, demonstrating the overflowed electrons significantly influence the lasing dynamics. The effective capture time under the lasing condition is estimated about 3 psec.

§ 6.1 Introduction

The capture of electrons and holes by quantum wells is of considerable current interest from both fundamental and applied point of views. The relevance of this problem to quantum well lasers motivated early as well as some recent studies. Luminescence and luminescence excitation spectroscopies have been used for the study of the carrier capture phenomenon [85],[86],[118]. Capture time were deduced either from capture efficiency or from time-resolved luminescence studies and ranged from 0.1 psec to less than 50 psec [85]-[88]. The carrier capture times have also received considerable theoretical attention recently and are of fundamental interest because the quantum mechanical aspects of the system play an important role in the capture process. There have have been predictions of strong resonances in the capture times as a function of quantum well thickness, arising from strong electronic resonances [119], with capture times ranging from 1 to 200 psec. A more recent theoretical indicates that there are also resonances resulting from the variation in the confined phonon modes as a function of quantum well thickness. However, no significant dependence on the well thickness has not been observed. From a device point of view, the efficiency of the carrier collection within the quantum well determines the quantum efficiency of quantum well lasers whereas the transfer rates to the QW govern the modulation speed of the quantum well laser. In § 3.3, we pointed out the significance of the capture rate

including carrier cooling and diffusion in lasing dynamics of gain-switched QW lasers under strong excitation condition. Here we directly observed the capture time as well as cooling time by a pump-probe measurement using 100-150 fsec dye laser pulses and discuss the influences of these phenomena on the lasing dynamics of gain-switched QW lasers.

§ 6.2 Carrier Capture Phenomena and Carrier Relaxation Process

6.2.1 *Experimental Procedure*

In order to observe the carrier capture phenomena and cooling process of hot carriers, pump-probe measurements are performed using femtosecond dye laser systems, as illustrated in Fig.6.1. The starting point for the present experiments is a dye laser (pyridine 1 or Styryl 9) with a cavity dumper, pumped by the second harmonic of a compressed, mode-locked Nd⁺-YAG laser. The dye laser output is typically 100 mW average power at 4.1 MHz repetition rate, with 700 fsec pulse width. We compress these pulses using a fiber-prism compressor. Using 100 mW input power, we obtain 100 fsec compressed pulses with an average power of 30 mW (~7 nJ). This laser system can produce wavelength-tunable 70-150 fsec pulses in the wavelengths ranging from 6000 Å to 8700 Å by using different kinds of dye. In these experiments, pyridine 1 (6800 Å-7600 Å) and Styryl 9 (8000 Å-8700 Å) were used to excite various energy states. Noncollinear pump-probe measurements were performed, and the temporal changes of the transmitted probe beam intensity were obtained as a function of delay time between the pump beam and the probe beam. The probe beam was perpendicularly polarized in order to suppress the influence of the coherent coupling artifact.

The sample used in this study was a quantum well laser with four 70 Å GaAs wells separated by 100 Å AlGaAs ($x=0.2$) barriers. The total thickness of the active region is 2500 Å and four QWs are placed at the center. The GaAs substrate and the buffer layer were removed by first polishing and then selectively etching. The remaining structure was epoxied on a transparent window for ease of handling. All the measurements were made at room temperature.

6.2.2 *Carrier Capture and Diffusion Process*

Dynamic behaviors of photo-excited carriers which transfer into QWs and relax to the bottom of QWs were investigated by pump-probe measurements. Figure 6.2 shows the measured differential (pump on minus pump off) transmission of the sample pumped and probed at the wavelength of 7350 Å. The photon energy of the pump pulse (1.685 eV) is slightly higher than the energy band-gap of AlGaAs ($x=0.2$) layers (1.672 eV). Therefore, all of the layers including GaAs QWs, AlGaAs barriers, and AlGaAs optical confinement layers are excited. The estimated carrier density in these AlGaAs layers is about $5-7 \times 10^{17} \text{ cm}^{-3}$. The result measured on a longer time scale is also shown in the inset figure of Fig.6.2, indicating that the decay time is about 20 psec. Figure 6.3 shows the result measured at the wavelength of 7590 Å. Since the

photon energy of the pump pulse (1.632 eV) is just below the energy-gap of AlGaAs ($x=0.2$) layers (1.672 eV), only in QWs carriers are excited. In this case, the decay process is due to the energy relaxation from the photo-excited state in QWs with a decay time of less than 1 psec. Since the total thickness of AlGaAs layers is wider compared to GaAs QW layers by about one order in this sample, the longer decay process is mainly attributed to the phenomena in the AlGaAs layers. Note that this decay does not result from the radiative or nonradiative recombination process because the recombination life time deduced from the measured photoluminescence decay time by the streak camera is in the order of nanosecond. Therefore this decay process comes from the diffusion of carriers from AlGaAs layer to the QWs. The theoretically estimated time to diffuse 1000 Å is about 10 psec assuming a typical diffusion coefficient at 300 K of $5 \text{ cm}^2\text{s}^{-1}$. This value is in rough agreement with the observed decay time.

6.2.3 *Cooling Process of Hot Carriers*

As shown before, the carrier relaxation process in QWs is much faster than the carrier diffusion. It is well-known that intra-band relaxation process and carrier heating effects significantly influence the dynamics of semiconductor lasers. Here, cooling process of photo-excited carriers are investigated by the pump-probe measurement.

Figures 6.4 (a) and (b) show the spectra of pump pulse and photo-luminescence from the sample at room temperature. The pulse duration of the pump pulse is about 150 fsec and the center wavelength is 8300 Å. Even though the excited energy state is near the band-edge of QWs, the broad P.L. spectra are observed in Fig.6.6 (b), indicating that carriers distribute in much higher energy states compared to the pumped state, that is, the carrier heating occurs by this intense excitation. When we use the pumping wavelength of 8050 Å (1.539 eV) so as to excite the higher energy level which is about 100 meV beyond the band-edge of QWs, carrier heating effects are realized in the initial stage of the excitation.

Figure 6.5 (a) and (b) show the measured differential transmission of the sample pumped at the wavelength of 8050 Å and probed at the wavelength of 8050 Å and 8300 Å, respectively. The inset figure of Fig.6.5 (a) is plotted on a longer time scale. Figure 6.5 (b) indicates that the carrier population at energy level of 8300 Å (1.493 eV), which is slightly beyond the band-edge states, increases with a time constant of 300 fsec owing to the carrier relaxation from the photo-excited state and subsequently saturates. On the other hand, in Fig.6.5 (a), two processes with different rise time are observed and the carrier population at energy level of 8050 Å increases with a first time constant of about 500 fsec and subsequently with a second time constant of about 1-2 psec. This

slower rise time is due to the cooling time of hot carriers, which consists with the result of Fig.6.2.

Figure 6.6 (a) and (b) show the measured differential transmission of the sample pumped about 20 meV beyond the band edge states by using the wavelength of 8350 Å (1.484 eV), and probed at the wavelength of 8350 Å and 8450 Å (1.466 eV; presumably band-edge states), respectively. It is found that the carrier relaxation occurs within 100 fsec. In this case, the relaxation mechanism is attributed to only carrier-carrier scattering because we excite at less than one phonon excess energy. As shown in Fig.6.5, the relaxation process presumably due to the optical phonon scattering is slower compared to carrier-carrier scattering [89]-[94]. In Fig.6.6 (b), negative signal observed at negative delay time is due to the interaction of the pump pulse with the polarization which is induced by the probe field [121]-[124].

§ 6.3 Effects of Carrier Capture Phenomena and Carrier Heating on Lasing Dynamics of Gain-Switched Quantum Well Lasers

We have studied the carrier relaxation phenomena and the carrier diffusion process in photo-excited QWs. The results say that the energy relaxation time of hot carriers is ranging from 0.1 to 2 psec which depends on excess energy of carriers and that the carrier diffusion time in the active layer is 10-20 psec. When we discuss the lasing dynamics of the gain-switched quantum well laser which is generating picosecond pulses, we should take into account the effects of capture process, diffusion, and relaxation phenomena of electrons and holes. Note that the strong stimulated emission by the gain switching effects occurs after 10-20 psec from the excitation, as discussed in § 2, where the transport of carriers from AlGaAs regions to QWs has almost finished and a thermal equilibrium condition is realized. It is reported that capture time of holes is faster than that of electrons^[119] and that the Coulomb attraction between electrons and holes also plays an important role in the capture process^[87], resulting in that only electrons overflow from the wells under the strong excitation condition because of light effective mass. Figures 6.7 (a) and (b) show pictures of the initial condition and the thermal equilibrium condition. In Fig.6.7 (a), a part of electrons and holes are captured in QWs and other carriers are diffusing in the AlGaAs layers. Under the thermal equilibrium condition, as illustrated in Fig.6.7 (b), there are overflowed electrons

which are attracted by holes in QWs. When we discuss the lasing dynamics, these conditions should be considered.

As discussed in § 3, when the number of QWs is large, lasing condition can be realized by the small carrier density. In this case, since the most part of electrons and holes are captured in QWs, as illustrated in Fig.6.8 (a), the only energy relaxation process plays an important role in the lasing dynamics. Even though the reduction of carrier density due to the strong stimulated emission is a little slower compared to the carrier relaxation time (0.1-1 psec), the effects of the relaxation process can be explained by considering the nonlinear gain saturation effects due to the spectral hole burning. However, note that the multi-mode oscillation with drastic spectral shifts reduces the influence of the spectral hole burning. On the other hand, when the number of wells is small or the excitation intensity is extremely strong, the carrier (electron) overflow occurs even under the thermal equilibrium condition, as illustrated in Fig.6.8 (b), where capture process including carrier diffusion and relaxation of overflowed electrons play a significant role in the lasing dynamics. In fact, in §3.2.3, we observed the tail structures in the output pulse forms from the gain-switched QW laser with 4 QWs which is strongly excited [120].

Figures 6.9 (a)-(f) show the calculated spectral dynamics of QW lasers with 12 QWs [(a)-(c)] and 4 QWs [(d)-(f)] under various excitation intensities on the basis of multi-mode rate equations as

discussed in § 3.2.4. In the QW laser with the smaller number of QWs, since higher carrier density is required for the lasing condition, carrier overflow easily occurs and causes the tail structures in the output pulse forms under strong excitation conditions. In this calculation the effective capture time τ_{cap} including carrier diffusion and relaxation of overflowed electrons is estimated to be about 3 psec. Even though this effective capture time depends on the carrier density and sample geometry such as the ratio of the thickness of AlGaAs region to that of GaAs QW region, this estimated value of 3 psec is in rough agreement with that deduced from the carrier diffusion time and the relaxation time of overflowed electrons achieved in our experiment.

§ 6.4 Concluding Remarks

We observed capture phenomena and cooling process of photo-excited carriers in quantum well (QW) structures by pump-probe measurements using wavelength-tunable 100-150 fsec ultrashort dye laser pulses. It is revealed that hot-carriers thermalize with relaxation times ranging from 0.1 psec to 2 psec, which depends on excess energy of carriers, and that the carrier diffusion speed dominantly determines the capture time of about 20 psec. The effects of carrier capture process and the carrier thermalization on the lasing dynamics of gain-switched QW lasers are also investigated, demonstrating the overflowed electrons significantly influence the lasing dynamics. The effective capture time under the lasing condition is estimated about 3 psec.

FEMTOSECOND LASER SYSTEM

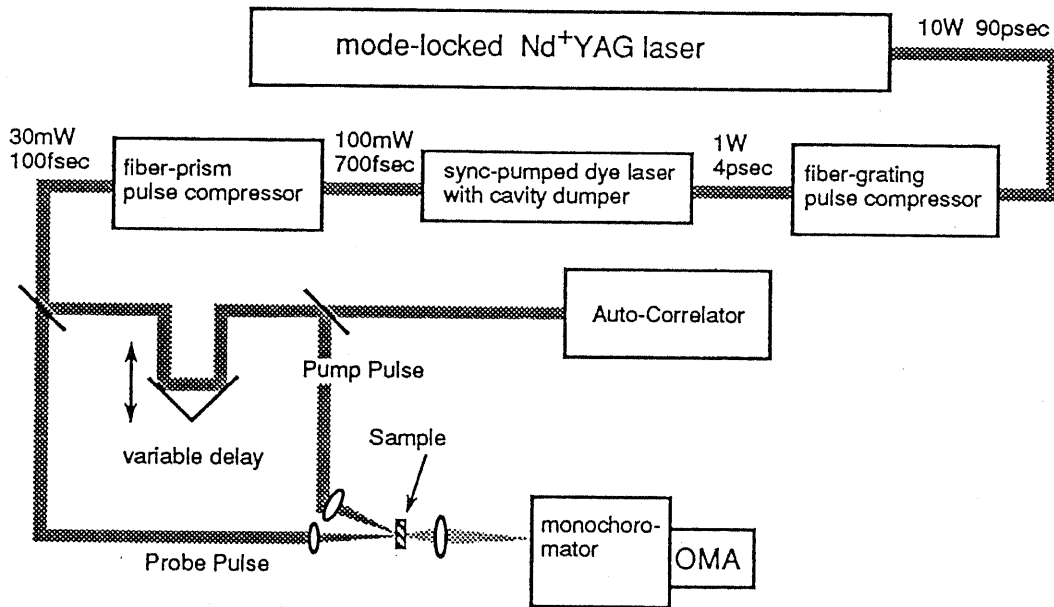


FIG. 6.1 Experimental setup for pump-probe measurement using 100fsec compressed dye laser pulses pumped by the frequency-doubled output of a compressed, mode-locked YAG laser.

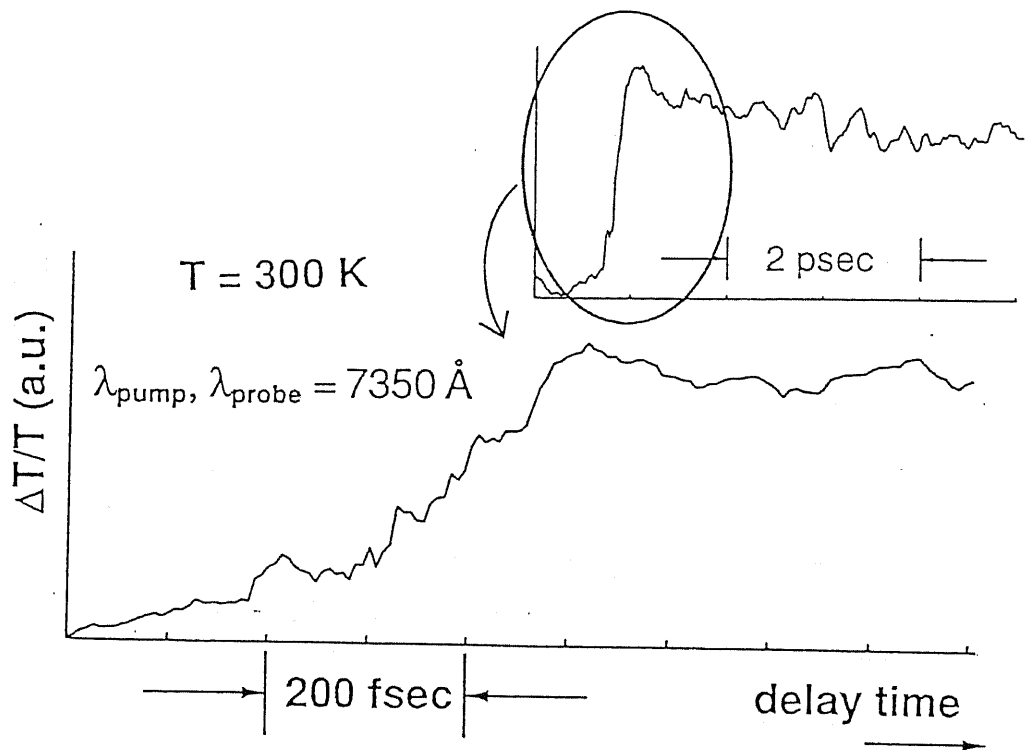


FIG. 6.2 Measured differential transmission of the sample at the wavelength of 7350 \AA . The photon energy of the pump pulse is slightly higher than the energy-gap of AlGaAs ($x=0.2$) layers. The inset figure shows the result of long time range measurement. The decay time is estimated to be about 20 psec.

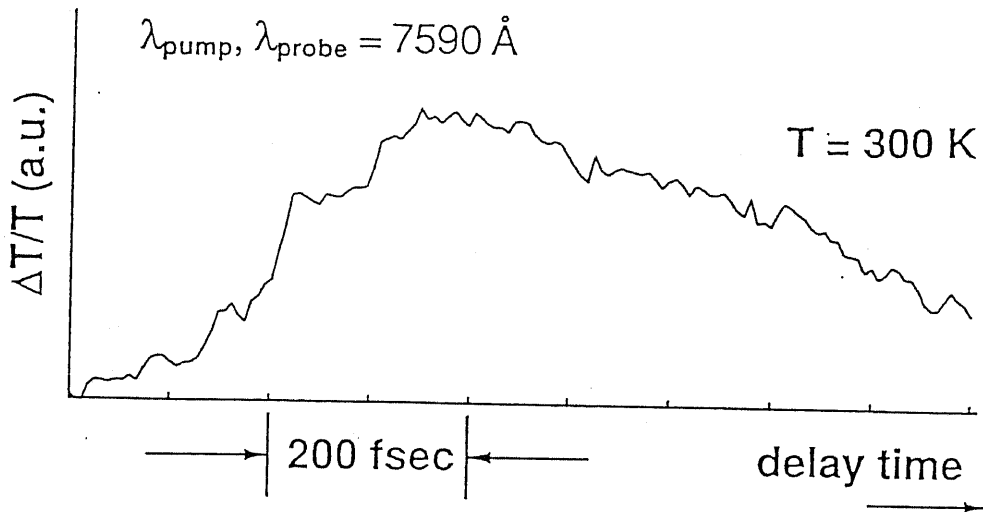


FIG. 6.3 Measured differential transmission of the sample at the wavelength of 7590 \AA . The photon energy of the pump pulse is just below the energy-gap of AlGaAs ($x=0.2$) layers. Therefore, only in QWs carriers are excited. The estimated decay time is less than 1 psec. This decay process is due to the energy relaxation of carriers.

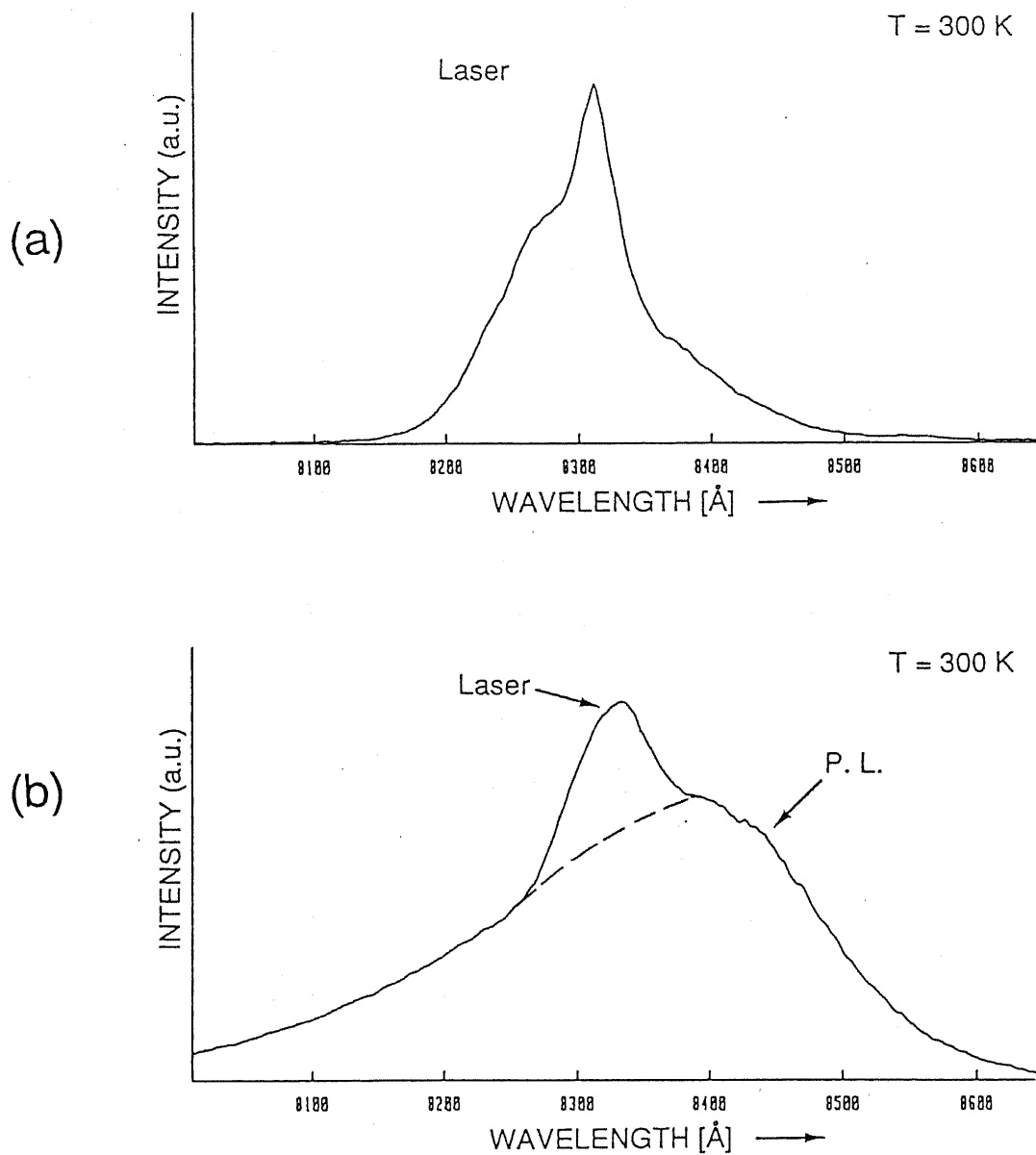


FIG. 6.4 Measured spectra of (a) pump pulse and (b) photoluminescence from the sample at room temperature. The pulse duration of the pump pulse is 150 fsec and the center wavelength is 8300 Å. Even though the excited energy state is near the bottom of QWs, the broad P.L. spectra are obtained in (b), indicating that the carrier heating occurs.

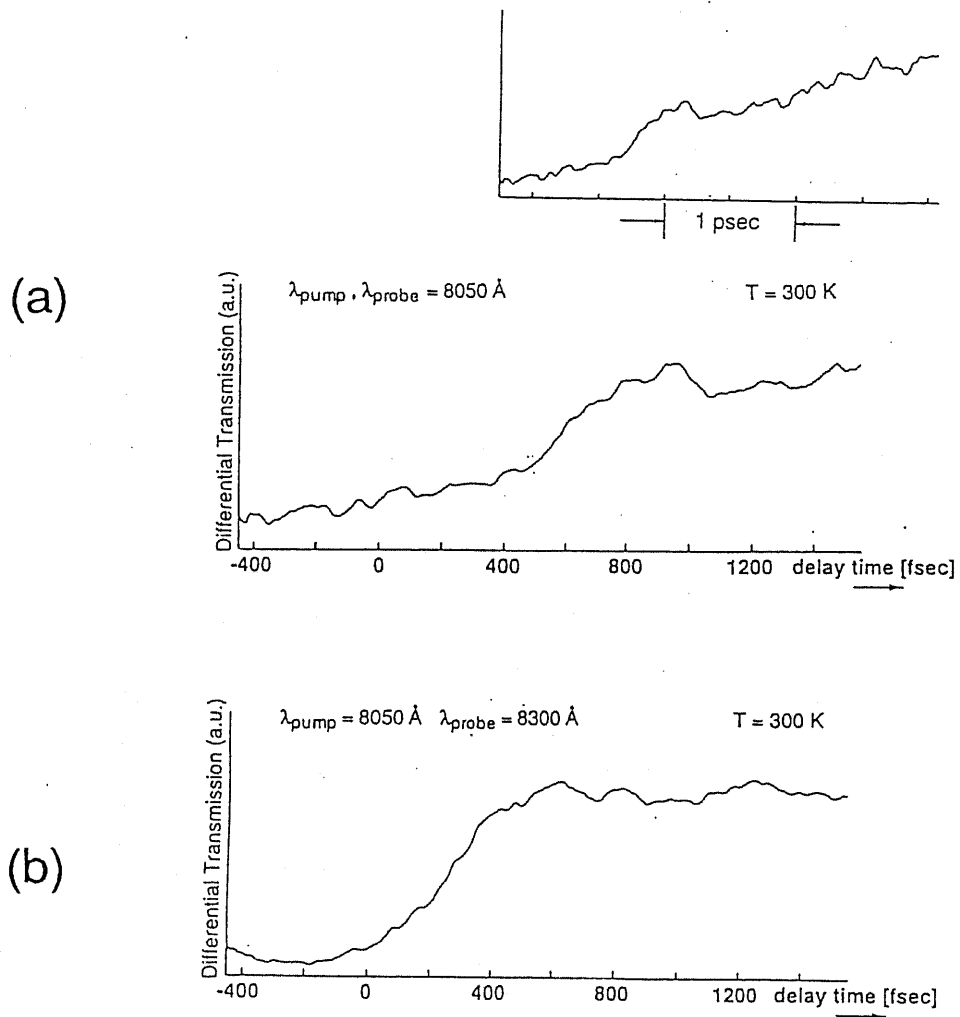


FIG. 6.5 Measured differential transmission of the sample pumped at the wavelength of 8050 \AA and probed at (a) the wavelength of 8050 \AA and (b) 8300 \AA , respectively. The inset figure of (a) is the same result plotted in the long time range.

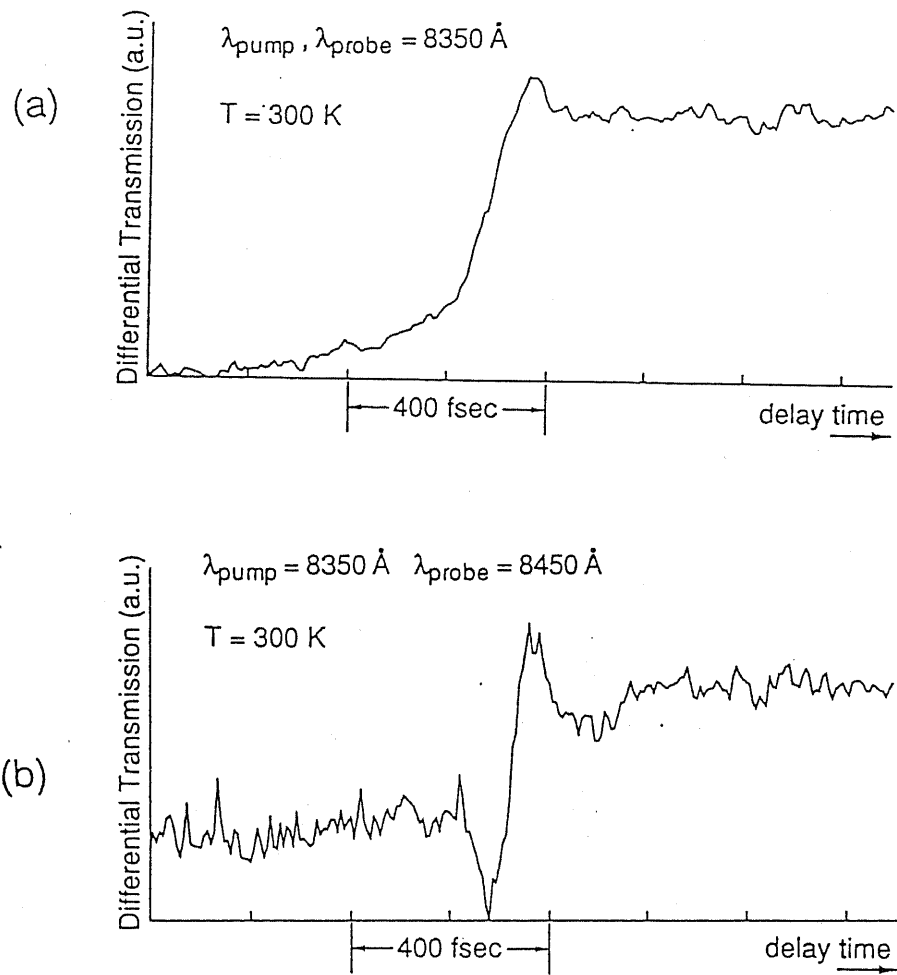


FIG. 6.6 Measured differential transmission of the sample pumped at the wavelength of 8350 \AA and probed at (a) the wavelength of 8350 \AA and (b) 8450 \AA , respectively.

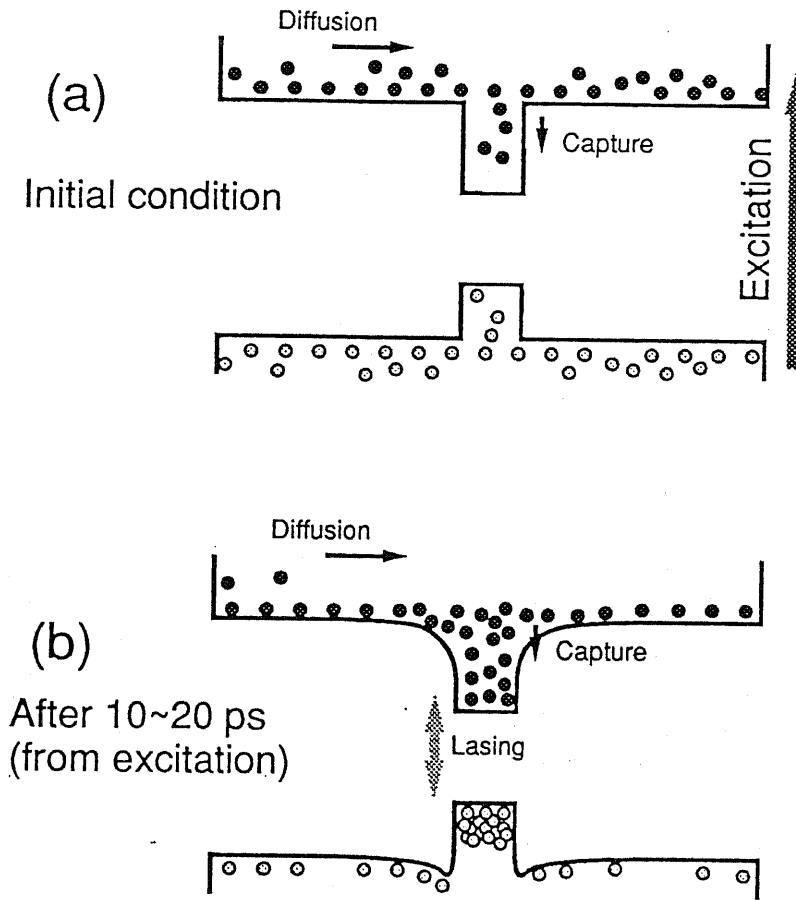


FIG. 6.7 Schematic illustrations of carrier distribution in the photo-excited active layer (a) at the initial stage of carrier capture phenomena, and (b) that of the gain-switching condition. Both conditions consist of electrons in QWs, holes in QWs, and electrons and holes in the AlGaAs layers which are diffusing. In gain-switching condition, there are overflowed electrons which are attracted by the Coulomb interaction.

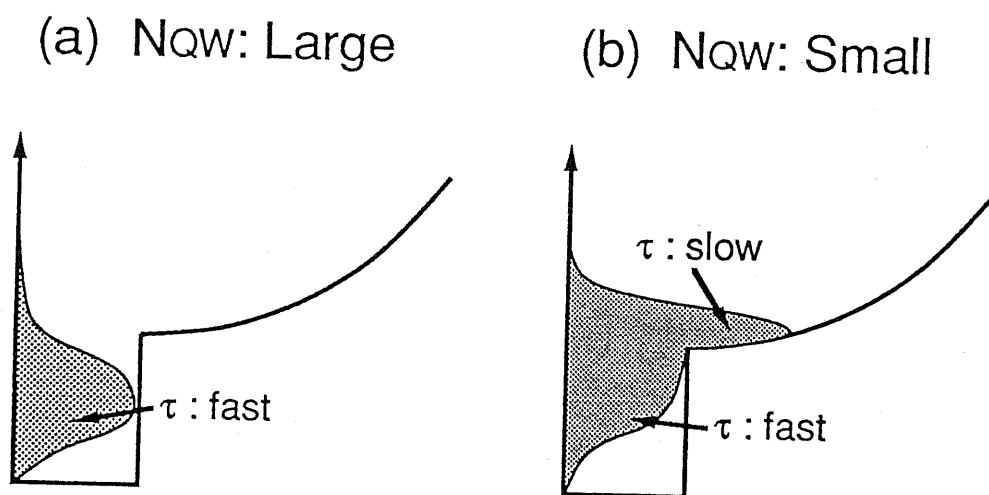


FIG. 6.8 (a) If the number of QWs is large, lasing condition can be realized by the small carrier density, resulting in the presence of electrons and holes in QWs. (b) When the number of wells is small or the excitation intensity is strong, the carrier (electron) overflow occurs, where capture process including carrier diffusion and relaxation of overflowed electrons play a significant role in the lasing dynamics.

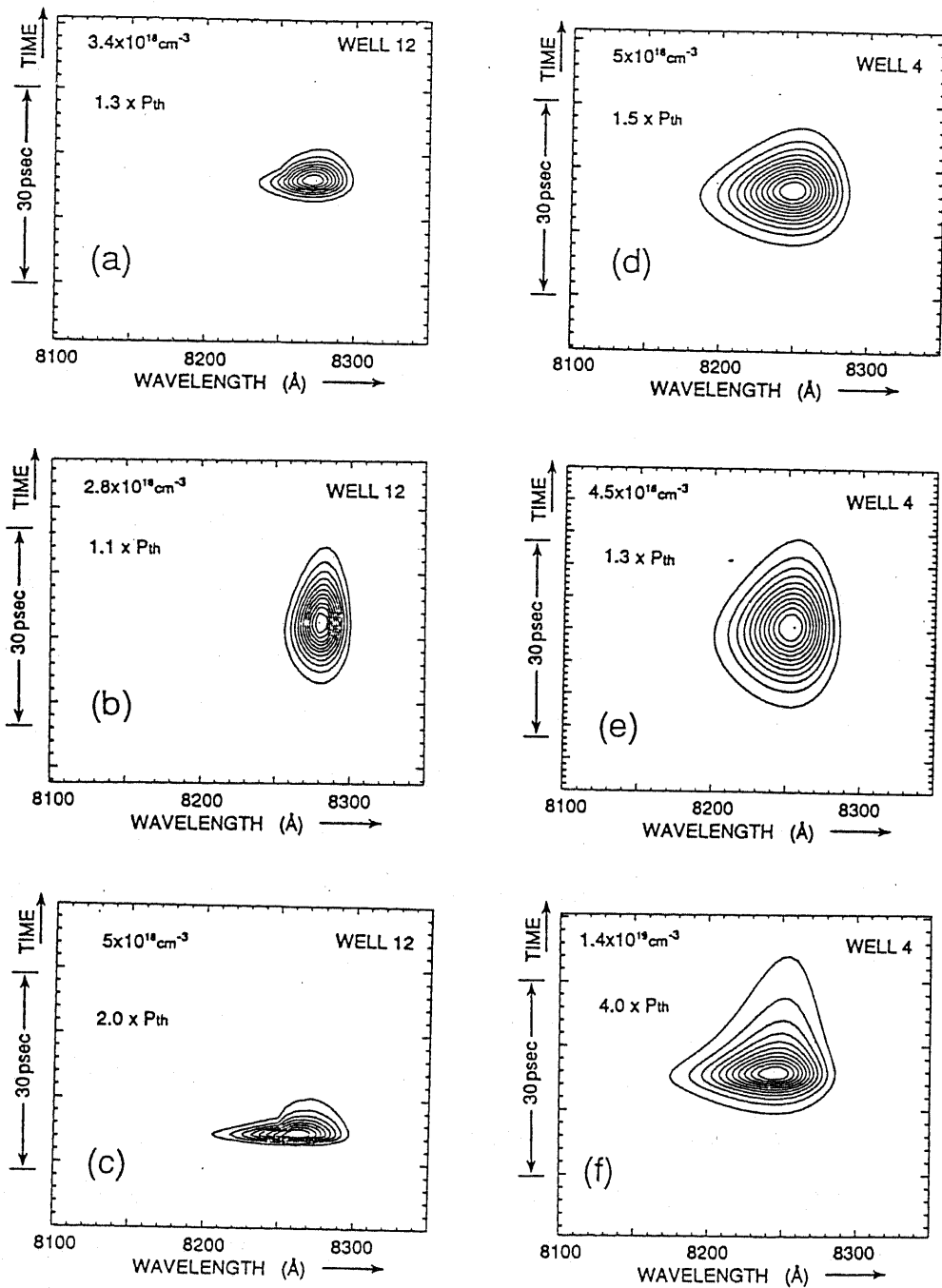


FIG. 6.9 Calculated spectral dynamics of QW lasers with 12 QWs [(a)-(c)] and 4 QWs [(d)-(f)] under various excitation conditions on the basis of multi-mode rate equations.

Chapter VII Conclusions

In this thesis, the author has studied picosecond lasing dynamics of gain-switched quantum well lasers.

In Chapter II, significance of the enhanced differential gain in picosecond optical pulse generation by the gain switching method is theoretically and experimentally demonstrated. An extremely short light pulse less than 1.3 psec is successfully generated by the optically pumped gain switching method in a GaAs/AlGaAs multi-quantum well laser. This value is the smallest one so far obtained in semiconductor lasers by the gain switching method. This short pulse generation results from the enhanced differential gain due to two dimensional properties of carriers in the quantum wells. Stochastic behavior of the spontaneous emission inside the cavity is for the first time pointed out. Experimental results using detuned InGaAsP distributed feedback lasers also demonstrate the significance of the differential gain for short pulse generation.

In Chapter III, picosecond spectral dynamics of gain-switched GaAs/AlGaAs quantum well (QW) lasers generating short optical pulses is investigated. Effects of QW structures such as the number of quantum wells and the barrier thickness on picosecond lasing dynamics are also clarified. It is found that dynamic gain behaviors are important for short pulse generation and that larger number of

QWs leads to shorter pulse generation. The significance of two dimensional carrier properties owing to the quantum confinement effects is also demonstrated by comparing the lasing dynamics of an uncoupled QW laser and a coupled QW laser.

In Chapter IV, repetitive gain-switching characteristics in quantum well lasers are studied. Extremely short interval pulse generation with 16 psec interval is successfully achieved in quantum well lasers through an optically pumped repetitive gain-switching method, demonstrating the superior performance of the quantum well laser as an ultrafast optoelectronic device. The significance of two-dimensional quantum confinement for high bit rate short pulse generation is also demonstrated.

In Chapter V, a novel technique to switch the lasing wavelength of picosecond pulses is demonstrated. This results from the enhanced band gap shrinkage effects and the dominant amplification of the initially present photons. Ultrafast logic gating operations (AND/NOT) utilizing these phenomena are successfully demonstrated.

In Chapter VI, carrier capture phenomena and carrier relaxation process are investigated by the pump-probe measurements using 100-150 fsec compressed dye laser pulses. It is revealed that the cooling times of hot-carriers are ranging from 0.1 to 2 psec and that the capture time limited by the carrier diffusion speed is about 20 psec . The effects of carrier capture process and

the carrier thermalization on the lasing dynamics of gain-switched QW lasers are also investigated, demonstrating the overflow of carriers significantly influences the lasing dynamics.

The author hopes that the present study contributes to the fundamental understanding of the short optical pulse generation in semiconductor lasers and its application to future ultrafast optoelectronic systems.

Appendix Lasing Dynamics of Quantum-
Well Wire (QWW) Lasers

Abstract

Lasing dynamics of a gain-switched quantum-well wire (QWW) laser as well as its gain properties are theoretically studied. The calculated results on the basis of multi-mode rate equations demonstrate that short pulses less than 3 psec with narrow spectra can be achieved in QWW lasers by lower operation power compared to the QW laser owing to both the highly enhanced differential gain properties and the lower threshold condition.

A.1 Introduction

Recent progress of direct write lithography technology combined with epitaxial growth technology for quantum-well structures leads to the possibility of realizing quantum-well wire (QWW) and quantum-well box (QWB) structures. In 1982, Arakawa and Sakaki proposed use of arrays of QWW and QWB as the active layer of a semiconductor laser [69]. Theoretical studies have discussed threshold current characteristics, modulation bandwidth, and spectral properties [70],[118]. The QWW and QWB effects in the semiconductor lasers are also experimentally demonstrated by placing the quantum well laser in a high magnetic field [119],[120]. In §2 and §3, we pointed out the significance of the enhanced differential gain and low dimensional carrier properties in the improvement of the lasing dynamics of gain-switched QW lasers. It is reported that the QWW laser has the extremely high differential gain property which is enhanced by a factor of three compared to the QW laser, that is, by one order compared to the double-heterostructure (DH) laser [118]. Here we theoretically investigate the lasing dynamics of gain switched QWW lasers on the basis of multi-mode rate equations.

A.2 Gain Properties of Quantum-Well Wire Lasers

With reduction of dimensionality of electron-motion freedom from QW to QWW structures, the density of states changes from a step-like function to a reciprocal of square-root function, having less broadening of carrier distribution. The gain envelop function $g(n,E)$ can be give n by Eq. (A.1).

$$g(n,E) = CM\rho_{\text{red}} [f_c(n,E) - f_v(n,E)] \quad (\text{A.1})$$

, where n is the carrier density, E is the lasing photon energy, ρ_{red} is the reduced density of states, f_c (f_v) is the conduction band (valence band) state occupation (Fermi) function which is a function of carrier concentration n through the quasi-Fermi energy, M is the square of the dipole matrix element, and C contains constants which are independent of the active layer geometry and material properties. In conventional double-heterostructures (DH), the value of M can be determined from Kane's model. In the case of GaAs, $M=1.33m_0 E_g (\equiv M_0)$, where m_0 is the electron mass and E_g is the band gap energy. In the QWW laser, the reduced density of states with respect to electrons and holes in the (i,k) subband is given by Eq. (A.2).

$$\rho_{\text{red}} = \left(\frac{2m_j^*}{\hbar^2} \right)^{1/2} \frac{1}{2\pi L_z L_y} \times \frac{1}{\sqrt{(E - \hbar^2 \pi^2 / 2m_j^* [(i/L_z)^2 + (k/L_y)^2])}} \quad (\text{A.2})$$

, where m_j^* ($j=l,h$) is the reduced mass with respect to heavy holes or light holes. In this case, M of the transition for (i,k) subband is maximum when the polarization of the electrical field is parallel with the quantum wire direction. The expression of M of the transition between the electrons and holes is given by Eq. (A.3).

$$M = \left(\frac{1}{E} \frac{\hbar^2 \pi^2}{2m_h^*} \left[\left(\frac{i}{L_z} \right)^2 + \left(\frac{k}{L_y} \right)^2 \right] \right) \frac{3}{2} M_0 \quad (\text{A.3})$$

This equation indicates that M is nearly $1.5M_0$ at equivalent band-gap edge. Figure A.1.1 shows the calculated bulk gain profiles of the QWW laser with $100 \text{ \AA} \times 100 \text{ \AA}$ wires at 300 K, plotted as a function of wavelength (or photon energy) and carrier densities ranging from $1 \times 10^{17} \text{ cm}^{-3}$ to $1 \times 10^{19} \text{ cm}^{-3}$. In this calculation, light holes are not included for the brief discussion. Narrow gain spectra are obtained in the QWW laser even at room-temperature.

A.3 Theoretical Analysis of Lasing Dynamics of Quantum-Well Wire Lasers

In §3.2, we both experimentally and theoretically studied the spectral dynamics of gain-switched QW lasers and its dependence on the number of QWs, demonstrating the significance of the enhanced differential gain due to narrow dynamic gain spectra which can be obtained in the QW laser with the larger number of QWs. Here, the lasing dynamics of QWW lasers in the gain switching are theoretically investigated on the basis of multi-mode rate equations which utilize the calculated gain properties as shown in Fig. A.1. Fig. A.2 (a) and (b) show the calculated spectral dynamics of the QWW laser when the excitation intensities are just above the threshold intensity and at 1.6 times the threshold intensity, respectively. The calculated results of the QW laser are also shown in Fig. A.3, where the excitation intensities are 1.1 times and 2.0 times as large as the threshold, respectively, and the number of wells is 12 for the narrow gain spectra. Note that the threshold excitation intensity of the QW laser is much higher than the QWW laser. Our calculated results indicate that short pulses less than 3 psec with narrow spectra are produced if the the normalized excitation intensity is beyond 1.1 times of the threshold intensity in the QWW laser, demonstrating that shorter pulses can be obtained by the smaller drive power compared to the QW laser owing to both the highly enhanced differential gain and the low

threshold condition. In addition, since the analyzed lasing spectra of the QWW laser do not drastically broaden with the increase of the excitation intensity, as shown in Fig. A.2, the QWW laser has an advantage that its lasing dynamics can be discussed on the basis of simple single mode rate-equations.

A.4 Summary

Lasing dynamics of a gain-switched quantum-well wire (QWW) laser as well as its gain properties are theoretically studied. The calculated results on the basis of multi-mode rate equations demonstrate that short pulses less than 3 psec with narrow spectra can be achieved in QWW lasers by lower operation power compared to the QW laser owing to both the highly enhanced differential gain properties and the lower threshold condition.

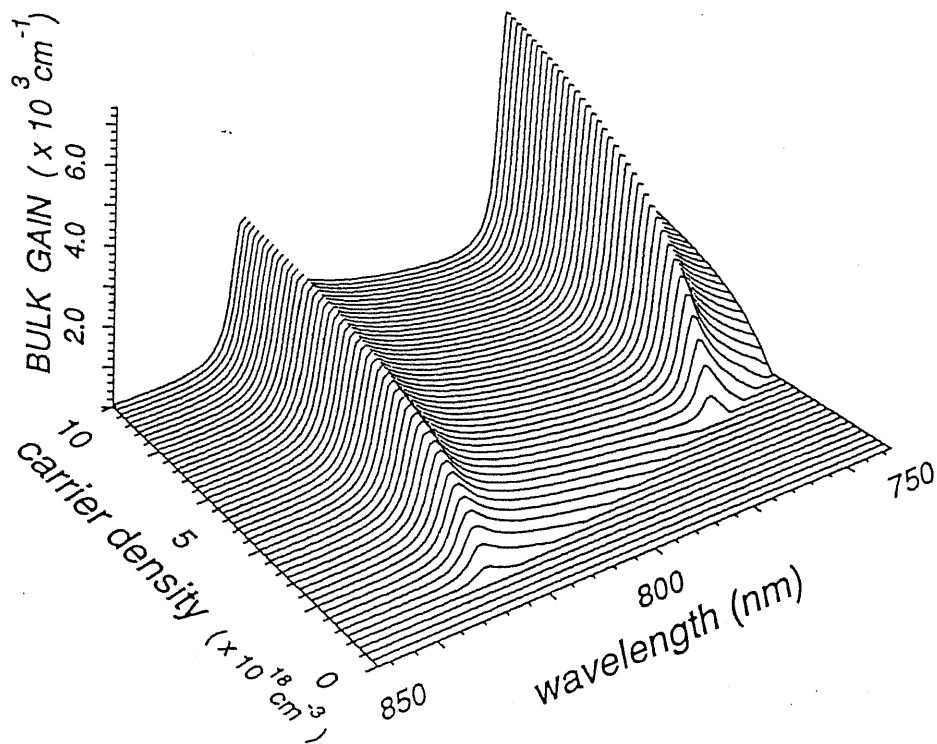


FIG. A.1 Calculated bulk gain profiles of a QWW laser with $100\text{\AA} \times 100\text{\AA}$ wires at 300K, plotted as a function of wavelength (or photon energy) and carrier densities ranging from $1 \times 10^{17} \text{ cm}^{-3}$ to $1 \times 10^{19} \text{ cm}^{-3}$. Narrow gain spectra and higher differential gain are obtained in the QWW laser.

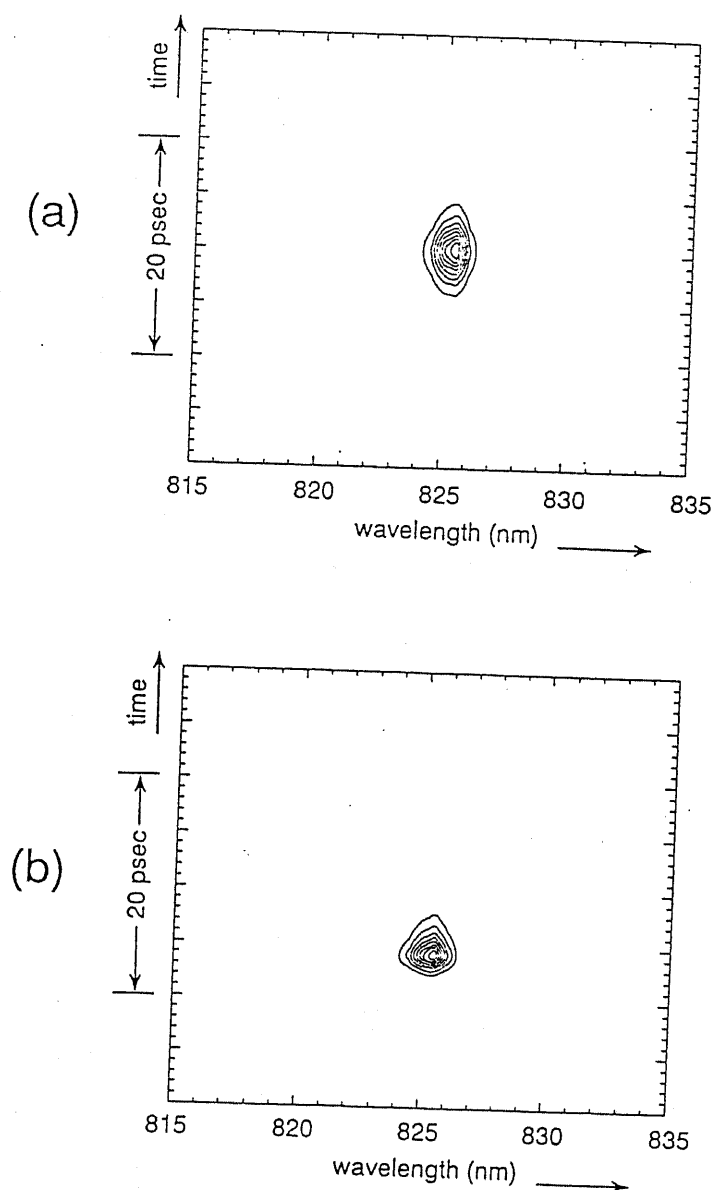


FIG. A.2 Calculated spectral dynamics of a quantum-well wire (QWW) laser when (a) the excitation intensities are just above the threshold intensity and (b) at 1.6 times the threshold intensity.

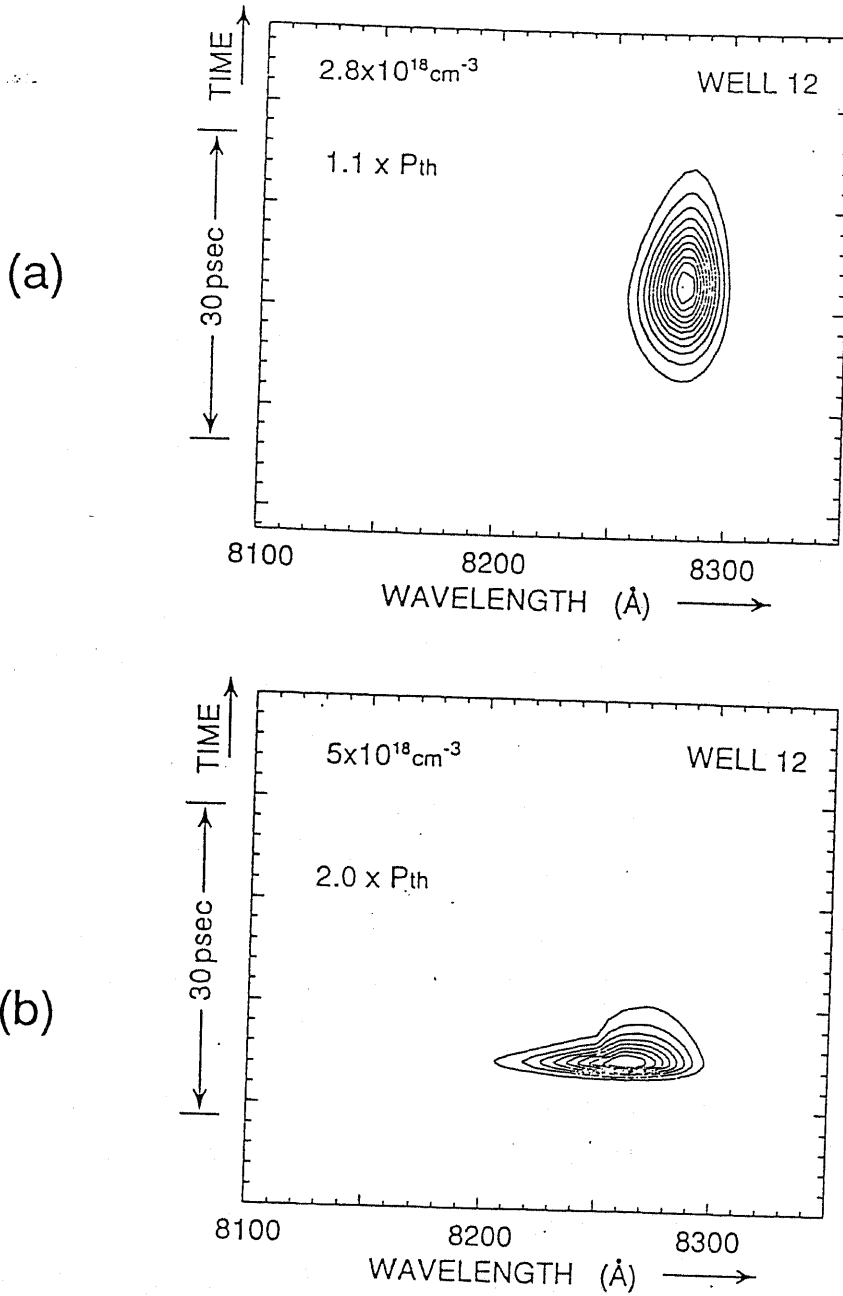


FIG. A.3 Calculated spectral dynamics of a quantum-well (QW) laser when (a) the excitation intensities are 1.1 times and (b) 2.0 times as large as the threshold, respectively, and the number of wells is 12.

References

- [1] S. L. Shapiro, ed.; *Ultrashort Light Pulses*, Springer-Verlag, (1977)
- [2] W. Kaiser, ed.; *Ultrashort Laser Pulses and Applications.*, Springer-Verlag, (1988)
- [3] R. L. Fork, B. I. Greene, and C. V. Shank, "Generation of pulses shorter than 0.1ps by colliding pulse mode locking," *Appl. Phys. Lett.*, Vol. **38**, p671 (1981)
- [4] E. B. Treacy, "Optical pulse compression with diffraction gratings," *IEEE J. Quantum Electron.*, Vol. **QE-5**, p454 (1969)
- [5] H. Nakatsuka, D. Grischkowsky, and A. C. Balant, "Nonlinear picosecond pulse propagation through optical fibers with positive group velocity dispersion," *Phys. Rev. Lett.*, Vol. **47**, p910 (1981)
- [6] C. V. Shank, R. L. Folk, R. Yen, R. H. Stolen, and W. J. Tomlinson, "Compression of femtosecond optical pulses," *Appl. Phys. Lett.*, Vol. **40**, p761 (1982)
- [7] R. L. Folk, C. V. Shank, and R. Yen, "Amplification of 70fs optical pulses to gigawatt powers," *Appl. Phys. Lett.*, Vol. **41**, p223 (1982)
- [8] R. L. Folk, O. E. Martinez, and J. P. Gordon, "Negative dispersion using pairs of prisms," *Opt. Lett.*, Vol. **9**, p150 (1984)
- [9] R. L. Fork, C. H. Brito Cruz, P. C. Becker, and C. V. Shank, "Compression of optical pulses to six femtosecond by using cubic phase compensation," *Optics Lett.*, Vol. **12**, p483 (1987)
- [10] C. V. Shank, R. L. Fork, R. F. Leheny, and J. Shah, "Dynamics of photoexcited GaAs band-edge absorption with subpicosecond resolution," *Phys. Rev. Lett.*, Vol. **42**, p112 (1979)

References

- [11] C. H. Brito Cruz, R. L. Fork, W. H. Knox, and C. V. Shank, "Spectral hole burning in large molecules probed with 10fs optical pulses," *Chem. Phys. Lett.*, Vol. **132**, p341 (1986)
- [12] C. V. Shank, R. L. Fork, C. H. Brito Cruz, and W. H. Knox, "Investigation of nonthermal population distributions with 10fs optical pulses," *Ultrashort Phenomena V*, Springer-Verlag, p179 (1986)
- [13] P. T. Ho, "Coherent pulse generation with a GaAlAs laser by active mode locking," *Electron. Lett.*, Vol. **21**, p211 (1985)
- [14] M. B. Holbrook, W. Sleat, and D. Bradley, "Bandwidth limited picosecond pulse generation in actively mode locked GaAlAs diode laser," *Appl. Phys. Lett.*, Vol. **37**, p59 (1980)
- [15] J. P. van der Ziel, "Mode locking in semiconductor lasers," in *Semiconductors and Semimetals*, Vol. **22B**, W. T. Tsang, Ed. New York: Academic, 1985
- [16] A. Olsson and C. L. Tang, "Active mode locking in linear and ring external cavity semiconductor lasers," *IEEE J. Quantum Electron.*, Vol. **QE-17**, p1977 (1981)
- [17] K. Y. Lau and A. Yariv, "Direct modulation and active mode locking of ultrahigh speed GaAlAs lasers at frequencies up to 18GHz," *Appl. Phys. Lett.*, Vol. **46**, p326 (1985)
- [18] K. Y. Lau and I. Ury, "Passive and active mode locking of a semiconductor laser without an external cavity," *Appl. Phys. Lett.*, Vol. **46**, p1117 (1985)
- [19] R. S. Tucker, S. K. Korotky, G. Eisenstein, U. Koren, L. W. Stulz, and J. J. Veselka, "20GHz active mode-locking of a 1.55 μ m InGaAsP laser," *Electron. Lett.*, Vol. **21**, p239 (1985)

References

- [20] S. W. Corzine, J. E. Bowers, G. Przybylek, U. Koren, B. I. Miller, and C. E. Socolich, "Active mode locked GaInAsP laser with subpicosecond output," *Appl. Phys. Lett.*, Vol. **52**, p348 (1988)
- [21] R. S. Tucker, U. Koren, G. Raybon, C. A. Burrus, B. I. Miller, T. L. Koch, G. Eisenstein, and A. Shahar, "40GHz active mode locking in a monolithic long cavity laser," *presented at the 11th IEEE Int. Semiconductor Laser Conf.*, Boston, MA, Sept. 1988, paper PD5
- [22] P. T. Ho, L. A. Glasser, E. P. Ippen, and H. A. Haus, "Picosecond pulse generation with a CW GaAlAs laser diode," *Appl. Phys. Lett.*, Vol. **33**, p241(1978)
- [23] A. Morimoto, T. Kobayashi, and T. Sueta, "Active mode locking of lasers using an electrooptic deflector," *IEEE J. Quantum Electron.*, Vol. **QE-24**, p94 (1988)
- [24] G. Eisenstein, R. S. Tucker, U. Koren, and S. K. Korotky, "Active modelocking characteristics of InGaAsP single mode fiber composite cavity lasers," *IEEE J. Quantum Electron.*, Vol. **QE-22**, p142 (1986)
- [25] J. E. Bowers, P. A. Morton, A. Mar, and S. W. Corzine, "Actively mode locked semiconductor lasers," *IEEE J. Quantum Electron.*, Vol. **QE-25**, p1426 (1989)
- [26] M. C. Wu, Y. K. Chen, T. Tunbun-Ek, R. A. Logan, M. A. Chin, and G. Raybon, "Transform-limited 1.4ps optical pulses from a monolithic colliding-pulse mode-locked quantum well laser," *Appl. Phys. Lett.*, Vol. **57**, p759 (1990)
- [27] E. P. Ippen, D. J. Eilenbert, and R. W. Dixon, "Picosecond pulse generation by passive mode locking of a diode laser," *Appl. Phys. Lett.*, Vol. **37**, p267 (1980)

References

- [28] P. W. Smith, Y. Silberberg, and D. A. B. Miller, "Mode locking semiconductor diode lasers using saturable excitonic nonlinearities," *J. Opt. Soc. Am. B*, Vol. 2, p1228 (1985)
- [29] Y. Silberberg and P. W. Smith, "Subpicosecond pulses from a mode locked semiconductor lasers," *IEEE J. Quantum Electron.*, Vol. QE-22, p759 (1986)
- [30] H. Yokoyama, H. Ito, and H. Inaba, "Generation of subpicosecond coherent optical pulses by passive mode locking of an AlGaAs diode laser," *Appl. Phys. Lett.*, Vol. 40, p105 (1982)
- [31] H. Ito, H. Yokoyama, S. Murata, and H. Inaba, "Picosecond optical pulse generation from a RF-modulated AlGaAs DH diode laser," *Electron. Lett.*, Vol. 15, p738 (1979)
- [32] H. J. Klein, D. Bimberg, H. Beneking, J. Kuhl, and E. O. Gobel, "High peak power picosecond light pulses from a direct modulated semiconductor laser," *Appl. Phys. Lett.*, Vol. 41, p394 (1982)
- [33] C. Lin, C. A. Burrus, G. Eisenstein, R. S. Tucker, P. Besomi, and R. J. Nelson, "11.2GHz picosecond optical pulse generation in gain-switched short cavity InGaAsP injection lasers by high-frequency direct modulation," *Electron. Lett.*, Vol. 20, p238 (1984)
- [34] J. P. van der Ziel and R. A. Logan, "Generation of short optical pulses in semiconductor lasers by combined dc and microwave current injection," *IEEE J. Quantum Electron.*, Vol. QE-18, p1340 (1982)
- [35] E. Scholl, D. Bimberg, H. Schumacher, and P. T. Landsberg, "Kinetics of picosecond pulse generation in semiconductor lasers with bimolecular recombination at high current injection," *IEEE J. Quantum Electron.*, Vol. QE-20, p394 (1984)

References

- [36] I. H. White, D. F. G. Gallagher, M. Osinsky, and D. Bowley, "Direct streak camera observation of picosecond gain-switched optical pulses from a 1.5 μ m semiconductor laser," *Electron. Lett.*, Vol. 21, p197 (1985)
- [37] R. A. Elliott, H. DeXiu, R. K. DeFreez, J. M. Hunt, and P. G. Rickman, "Picosecond optical pulse generation by impulse train current modulation of a semiconductor laser," *Appl. Phys. Lett.*, Vol. 42, p1012 (1983)
- [38] D. Bimberg, K. Ketterer, H. E. Scholl, and H. P. Vollmer, "Generation of 4ps light pulses from directly modulated V-groove lasers," *Electron. Lett.*, Vol. 20, p640 (1984)
- [39] S. Lundqvist, T. Anderson, and S. T. Eng, "Generation of tunable single-mode picosecond pulses from an AlGaAs semiconductor laser with grating feedback," *Appl. Phys. Lett.*, Vol. 43, p715 (1983)
- [40] N. Onodera, H. Ito, and H. Inaba, "Fourier transform-limited single mode picosecond optical pulse generation by a distributed feedback InGaAsP diode laser," *Appl. Phys. Lett.*, Vol. 45, p843 (1984)
- [41] Y. T. Lee, A. Shimizu, I. Tanaka, and T. Kamiya, "Gain-switched distributed feedback laser suitable for ultrafast optical trigger," *Extended Abst. of Conf. on Solid State Devices and Materials*, p111 (1987)
- [42] K. Kamite, H. Sudo, M. Sugano, H. Soda, T. Kusunoki, and H. Ishikawa, "14GHz single-mode picosecond optical pulse train generation in Zn doped distributed feedback lasers," *Appl. Phys. Lett.*, Vol. 54, p208 (1989)
- [43] T. L. Koch and J. E. Bowers, "Nature of wavelength chirping in directly modulated semiconductor lasers," *Electron. Lett.*, Vol. 20, p1038 (1984)

References

- [44] A. Takada, T. Sugie, and M. Saruwatari, "Picosecond optical pulse compression from gain-switched 1.3 μ m distributed feedback laser diode through highly dispersive single mode fiber," *Electron. Lett.*, Vol. 21, p969 (1985)
- [45] R. Takahashi, H. F. Liu, M. Osinsky, and T. Kamiya, "Picosecond single mode pulse compression using a 1.3 μ m Fabry-Perot laser diode, a dispersion-shifted fiber, and a grating monochromator," *Appl. Phys. Lett.*, Vol. 55, p2377 (1989)
- [46] G. J. Aspin, J. E. Carroll, and R. G. Plumb, "The effect of cavity length on picosecond pulse generation with highly rf modulated AlGaAs double heterostructure lasers," *Appl. Phys. Lett.*, Vol. 39, p860 (1981)
- [47] J. M. Wiesenfeld and J. Stone, "Picosecond pulse generation in optically pumped ultrashort-cavity InGaAsP, InP, and InGaAs film," *IEEE J. Quantum Electron.*, Vol. QE-22, p119 (1986)
- [48] J. R. Karin, L. G. Melcer, R. Nagarajan, J. E. Bowers, S. W. Corzine, P. A. Morton, R. S. Geels, and L. A. Coldren, "Generation of picosecond pulses with a gain-switched GaAs surface-emitting laser," *Appl. Phys. Lett.*, Vol. 57, p963 (1990)
- [49] Y. Arakawa, T. Sogawa, M. Nishioka, M. Tanaka, and H. Sakaki, "Picosecond pulse generation (<1.8psec) in a quantum well laser by a gain switching method," *Appl. Phys. Lett.*, Vol. 51, p1295 (1987)
- [50] T. Sogawa, Y. Arakawa, and T. Kamiya, "picosecond pulse generation in detuned distributed feedback lasers," *Electron. Lett.*, Vol. 24, p170 (1988)
- [51] T. Sogawa, Y. Arakawa, M. Tanaka, and H. Sakaki, "Observation of a short optical pulse (<1.3 psec) from a gain-switched quantum well laser," *Appl. Phys. Lett.* Vol. 53, p1580 (1988)

References

- [52] D. Z. Tsang, J. N. Walpole, S. H. Groves, J. J. Hsieh, and J. P. Donnelly, " Intracavity loss modulated GaInAsP diode lasers," *IEEE Trans. Electron. Devices*, Vol. **ED-27**, p2192 (1980)
- [53] D. Z. Tsang, J. N. Walpole, S. H. Groves, J. J. Hsieh, and J. P. Donnelly, " Intracavity loss modulated GaInAsP diode lasers," *Appl. Phys. Lett.*, Vol. **38** p120 (1981)
- [54] D. Z. Tsang and J. N. Walpole, " Q-switched semiconductor lasers," *IEEE J. Quantum Electron.*, Vol. **QE-19**, p145 (1983)
- [55] T. P. Lee and R. H. R. Roldan, "Repetitively Q-switched light pulses from GaAs injection lasers with tandem double-section stripe geometry semiconductor lasers," *IEEE J. Quantum Electron.*, Vol. **QE-6**, p339 (1970)
- [56] H. Ito, N. Onodera, K. Gen-ei, and H. Inaba, "Self Q-switched picosecond optical pulse generation with tandem type AlGaAs TJS laser," *Electron. Lett.* , Vol. **17**, p15 (1981)
- [57] T. Tsukada and C. L. Tang, " Q-switching of semiconductor lasers," *IEEE J. Quantum Electron.*, Vol. **QE-13**, p37 (1977)
- [58] Y. Arakawa, A. Larsson, J. Paslasky, and A. Yariv, "Active Q-switching in a multi-quantum well laser with a internal loss modulation," *Appl. Phys. Lett.*, Vol. **48** p561 (1986)
- [59] L. Esaki and R. Tsu, "Superlattice and negative differential conductivity in semiconductors," *IBM J. Res. Develop.*, Vol. **14**, p61 (1970)
- [60] R. Dingle, A. C. Gossard, and W. Wiegman, "Direct observation of super lattice formation in a semiconductor heterostructure," *Phys. Rev. Lett.*, Vol. **34**, p1327 (1975)

References

- [61] J. P. van der Ziel, R. Dingle, R. C. Miller, W. Wiegman, and W. A. Nordland Jr., "Laser oscillation from quantum well states in very thin GaAl-Al_{0.2}Ga_{0.8}As multilayer structures," *Appl. Phys. Lett.*, Vol. **26** p463 (1975)
- [62] N. Holonyak Jr, R. M. Kolbas, R. D. Dupius, and P. D. Dapkus, "Quantum well heterostructure lasers," *IEEE J. Quantum Electron.*, Vol. **QE-16**, p170 (1980)
- [63] W. T. Tsang, "Extremely low threshold (AlGa)As modified multi quantum well heterostructure lasers grown by molecular beam epitaxy," *Appl. Phys. Lett.*, Vol. **39** p786 (1981)
- [64] T. Fujii, S. Yamakoshi, K. Nanbu, O. Wada, and S. Hiyamizu, "MBE growth of extremely high quality GaAs-AlGaAs GRIN-SCH lasers with a superlattice buffer layer," *J. Vac. Sci. Technol.*, Vol. **2**, p259 (1984)
- [65] P. L. Derry, A. Yariv, and K. Y. Lau, "Ultralow-threshold graded-index separate-confinement single quantum well buried heterostructure (Al,Ga)As lasers with high reflectivity coatings," *Appl. Phys. Lett.*, Vol. **50** p1773 (1987)
- [66] K. Y. Lau, P. L. Derry, and A. Yariv, "Ultimate limit in low threshold quantum well GaAlAs semiconductor lasers," *Appl. Phys. Lett.*, Vol. **52** p88 (1988)
- [67] R. Chin, N. Holonyak Jr, B. A. Bojak, K. Hess, R. D. Dupius, and P. D. Dapkus, "Temperature dependence of threshold current for quantum well AlGaAs-GaAs heterostructure laser diodes," *Appl. Phys. Lett.*, Vol. **36** p19 (1979)
- [68] K. Hess, B. A. Bojak, N. Holonyak Jr., R. Chin, and P. D. Dapkus, "Temperature dependence of threshold current for a quantum well heterostructure laser," *Solid-State Electron.*, Vol. **23**, p585 (1980)

References

- [69] Y. Arakawa and H. Sakaki, "Multiquantum well laser and its temperature dependence of the threshold current," *Appl. Phys. Lett.*, Vol.40 p939 (1982)
- [70] Y. Arakawa, K. Vahala, and A. Yariv, "Quantum noise and dynamics in quantum well and quantum wire lasers," *Appl. Phys. Lett.*, Vol.45 p950 (1984)
- [71] Y. Arakawa and A. Yariv, "Theory of gain, modulation response, and spectral linewidth in AlGaAs quantum well lasers," *IEEE J. Quantum Electron.*, Vol. QE-21, p1666 (1985)
- [72] Y. Arakawa and A. Yariv, "Quantum well lasers - gain, spectra, dynamics," *IEEE J. Quantum Electron.*, Vol. QE-22, p1887 (1986)
- [73] K. Uomi, N. Chinone, T. Ohtoshi, and T. Kajimura, "High relaxation oscillation frequency (beyond 10GHz) of AlGaAs multiquantum well lasers," *Jpn. J. Appl. Phys.*, Vol. 24, pL539 (1986)
- [74] K. Uomi, T. Mishima, and N. Chinone, "Ultrahigh relaxation oscillation frequency (up to 30GHz) of highly p-doped GaAs/AlGaAs multiple quantum well lasers," *Appl. Phys. Lett.*, Vol. 51, p78 (1987)
- [75] H. Haug, "Quantum mechanical rate equation for semiconductor lasers," *Phys. Rev.*, Vol. 184, p338 (1969)
- [76] R. Roldan, "Spikes in the light output of room-temperature GaAs junction lasers," *Appl. Phys. Lett.*, Vol. 11, p346 (1967)
- [77] Y. Suematsu and K. Huruta, "Theoretical spontaneous emission factor of injection lasers," *Trans. of IECE Japan*, Vol. E-60, p467 (1977)
- [78] K. Petermann, "Calculated spontaneous emission factor for double-heterostructure injection lasers with gain-induced waveguiding," *IEEE J. Quantum Electron.*, Vol. QE-15, p566 (1979)

References

- [79] J. C. Goodwin and B. K. Garside, "Measurement of spontaneous emission factor for injection lasers," *IEEE J. Quantum Electron.*, Vol. **QE-18**, p1264 (1982)
- [80] A. Icsevgi and W. E. Lamb, Jr., "Propagation of light pulses in a laser amplifier," *Phys. Rev.*, Vol. **185**, p517 (1969)
- [81] K. Kamite, H. Sudo, M. Yano, H. Ishikawa, and H. Imai, "DFB laser with bandwidth larger than 9GHz," *Tech. Dig. of IEEE Semiconductor Laser Conf.*, pap. M-4 (1986)
- [82] H. Nishimoto, M. Yamaguchi, I. Mito, and K. Kobayashi, "High frequency response for DFB LD due to a wavelength detuning effect," *IEEE J. Lightwave Technol.*, Vol. **LT-5**, p1399 (1987)
- [83] H. Ishikawa, H. Soda, K. Wakao, K. Kihara, K. Kamite, Y. Kotaki, M. Matsuda, H. Sudo, S. Yamakoshi, S. Isozumi, and H. Imai, "Distributed feedback laser emitting at 1.3 μ m for gigabit communication systems," *IEEE J. Lightwave Technol.*, Vol. **LT-5**, p848 (1987)
- [84] K. Ketterer, E. H. Bottcher, and D. Bimberg, "Picosecond spectra of gain-switched AlGaAs/GaAs multiquantum well lasers," *Appl. Phys. Lett.*, Vol. **53**, p2263 (1988)
- [85] D. J. Westland, D. Mihailovic, J. F. Ryan, and M. D. Scott, "Optical time-of-flight measurement of carrier diffusion and trapping in an InGaAs/InP heterostructure," *Appl. Phys. Lett.*, Vol. **51**, p590 (1987)
- [86] J. Feldmann, G. Peter, E. O. Gobel, K. Leo, H.-J. Polland, K. Ploog, K. Fujiwara, and T. Nakayama, "Carrier trapping in single quantum well with different confinement structures," *Appl. Phys. Lett.*, Vol. **51**, p226 (1987)

References

- [87] B. Deveaud, J. Shah, T. C. Damen, and W. T. Tsang, "Capture of electrons and holes in quantum wells," *Appl. Phys. Lett.*, Vol. 52, p1886 (1988)
- [88] D. Y. Oberli, J. Shah, J. L. Jewell, and T. C. Damen, "Dynamics of carrier capture in an InGaAs/GaAs quantum well trap," *Appl. Phys. Lett.*, Vol. 54, p1028 (1989)
- [89] W. H. Knox, C. Hirlimann, D. A. B. Miller, J. Shah, D. S. Chemla, and C. V. Shank, "Femtosecond excitation of nonthermal carrier populations in GaAs quantum wells," *Phys. Rev. Lett.*, Vol. 56, p1191 (1986)
- [90] W.Z.Lin, J.G.Fujimoto, E.P.Ippen, and R. A. Logan, "Femtosecond dynamics of highly excited carriers in AlGaAs," *Appl. Phys. Lett.*, Vol. 51, p161 (1987)
- [91] R. W. Schoenlein, W .Z. Lin, E. P. Ippen, and J. G. Fujimoto, "Femtosecond hot carrier energy relaxation in GaAs," *Appl. Phys. Lett.*, Vol. 51, p1442 (1987)
- [92] W. H. Knox, D. S. Chemla, G. Livescu, J. E. Cunningham, and J. E. Henr, "Femtosecond carrier thermalization in dense fermi seas," *Phys. Rev. Lett.*, Vol. 61, p1290 (1988)
- [93] W. H. Knox, D. S. Chemla, G. Livescu, J. E. Henry, J. E. Cunningham, and, S. M. Goodnick, "Femtosecond carrier-carrier scattering dynamics in p-type and n-type modulation-doped quantum wells," *Ultrafast Phenomena VI*, Springer-Verlag, p210 (1988)
- [94] W. Z. Lin, R. W. Schoenlein, M. J. LaGasse, B. Zysset, E. P. Ippen, and J. G. Fujimoto, "Ultrafast scattering and energy relaxation of optically excited carriers in GaAs and AlGaAs," *Ultrafast Phenomena VI*, Springer-Verlag, p294 (1988)

References

- [95] Jagdeep Shah, "Ultrafast luminescence spectroscopy using sum frequency generation," *IEEE J. Quantum Electron.*, Vol. **QE-24**, p276 (1988)
- [96] P. C. Becker, H. L. Fragnito, C. H. Brito Cruz, R. L. Fork, J. E. Cunningham, J. E. Henry, and C. V. Shank, "Femtosecond photon echoes from band-to-band transitions in GaAs," *Phys. Rev. Lett.*, Vol. **61**, p1647 (1988)
- [97] J. -Y. Bigot, M. T. Portella, R. W. Schoenlein, C. V. Shank, and J. E. Cunningham, "Two-dimensional carrier-carrier screening studied with femtosecond photon echoes," *Ultrafast Phenomena VII*, Springer-Verlag, p239 (1990)
- [98] H. Kromer and H. Okamoto, "Some design consideration for multiquantum well lasers," *Japan J. Appl. Phys.*, Vol. **23**, p970 (1984)
- [99] A. Yariv, C. Lindsey, U. Sivan, "Approximate analytic solution for electronic wave function and energies in coupled quantum wells," *J. Appl. Phys.*, Vol. **58**, p3669 (1985)
- [100] B. S. Goldstein and J. D. Welch, "Microwave modulation of a GaAs injection laser," *Proc. IEEE*, , **52**, p715 (1964)
- [102] T. Ikegami and Y. Suematsu, "Resonance-like characteristics of the direct modulation of a junction laser," *Proc. IEEE*, , **55**, p122 (1967)
- [103] T. Ikegami and Y. Suematsu, "Direct modulation of semiconductor junction lasers," *Trans. of IECE Japan*, Vol. **51-B**, p51 (1968)
- [104] K. Y. Lau and A. Yariv, "Ultra high speed semiconductor lasers," *IEEE J. Quantum Electron.*, Vol. **QE-21**, p121 (1985)
- [105] R. S. Tucker, "High speed modulation properties of semiconductor lasers," *IEEE J. Lightwave Technol.*, Vol. **LT-3**, p1180 (1985)

References

- [106] W. Harth, "Large-signal direct modulation of injection lasers," *Electron. Lett.*, Vol. **9**, p532 (1973)
- [107] S. Tarucha and K. Otsuka, "Response of semiconductor laser to deep sinusoidal injection current modulation," *IEEE J. Quantum Electron.*, Vol. **QE-17**, p810 (1981)
- [108] E. Hemery, L. Chusseau, and J.-M. Lourtioz, "Dynamic behaviors of semiconductor lasers under strong sinusoidal current modulation: Modeling and experiments at 1.3 μ m," *IEEE J. Quantum Electron.*, Vol. **QE-26**, p633 (1990)
- [109] D. Hulin, A. Mysyrowicz, A. Antonetti, A. Migus, W. T. Masselink, H. Morkoc, H. M. Gibbs, and N. Peyghambarian, "Ultrafast all-optical gate with subpicosecond on and off response time," *Appl. Phys. Lett.*, Vol. **49**, p749 (1986)
- [110] H. M. Gibbs, S. S. Tarng, J. L. Jewell, D. A. Weinberger, K. Tai, A. C. Gossard, S. L. MaCall, A. Passner, and W. Wiegmann, "Room-temperature excitonic optical bistability in a GaAs-AlGaAs superlattice etalon," *Appl. Phys. Lett.*, Vol. **41**, p221 (1982)
- [111] D. A. B. Miller, D. S. Chemla, T. C. Damen, A. C. Gossard, W. Wiegmann, T. H. Wood, and C. A. Burrus, "Novel hybrid optical bistable switch: The quantum well self electrooptic effect device," *Appl. Phys. Lett.*, Vol. **45**, p13 (1984)
- [112] G. J. Lasher, "Analysis of a proposed bistable injection laser," *Solid State Electron.*, Vol. **7**, p707 (1964)
- [113] H. Kawaguchi and G. Iwane, "Bistable operation in semiconductor lasers with inhomogeneous excitation," *Electron. Lett.*, Vol. **17**, p167 (1981)

References

- [114] T. Sanada, T. Odagawa, T. Machida, K. Wakao, and S. Yamakoshi, "New reset method for optical bistable laser diodes," *Extended Abst. of Conf. on Solid State Devices and Materials*, p321 (1989)
- [115] J. L. Oudar, C. Tanguy, J. P. Chambaret, and D. Hulin, "Ultrafast optical switching based on stimulated emission in GaAs/AlGaAs multiple quantum wells," *Ultrafast Phenomena VI*, Springer Verlag, p179 (1988)
- [116] S. Tarucha, H. Kobayashi, Y. Horikoshi, and H. Okamoto, "Carrier induced energy gap shrinkage in current injection GaAs/AlGaAs MQW heterostructures," *Japan J. Appl. Phys.*, Vol. **23**, p874 (1984)
- [117] T. Sogawa and Y. Arakawa, "60GHz high relaxation oscillation frequency in a quantum well laser," *Extended Abst. of Int. Conf. on Solid State Devices and Materials*, p561 (1990)
- [118] E. O. Gobel, H. Jung, J. Kuhl, and K. Ploog, "Recombination enhancement due to carrier localization in quantum well structures," *Phys. Rev. Lett.*, Vol. **51**, p1588 (1983)
- [119] J. A. Brum and G. Bastard, "Resonant carrier capture by semiconductor quantum wells," *Phys. Rev. B.*, Vol. **33**, p1420 (1986)
- [120] T. Sogawa and Y. Arakawa, "Picosecond Spectral Dynamics of Gain-Switched Quantum Well Lasers and Its Dependence on Quantum Well Structures," *Journal of Applied Physics*, Vol. **67**, p2675, 1990
- [121] B. Fluegel, N. Peyghambarian, G. Olbright, M. Lindberg, S. W. Koch, M. Joffre, D. Hulin, A. Migus, and A. Antonetti, "Femtosecond Studies of Coherent Transitions in Semiconductors," *Phys. Rev. Lett.*, Vol. **59**, p2588 (1987)

References

- [122] M. Joffre, D. Hulin, J. P. Chambaret, A. Migus, A. Antonetti, and C. Benoit a la Guillaume, "Bleaching of an Exciton Line Using Sub-T2 Pulses: Artifact or Reality?," *Ultrafast Phenomena VI*, Springer-Verlag, p223 (1988)
- [123] N. Peyghambarian, B. Fluegel, S. W. Koch, J. Sokoloff, M. Lindberg, M. Joffre, D. Hulin, A. Migus, and A. Antonetti, "Femtosecond Transients and Dynamic Stark Effect in Semiconductors," *Ultrafast Phenomena VI*, Springer-Verlag, p218 (1988)
- [124] C. H. Brito Cruz, J. P. Gordon, P. C. Becker, R. L. Fork, and C. V. Shank, "Dynamics of Spectra Hole Burning," *IEEE J. Quantum Electron.*, Vol. QE-24, p261 (1988)

Publication List

Journal

- [1] Y. Arakawa, T. Sogawa, M. Nishioka, M. Tanaka, and H. Sakaki, "Picosecond Pulse Generation (<1.8 ps) in a Quantum Well Laser by a Gain Switching Method," *Applied Physics Letters*, Vol. **51**, p1295, 1987
- [2] T. Sogawa, Y. Arakawa, and T. Kamiya, "Picosecond Pulse Generation in Detuned Distributed Feedback Lasers," *Electronics Letters*, Vol. **24**, p170, 1988
- [3] T. Sogawa, Y. Arakawa, and T. Kamiya, "Enhanced Differential Gain for Short Pulse Generation in Semiconductor Lasers," *Ultrafast Phenomena V*, Springer-Verlag, p70, 1988
- [4] T. Sogawa, Y. Arakawa, M. Tanaka, and H. Sakaki, "Observation of a Short Optical Pulse (<1.3 ps) from a Gain-Switched Quantum Well Laser," *Applied Physics Letters*, Vol. **53**, p1580, 1988
- [5] T. Sogawa and Y. Arakawa, "Picosecond Spectral Dynamics of Gain-Switched Quantum Well Lasers and Its Dependence on Quantum Well Structures," *Journal of Applied Physics*, Vol. **67**, p2675, 1990
- [6] T. Sogawa and Y. Arakawa, "Picosecond Lasing Dynamics of Gain-Switched Quantum Well Lasers and Its Dependence on Quantum Well Structures," *to be published in IEEE Journal of Quantum Electronics*
- [7] T. Sogawa and Y. Arakawa, "Wavelength Switching of Picosecond Pulse (<10 psec) in a Quantum Well Laser and Its All-Optical Logic Gating Operations," *to be published in Applied Physics Letters*

Publication List

- [8] T. Sogawa and Y. Arakawa, "Picosecond Dynamics in Gain-Switched Uncoupled and Coupled Quantum Well Lasers," *to be published in Applied Physics Letters*
- [9] T. Sogawa, A. Ishikawa, and Y. Arakawa, "Carrier Capture Process in Quantum Well Structures and Its Effects on Lasing Dynamics," *in preparation*

Presentations

A. *International Conference*

- [1] T. Sogawa, Y. Arakawa, and T. Kamiya, "Enhanced Differential Gain for Short Pulse Generation in Semiconductor Lasers," *International Conference on Ultrafast Phenomena*, July 1988, Japan
- [2] T. Sogawa, Y. Arakawa, M. Tanaka, and H. Sakaki, "Picosecond Pulse Generation in Quantum Well Lasers by a Gain Switching Method," *XVI International Quantum Electronics Conference*, July 1988, Japan
- [3] Y. Arakawa, T. Sogawa, M. Tanaka, and H. Sakaki, "Picosecond Lasing Dynamics in Quantum Well Lasers and Its Dependence on the Number of Quantum Wells," *Topical Meeting on Picosecond Electronics and Optoelectronics*, March 1989, Salt Lake City, U.S.A.
- [4] T. Sogawa, Y. Arakawa, M. Tanaka, and H. Sakaki, "Spectral Dynamics of Gain-Switched Quantum Well Lasers," *Conference on Quantum Electronics and Laser Science '89*, April 1989, Baltimore, U.S.A.
- [5] T. Sogawa and Y. Arakawa, "Picosecond Lasing Dynamics in Coupled Quantum Well Lasers," *International Quantum Electronics Conference*, May 1990, Anaheim U.S.A.
- [6] T. Sogawa and Y. Arakawa, "60GHz Relaxation Oscillation Frequency in a Quantum Well Laser," *International Conference on Solid State Devices and Materials*, August 1990, Japan
- [7] T. Sogawa and Y. Arakawa, "Wavelength Control of Picosecond Pulses (<10ps) in Quantum Well Lasers by Localized and Unlocalized Pumping Pulses," *IEEE International Semiconductor Laser Conference*, September 1990, Switzerland

B. *Domestic (in Japanese)*

- [1] T. Sogawa, Y. Arakawa, M. Nishioka, M. Tanaka, and H. Sakaki, "Picosecond Pulse Generation in Quantum Well Lasers," *34th Spring Meeting of The Japan Society of Applied Physics and Related Societies*, March 1987, Tokyo
- [2] T. Sogawa, Y. Arakawa, M. Nishioka, M. Tanaka, and H. Sakaki, "Picosecond Pulse (<1.8ps) Generation in Quantum Well Lasers by a Gain Switching Method," *48th Autumn Meeting of The Japan Society of Applied Physics*, October 1987, Nagoya
- [3] T. Sogawa, Y. Arakawa, M. Tanaka, and H. Sakaki, "Picosecond Pulse Generation in Quantum Well Lasers," *5th Semiconductor Laser Symposium*, February 1988, Tokyo
- [4] T. Sogawa, Y. Arakawa, and T. Kamiya, "Effects of Enhanced Differential Gain on Short Pulse Generation in Semiconductor Lasers," *35th Spring Meeting of The Japan Society of Applied Physics and Related Societies*, March 1988, Tokyo
- [5] T. Sogawa, Y. Arakawa, M. Tanaka, and H. Sakaki, "Picosecond Pulse (<1.3ps) Generation in Gain Switched Quantum Well Lasers," *35th Spring Meeting of The Japan Society of Applied Physics and Related Societies*, March 1988, Tokyo
- [6] T. Sogawa, Y. Arakawa, and T. Kamiya, "Short Pulse Generation in Detuned Distributed Feedback Lasers," *5th Meeting on Ultrafast Optoelectronics*, March 1988, Tokyo
- [7] T. Sogawa, Y. Arakawa, M. Tanaka, and H. Sakaki, "Time-Resolved Spectra of Gain-Switched Quantum Well Lasers," *49th Autumn Meeting of The Japan Society of Applied Physics*, October 1988, Toyama

- [8] T. Sogawa, Y. Arakawa, M. Tanaka, and H. Sakaki, "Picosecond Spectral Dynamics of Gain-Switched Quantum Well Lasers and Its dependence on the Number of Quantum Wells," *36th Spring Meeting of The Japan Society of Applied Physics and Related Societies*, April 1989, Chiba
- [9] T. Sogawa, Y. Arakawa, M. Tanaka, and H. Sakaki, "Picosecond Lasing Dynamics of Gain-Switched Quantum Well Lasers; Dependence on the Barrier Thickness," *50th Autumn Meeting of The Japan Society of Applied Physics*, September 1989, Fukuoka
- [10] T. Sogawa, and Y. Arakawa, "Picosecond Lasing Dynamics of Gain-Switched Quantum Well Lasers," *Meeting on Electronics Materials and Optical Quantum Devices*, December 1989, Tokyo
- [11] T. Sogawa, and Y. Arakawa, "Picosecond Wavelength Switching Phenomena of Gain-Switched Quantum Well Lasers," *51th Autumn Meeting of The Japan Society of Applied Physics*, September 1990, Iwate
- [12] T. Sogawa, and Y. Arakawa, "Effects of Quantum Confinement on Repetitive Gain-Switching Characteristics," *51th Autumn Meeting of The Japan Society of Applied Physics*, September 1990, Iwate
- [13] T. Sogawa, and Y. Arakawa, "Picosecond Lasing Dynamics of Gain-Switched Quantum Well Lasers: Short Optical Pulse generation and Wavelength Switching," *Symposium on Ultrafast Optical Engineering*, October 1990, Shizuoka
- [14] T. Sogawa, A. Ishikawa, and Y. Arakawa, "Carrier Capture Process in Quantum Well Structures and Its Effects on Lasing Dynamics," *37th Spring Meeting of The Japan Society of Applied Physics and Related Societies*, March 1991, Kanagawa